Cooperative Research in C1 Chemistry

Report on research conducted from May 1, 1999 to April 30, 2000
DOE Cooperative Agreement No. DE-FC26-99FT40540

Prepared by the Consortium for Fossil Fuel Liquefaction Science

Gerald P. Huffman, Director
CFFLS / University of Kentucky
111 Whalen Building
533 S. Limestone Street
Lexington, KY 40506

Phone: (859)257-4027
FAX: (859)257-7215
E-mail: cffls@pop.uky.edu
Web page: www.cffls.uky.edu

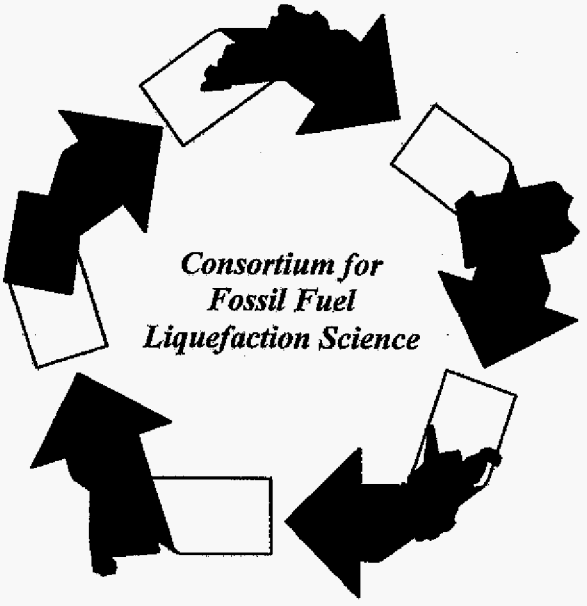

University of Kentucky *West Virginia University* *University of Pittsburgh*

University of Utah *Auburn University*

DISCLAIMER

Table of Contents

Cooperative Research in C1 Chemistry

Prepared by the Consortium for Fossil Fuel Liquefaction Science

July, 2000

Introduction

C1 chemistry refers to the conversion of simple carbon-containing materials that contain one carbon atom per molecule into valuable products. The feedstocks for C1 chemistry include natural gas, carbon dioxide, carbon monoxide, methanol and synthesis gas (a mixture of carbon monoxide and hydrogen). Synthesis gas, or syngas, is produced primarily by the reaction of natural gas, which is principally methane, with steam. It can also be produced by gasification of coal, petroleum coke, or biomass. The availability of syngas from coal gasification is expected to increase significantly in the future because of increasing development of integrated gasification combined cycle (IGCC) power generation.

Because of the abundance of remote natural gas, the advent of IGCC, and environmental advantages, C1 chemistry is expected to become a major area of interest for the transportation fuel and chemical industries in the relatively near future. The CFFLS will therefore perform a valuable national service by providing science and engineering graduates that are trained in this important area.

Syngas is the source of most hydrogen. Approximately 10 trillion standard cubic feet (SCF) of hydrogen are manufactured annually in the world. Most of this hydrogen is currently used for the production of ammonia and in a variety of refining and chemical operations. However, utilization of hydrogen in fuel cells is expected to grow significantly in the next century.

Syngas is also the feedstock for all methanol and Fischer-Tropsch plants. Currently, world consumption of methanol is over 25 million tons per year. There are many methanol plants in the U.S. and throughout the world. Methanol and oxygenated transportation fuel products play a significant role in the CFFLS C1 program. Currently, the only commercial Fischer-Tropsch plants are overseas, principally in South Africa (SASOL). However, new plants are being built or planned for a number of locations. One possible location for future F-T plant development in the U.S. is in the Alaskan oil fields.

Program Goals and First Year Accomplishments

The principal objectives of the CFFLS C1 research program are as follows:

- Develop technology for conversion of C1 source materials (natural gas, synthesis gas, carbon dioxide and monoxide, and methanol) into clean, high efficiency transportation fuel, especially diesel fuel.
- Develop improved processes to convert natural gas into syngas.
- Develop new processes for producing hydrogen from natural gas and other hydrocarbons.

A further general goal is to develop improved understanding of catalytic reaction mechanisms for all of these processes.

A brief summary of the principal accomplishments of the research program during its first year is given below.

- Fischer-Tropsch fuels containing oxygen have been synthesized.
- Higher ethers (C6-C8) have been synthesized from olefins, methanol and ethanol.
- Dimethyl and diethyl carbonates have been produced from the reaction of methanol and carbon monoxide.
- A small diesel engine has been set up to test the effects of these fuels, either alone or as additives, on particulate matter emissions and cetane level.
- Nanoscale, binary, Fe-based catalysts have been shown to have significant catalytic activity for the decomposition of methane to produce pure hydrogen.
- An environmentally safe catalyst for the hydroisomerization of straight-chain alkanes has been developed that may be useful for producing low pour point diesel fuel from F-T wax.
- Work on CO_2 reforming of methane to synthesis gas has been initiated.
- The reaction of CO_2 with ethylbenzene to produce styrene, which is a high volume, high value chemical, appears to a promising method of utilizing a greenhouse gas.
- In situ measurement capability has been developed for several analytical techniques to allow determination of catalyst structures and product suites during C1 reactions.

The remainder of this report presents a brief summary of the work carried out on each project.

Oxygenated Fischer-Tropsch Derived Diesel Fuel

Irving Wender and John W. Tierney
Department of Chemical and Petroleum Engineering, 1249 Benedum Hall,
University of Pittsburgh, Pittsburgh, PA 15261

There is a growing need to provide clean and efficient diesel fuels in improved diesel engines to replace gasoline now used in trucks, sports utility vehicles (SUVs) and other means of transportation. The gain in efficiency will be large with subsequent smaller releases of global warming gases. These new fuels must have high cetane numbers and, importantly, must meet new emission standards, especially in the lowering of particulate matter emissions. Exhaust particulate emissions from diesel engines can be as much as ten times greater than those from gasoline engines. As a result, focus on reduction of particle matter emissions from diesel engines is an environmental problem of great concern.

It is known that, when an oxygenated fuel blend is combusted, it can effectively deliver oxygen to the pyrolysis zone of a burning fuel, resulting in reduced particle matter generation. Data indicate that particle matter emission reductions of 4-10% can be achieved for each 1% of oxygen blended into diesel fuel by incorporation of certain oxygenated compounds, e.g, a glycol ether. Southwest Research Institute (SwRI) blended 15 % of dimethyl acetal, which has 6% oxygen, into superclean diesel from petroleum; particle matter emissions went down by 40% by this addition. It is important to determine whether the kind of oxygen in the additive is important and whether oxygenates of different structures, added together, reinforce each other.

As proposed, we listed a number of oxygenated compounds that could be added to diesel fuel to lower particle matter emissions. However, Dr. Bill Piel of the Oxygenate Analysis Project has furnished us with a list of some forty oxygenated compounds that are currently being surveyed as candidates for addition to petroleum low sulfur diesel fuel.

We have therefore directed our efforts to obtain high cetane oxygenated diesel fuel in the other direction highlighted in our proposal, namely via the preparation of oxygenated diesel fuel via the Fischer-Tropsch reaction. This approach does not use added oxygenated compounds which, while likely a viable direction, could have certain costs involving solubility, toxicity and other possible problems.

The Fischer-Tropsch (F-T) reaction converts synthesis gas, composed of various proportions of carbon monoxide and hydrogen, to straight-chain paraffins (alkanes) with cobalt catalysts and to a mixture of straight-chain paraffins and olefins with iron catalysts. The Shell F-T plant in Malayasia, with a cobalt catalyst, used the F-T process to produce diesel fuel with a cetane number of about 70; the fuel contained no aromatics and no sulfur. The state of California has imported some of this F-T diesel fuel from Shell and added small amounts to petroleum-derived diesel fuels to meet their diesel fuel environmental standards.

Our project aims to convert synthesis gas to F-T products from which environmentally clean diesel fuels containing 4-10 wt% oxygen in the hydrocarbon chain can be produced. The F-T diesel fuel has a high cetane number which would probably be reduced to about 60 by the addition of oxygen atoms in the chain. It is soluble in petroleum-derived diesel fuel and should be effective in reducing particle matter emissions. The F-T product, as has been done in California, would be used an additive to diesel from petroleum to help reduce emissions and raise cetane number.

For this purpose, a fixed bed continuous F-T unit has been constructed and is now operational. F-T products, from gases to waxes, have been produced using a cobalt catalyst. Present work is centered on a system for analysis of the complex mixture of products; this should be completed in the next two months. The F-T unit is an automatic high-pressure fixed bed reaction system. A computer is used to control the oven temperature, mass flow meters and sampling valves. Temperatures, flow rates and sampling times are also recorded by computer. Three GC columns are equipped to analyze the complex products of the F-T reaction. A HP Chemstation is used to control the GCs and analyze the collected data. A Visual Basic program was written to integrate the FC data and calculate the conversions and product distributions. A GC-MS is used to identify the components in products of the F-T synthesis.

A ruthenium-promoted Co/Al_2O_3 catalyst was prepared by incipient wetness impregnation. The support was γ-Al_2O_3 calcined at 500°C for 10 hours before impregnation. Cobalt nitrate and ruthenium nitrosyl nitrate were dissolved in de-ionized water and co-impregnated into γ-Al_2O_3 to form a catalyst with 20% Co and 0.5 wt% Ru. The catalyst was dried at 110°Cfor 12 hours and calcined in air at 300°C for 2 hours. $RuCo/Al_2O_3$ (0.2 to 2 g) was mixed with quartz sand and loaded into the reactor. The catalyst was reduced in pure H_2 at a rate of 50 ml/min, the temperature ramping from ambient to 350°C at 1°C, holding at 350°C for 10 hours. After reduction, the temperature was lowered to the reaction temperature. CO and H_2

flow rates were increased to a set value gradually in two hours while decreasing the argon (Ar) flow rate to avoid an initial temperature overshoot. Finally the Ar flow was maintained at 10 ml/min as a reference to calculate the CO conversion by

$$\text{Conversion} = [(C_{Ar})^{out}/(C_{Ar})^{in} - (C_{CO})^{in}/(C_{CO})^{in}]/[(C_{Ar})^{out}/(C_{Ar})^{in}]$$

F-T reactions were conducted at various temperatures and pressures. A good conversion of 36% was obtained at 220°C, 18 psi and 4.8 NL/hr.g. The activity remained constant during the run. The product is highly paraffinic. No wax product was collected at this reaction pressure. The conversion of CO and the average chain length of the product increased with increase in pressure. A substantial amount of wax was obtained at a pressure of 100 psig. Oxygenates were barely detectable in the F-T product on $RuCo/Al_2O_3$ at 220.

Oxygenates were obtained when the F-T reaction was conducted at lower temperatures. These oxygenates are mainly primary alcohols., identified by GC-MS. The alcohols ranged from C_6 to C_{19} as shown in Figure 1. At the initial stage of the reaction at 200°C and 100 psig, 3.2% of oxygenates were obtained in the collected oil product; the amount of oxygenates increased with time-on-stream. It increased to 6.2% after three days of reaction. Oxygenates could be further increased by lowering the temperature and raising the pressure of the F-T reaction. At 190°C and 200 psig, 10.2% of oxygenates were obtained in the collected oil product.

Product distributions of the collected oil fraction of the F-T product on $RuCo/Al_2O_3$ are shown in Figure 2. The amounts of oxygenates, olefins and paraffins are 10.2%, 26.5% and 63.3% respectively. The lower molecular weight products are rich in oxygenates and olefins; higher molecular weight products are more paraffinic.

Probe molecules containing oxygen, such as alcohols, ethers and unsaturated oxygen-containing molecules such as vinyl ethers are being added to the F-T reactions. The goal is to incorporate oxygen atoms into the F-T products to reduce particulate matter emissions while maintaining high cetane numbers.

Figure 1. Product Distribution of Oil Fraction

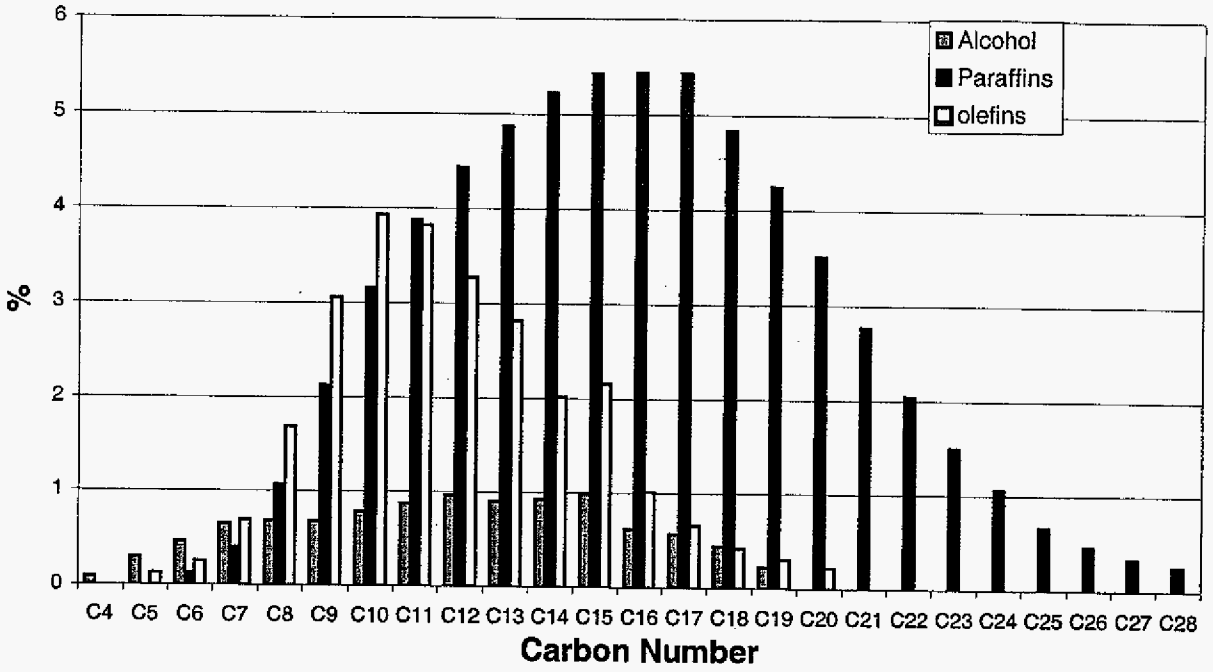

Figure 2. Distribution of Alcohols.

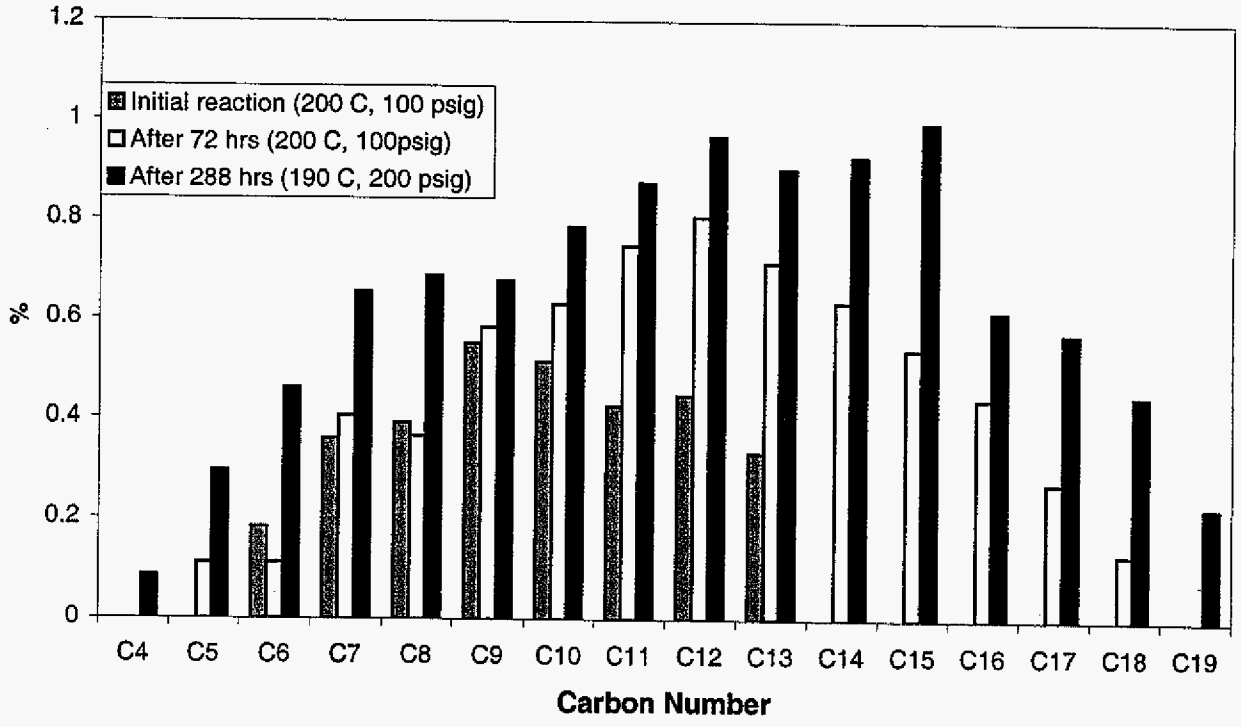

Synthesis of Higher Carbon Ethers from Methanol and Olefins

Jing Liu, Shaobin Wang, and James A. Guin
Department of Chemical Engineering, Auburn University

Oxygenated compounds such as ethers have a great potential as environmental enhancing additives for transportation fuels. The oxygenates can be produced from methanol and olefins or directly from alcohols, which can be produced from syngas by the Fischer-Tropsch process. The objective of our research is to study the production of higher (C_6 or greater) ethers which have desirable properties as transportation fuel additives. Higher molecular weight oxygenates have lower water solubility and vapor pressures than lower molecular weight oxygenates, e. g. MTBE, which have recently come under environmental pressures. The goal of the current project is to develop optimal reaction conditions and to develop new and improved catalysts for the reactions involved. In the previous year, our study has been focused on kinetics, reaction conditions and new catalysts for the production of a C_7 ether, 2,3 dimethyl-2-methoxybutane (DM2MB), from dimethyl butenes and methanol. We have also investigated the production of other higher ethers from this olefin and butanol, propanol and ethanol as well as binary mixtures of these alcohols. We have explored the development of new catalysts for these reactions as well. Reactions were performed in microautoclave reactors at several conditions using the commercial catalyst, Amberlyst-15, as well as several new laboratory-prepared catalysts and relevant kinetic and equilibrium parameters have been determined. Performance of the new laboratory developed catalysts has also been studied.

I. Catalytic behavior of the reference catalyst: Amberlyst 15.

As part of our first year's work, the reaction parameters for the production of one higher ether oxygenate, 2,3-dimethyl-2-methoxybutane (DM2MB), were investigated in a batch reactor at 50-70 °C using a macroporous cation exchange resin, Amberlyst 15, as catalyst for the etherification of 2,3-dimethyl-1-butene (DM1B) and 2,3-dimethyl-2-butene (DM2B) with methanol. The basic reaction scheme for olefins and DM2B with methanol is given below with the kinetic rate constants numbered as shown in the diagram. The kinetic rate constants were obtained by fitting the experimental data to kinetic equations based on a pseudohomogeneous model. Experimental results obtained in our investigations reveal the effect of temperature on simultaneous etherification and isomerization of DM1B and DM2B and differences in the reactivities of the

two olefins were studied. Kinetic and equilibrium parameters obtained from the Arrhenius and Van't Hoff equations agreed well with the values obtained from similar studies in the literature. The details of our work in the above area have been presented in a paper submitted for publication [1].

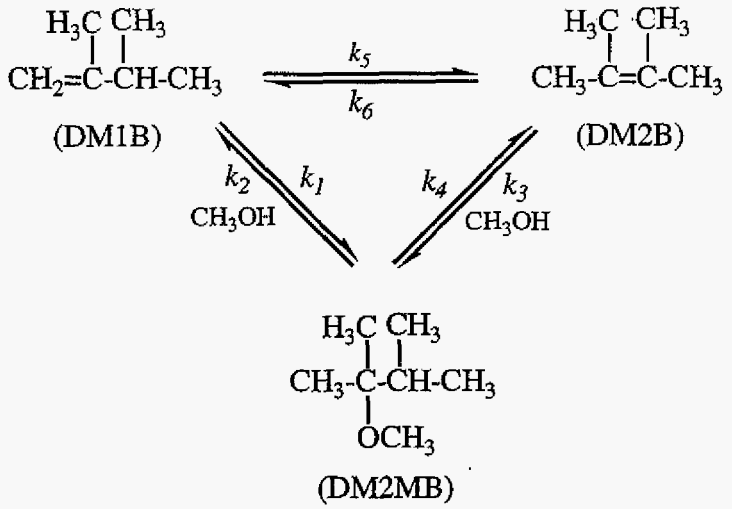

In our more recent work, we have studied the etherification reactions of butanol, propanol and ethanol with DM1B to compare the results with our work using methanol. The reaction routes with other alcohols are similar to the ones shown with methanol. The basic procedures were as follows: Amberlyst 15 was used as the catalyst. Before use, the catalyst was sieved and dried overnight in a vacuum oven at 90 °C. A catalyst particle size range of 0.4-0.7 mm was used in the kinetic experiments. Batch reactions were performed in 20 cm^3 316ss tubing bomb microreactors (TBMRS) agitated in a fluidized sand bath. TBMRS were charged with 250 psig He (inert) pressure in order to guarantee a liquid-phase reaction. Products were analyzed with a Varian 3300 gas chromatograph equipped with a FID using heptane as an internal standard at 35°C. The product ether DM2MB was identified by GC/MS.

Reaction rate constants obtained by fitting the data shown in Figures 1 and 2 for the reactions of DM1B with four different alcohols at 70°C are shown in Table 1. Not all of the results in Table 1 are in the same order as those reported in the literature. The finding that the etherification rate constant of methanol is greater than that of ethanol is different from the results obtained in the etherification of isobutene[2]. In the etherification of isobutene, an activity order of n-butanol = n-propanol > ethanol > methanol has been found, which was explained by the

effect of alcohols on the acidity of active sites. The acidity in the resin interior decreases in the order n-propanol > ethanol > methanol [3]. This leads to increase in both etherification and isomerization reaction rates. In our work shown in Table 1, all rate constants, except those for methanol etherification, are in an agreement with above explanation. These results imply that the effect of alcohols on the acidity of the proton may not be the only reason for the different reactivities.

Table 1. Rate Constants for Reactions with Different Alcohols at 70 °C

Alcohol	$k_1 \times 10^4$ (L·mol^{-1}·min^{-1})	$k_3 \times 10^4$ (L·mol^{-1}·min^{-1})	$k_5 \times 10^4$ (min^{-1})
Methanol	**2.48**	**1.0**	**39**
Ethanol	**1.94**	**0.88**	**49.6**
n-Propanol	**4.1**	**1.6**	**117**
n-Butanol	**6.5**	**2.0**	**196**

Figures 1 and 2 show the concentration profiles of ethers and isomer DM2B with time, respectively. The order of the isomer DM2B concentrations is the same as that of rate constants shown in Table 1. Also, as shown in Figure 1, except for the ether formed from methanol, the order of the ether concentrations is the same as that of rate constants in Table 1. The much higher concentration of methyl ether may be attributed to a consequence of the isomerization reaction. In the isomerization reaction, less DM2B is formed from DM1B in the presence of methanol. Due to the slower rate of isomerization, more DM1B, which is more active in etherification, will be available for the etherification and thus ether production with methanol is higher. For ethanol, n-propanol, n-butanol, the effect of isomerization on etherification is not apparent. Similar behaviors in etherification rates of isoamylenes with different alcohols were also reported by Linnekoski et al. [4]. They believed that the special reactivity of methanol might be related to its small molecule size, which provides easier access to the olefin DM1B, which has two branch methyl groups.

Figures 3-8 show concentration profiles of ethers and isomer DM2B in reaction of DM1B with equimolar binary mixtures of methanol/n-butanol, ethanol/n-butanol and n-propanol/n-

butanol, respectively. In Figure 3, the concentrations of methyl ether and butyl ether from binary alcohol mixtures are lower than those from pure alcohols at same reaction time. This result is due to the sharing of DM1B between the two alcohols. Analogous results are observed in Figure 4 and 5. It's interesting to note that the concentrations of butyl ether were always lower than the other ether when alcohol mixtures were used, despite the fact that the reaction rate constant of butyl ether is the highest with pure alcohol. These interesting results may be attributed to the different distribution coefficients for various alcohols. For example, Ancillotti et al. [2] experimentally determined the distribution coefficients for a methanol/n-butanol mixture on Amberlyst 15 resin, obtaining 1.14 for the methanol and 0.67 for the n-butanol. The sum of the ether concentration in reactions with alcohol mixtures lies approximately between the concentrations of ether in the reaction of DM1B with pure alcohols. Similar results for the isomer DM2B can be found in Figures 6-8.

II. Design and evaluation of new catalyst systems for ether production.

1. Acid-treated solid catalysts

Several acid-treated solid catalysts were prepared and their catalytic activity in the etherification of 23DM1B with methanol was investigated. The effects of acid property and nature of solid on activity were studied. Among the catalysts prepared, SiO_2-H_2SO_4 exhibits high activity and ether yield, which is better than the commercial ion-exchange resin catalysts. The factors influencing the catalytic behavior of SiO_2-H_2SO_4 catalysts were also investigated.

It is believed that acid treatment on solids will change their acid/base properties and their catalytic behavior will depend on nature of solids and acids employed as well as the preparation methods. Various acid-treated solid catalysts were prepared and tested under the same conditions and their catalytic activities were compared with the data obtained using some typical commercial ion-exchange resin catalysts. During the investigation, we firstly used several inorganic acids to modify the solids and found that sulfuric acid treated catalysts exhibited higher activity in terms of conversion and ether yield than that of other acids such as hydrochloric acid and nitric acid. Therefore, further study was concentrated on sulfuric acid treated catalysts.

Table 2 shows the catalytic behavior of the prepared solid catalysts and commercial catalysts. Three commercial catalysts show varying activity and the Amberlyst 15 exhibits the best performance, however, it shows low selectivity to ether production. The catalytic activity is believed to be related to the acidity of the catalysts [5]. Among the acid-treated catalysts, SiO_2-H_2SO_4 shows similar activity to Amberlyst 15. Montmorillonite-H_2SO_4 gives moderate conversion and high ether yield. Others show low activity but high ether selectivity around 50%. Based on Table 2, SiO_2-H_2SO_4 is a good candidate and deserves further investigation.

Table 2. Catalytic activity of various acid-treated solids and commercial catalysts in 23DM1B etherification with methanol. *

Catalyst	23DM1B conv (%)	23DM2B sel (%)	Ether sel (%)	Ether yield (%)
Amberlyst 15	91.0	78.7	20.6	18.8
Nafion	29.0	44.0	53.9	15.6
Nafion SAC-13	3.2	21.7	58.9	1.9
Bentonite-H_2SO_4	17.0	36.6	59.6	10.1
Montmorillonite-H_2SO_4	44.4	46.2	52.6	23.4
C-H_2SO_4	3.2	30.5	54.9	1.8
SiO_2-H_2SO_4	90.3	80.0	19.6	17.7
ZrO_2- H_2SO_4	0	0	0	0
Fe_2O_3- H_2SO_4	0	0	0	0
Al_2O_3- H_2SO_4	0	0	0	0

*** Reaction conditions: 0.5 g catalyst, 0.2 g methanol+ 0.5 g 23DM1B + 4g heptane, 80°C, 2h. Catalysts were obtained by treating 3 g SiO_2 in 25 ml sulfuric acid solution (0.5 M) and calcined at 300° C for 2h.**

In order to achieve high selectivity and ether yield over the SiO_2-H_2SO_4 system, we have studied some modifications of SiO_2-H_2SO_4 by varying the sulfur content and calcination temperature. Figure 9 and Figure 10 show the results, respectively. Calcination temperature affects the catalytic activity. High temperature calcination reduces 23DM1B conversion but enhances the ether selectivity. The highest ether yield is obtained at 400°C. Sulfuric acid treatment will increase the 23DM1B conversion and ether yield and the conversion will reach the highest level of 75% at the sulfur acid volume of 15 ml. However, the best ether yield of 30% is attained at a sulfuric acid volume of 20 ml.

2. Sulfated zirconia and supported sulfated zirconia catalysts.

A series of superacid catalysts such as sulfated zirconia(SZ), tungstated zirconia and supported sulfated zirconia were prepared. The effect of support in the supported sulfated zirconia system on the catalytic activity was investigated. It was found that silica supported sulfated zirconia catalysts produced high ether yield and the composition of this type of catalyst was optimized. Some metal oxide-promoted SZ/SiO_2 catalysts were also prepared and the effect of these promoters on catalytic activity was investigated.

Sulfate, tungstate and molybdate oxide containing solids are found to show high acidity and can be active for some acid-catalyzed reactions. We have prepared sulfated zirconia, tungstated zirconia and supported sulfated zirconia catalysts and investigated their activity. Figure 11 shows the results of 23DM1B etherification with methanol over the various laboratory-prepared and commercial catalysts. Sulfated zirconia exhibits higher conversion than that of Nafion SAC-13 while tungstated zirconia shows the lowest activity but similar isomerization selectivity to that of Nafion SAC-13 and SZ. Silica supported SZ gives a similar conversion and ether yield to that over Nafion NR50, but still lower than that of the Amberlyst 15. Acid-treated SZ/SiO_2 exhibits much high conversion with a desirably lower selectivity for isomerization, giving an ether yield of 30%, which is higher than that of the Amberlyst 15 reference catalyst.

Sulfated zirconia supported on other solids such as alumina, bentonite (BT), and montmorillonite (MT) were also prepared and tested. It was found that the catalytic activity follows an order of SZ/SiO_2> SZ/MT >SZ/BT > SZ/Al_2O_3. Further investigation on the SiO_2 supported system with added W and Mo oxides was also conducted and the results revealed that SiO_2 supported sulfated zirconia give higher activity than the other two catalysts.

The effects of varying the compositions of $Zr(SO_4)_2$ and SiO_2 in acid-treated SZ/SiO_2 and calcination temperature were further investigated and the results are presented in Figures 12 and 13, respectively. It is seen that the loading of $Zr(SO_4)_2$ in $SZ/SiO_2(H_2SO_4)$ greatly influences the catalytic activity and selectivity. Both 23DM1B conversion and 23DM2B selectivity generally increase as the $Zr(SO_4)_2$ loading increases. Ether yield increases with increasing $Zr(SO_4)_2$ loading and reaches a stable level of *ca.* 30% when the wt% $Zr(SO_4)_2$ exceeds 50%. Calcination temperature also exerts an influence on catalytic behavior. Catalysts calcined at 400-550 °C can give a much high conversion over 80%. When catalysts were calcined at higher temperatures over 600 °C, the selectivity to ether was remarkably enhanced, although the overall conversion

drops off. In terms of ether yield, 600 °C was the optimal temperature at which the highest ether yield was achieved.

It has been reported that certain metal oxides in supported SZ catalysts show a promoting effect on the acidity of those catalysts and thus we have prepared some promoted catalysts using Mn, Ni, Fe and Pt as promoters. The results showed that Ni and Pt increase the catalytic activity, Fe will have no significant influence on 23DM1B conversion while Mn reduces the catalytic activity.

3. Si-MCM41 supported catalysts

Three types of silica with different textural properties were employed as supports to prepare the supported sulfated zirconia and the effect of pore structure on catalytic behavior was investigated. The pore structure of the catalyst was found to affect the catalytic activity. Mesoporous Si-MCM41 supported SZ produced higher ether yields.

It is generally known that the pore structure of catalysts will influence the adsorption and catalytic activity. From what has been shown above, it is seen that SiO_2 is the best support for our acid catalysts. We, therefore, further investigated the effect of pore structure in the SZ/SiO_2 system. Three SiO_2 precursors with varying pore structure (fused SiO_2, silica gel and Si-MCM41) were used to prepare supported sulfated zirconia catalysts and the results demonstrate that SZ/Si-MCM41 exhibits much high activity than that of other two catalysts. This effect can be attributed to the variation of pore size.

As has been shown in the last section, the catalytic behavior of SZ and supported SZ catalysts depends on preparation methods. Figure 14 presents the catalytic activity of SZ/Si-MCM41 with the variation of $Zr(SO_4)_2$ loading. It is seen that SZ/Si-MCM41 shows the highest conversion activity at a $Zr(SO_4)_2$ loading of 50%. The highest ether yield of ca. 30% is achieved at the loading of 40-50%.

III. Future work.

The kinetic studies on the etherification reactions will be further studied using the most active catalysts developed in our previous investigations. The reaction mechanisms and kinetic models will be also developed. These catalysts will be tested in new reaction routes of alcohol coupling

to produce ethers instead of reactions between alcohols and olefins. Catalysts with optimal composition for ether selectivity and yield will be developed by characterization /testing.

References:

1. Liu, J., Wang S., Guin, J. A., *Fuel Processing Technology,* submitted.
2. Ancillotti, F.,Mauri, M. M., Pescarollo, E., *J. Catal.* 46, 49-57 (1977).
3. Casey, W. J., Pietrzyk, D. J., *Anal. Chem.* 45, 1404-1409 (1973).
4. Linnekoshi, J. A., Paakkonen-Kiviranta, P., Krause, A.O., Rihko-struckmann, L. K., *Ind. Eng. Chem. Res.* 38, 4563-4570 (1999).
5. Wang S., Liu, J., and Guin, J. A., *J. Catal.*, submitted.

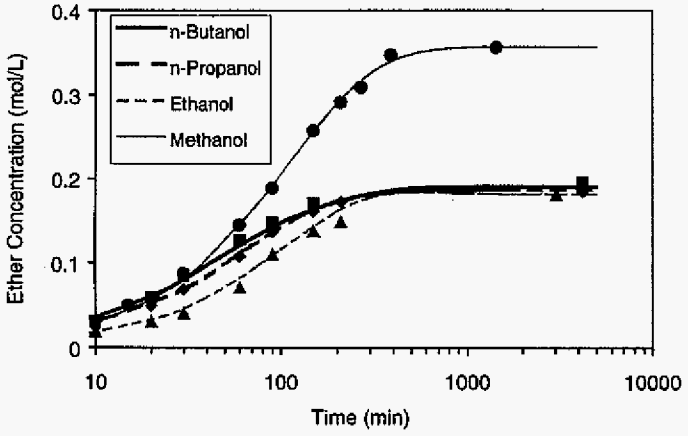

Figure 1. Concentration profiles of ethers for olefin etherification reactions with four different alcohols at 70°C.

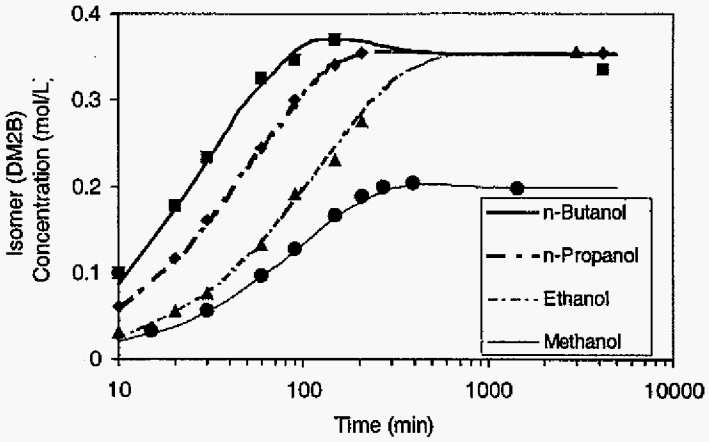

Figure 2. Concentration profiles of isomer DM2B for olefin etherification reactions with four different alcohols at 70°C.

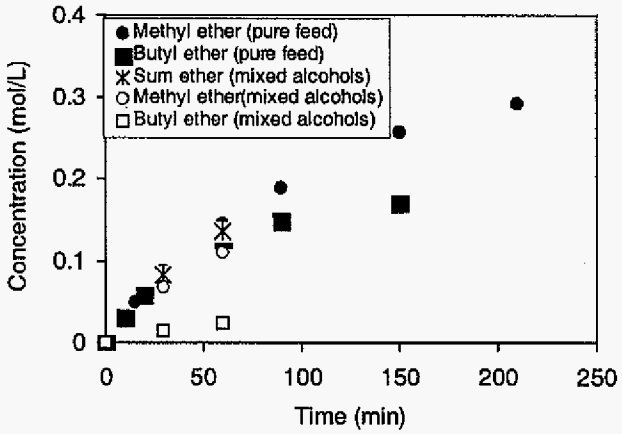

Figure 3. Comparison of ether concentrations for olefin etherification reactions with pure and binary equimolar alcohol mixtures.

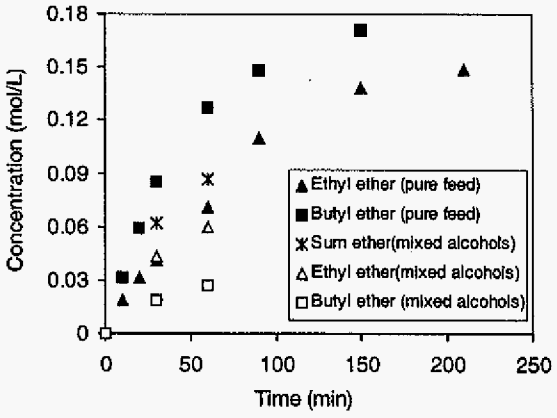

Figure 4. Comparison of ether concentrations for olefin etherification reactions with pure and binary equimolar alcohol mixtures.

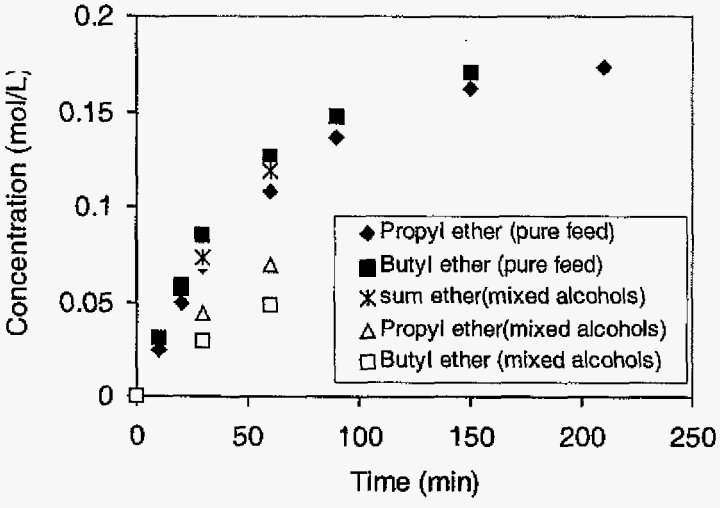

Figure 5. Comparison of ether concentrations for olefin etherification reactions with pure and binary equimolar alcohol mixtures.

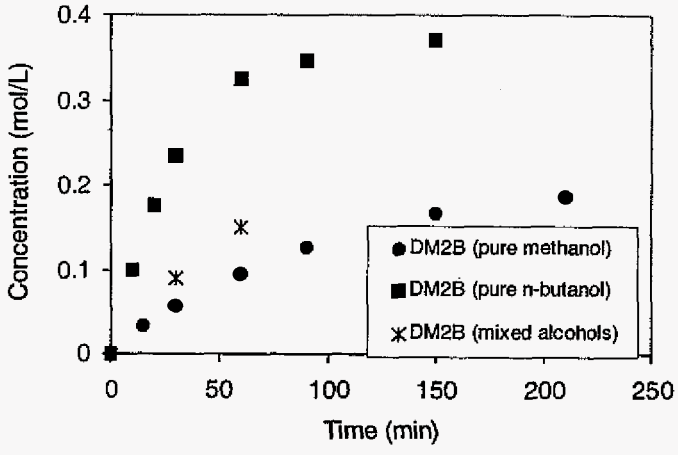

Figure 6. Comparison of isomer DM2B concentrations for olefin etherification reactions with pure and binary equimolar alcohol mixtures.

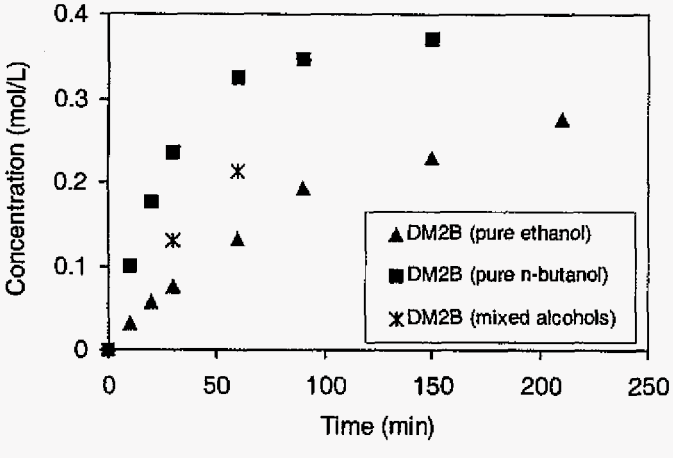

Figure 7. Comparison of isomer DM2B concentrations for olefin etherification reactions with pure and binary equimolar alcohol mixtures.

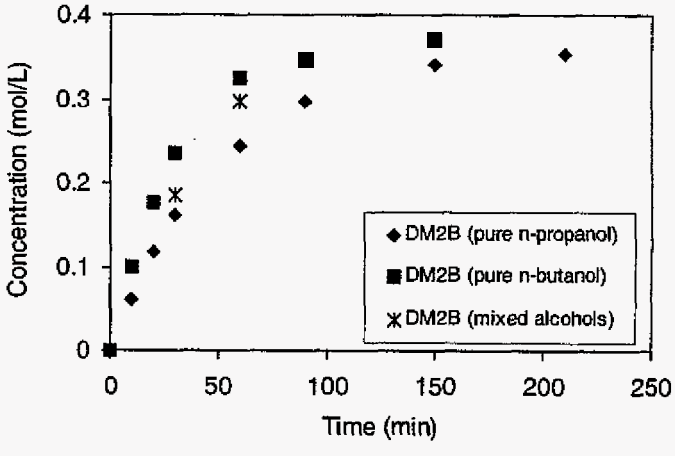

Figure 8. Comparison of isomer DM2B concentrations for olefin etherification reactions with pure and binary equimolar alcohol mixtures.

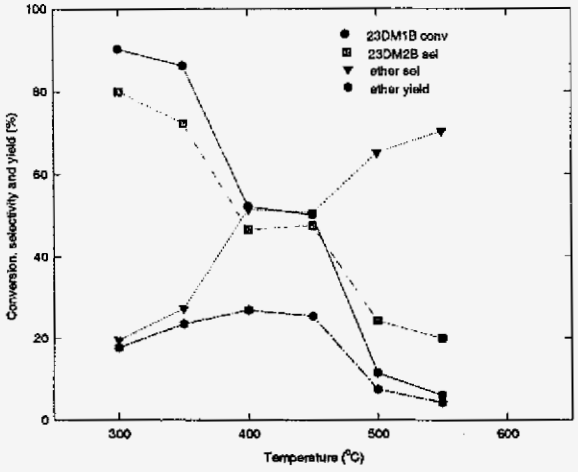

Figure 9. Effect of calcination temperature on activity of SiO_2-H_2SO_4 catalysts.

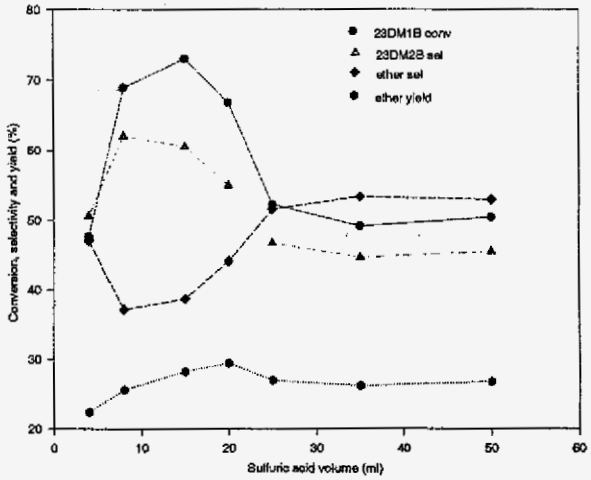

Figure 10. Effect of sulfuric acid volume used for treatment of SiO_2 on activity of SiO_2-H_2SO_4 catalysts.

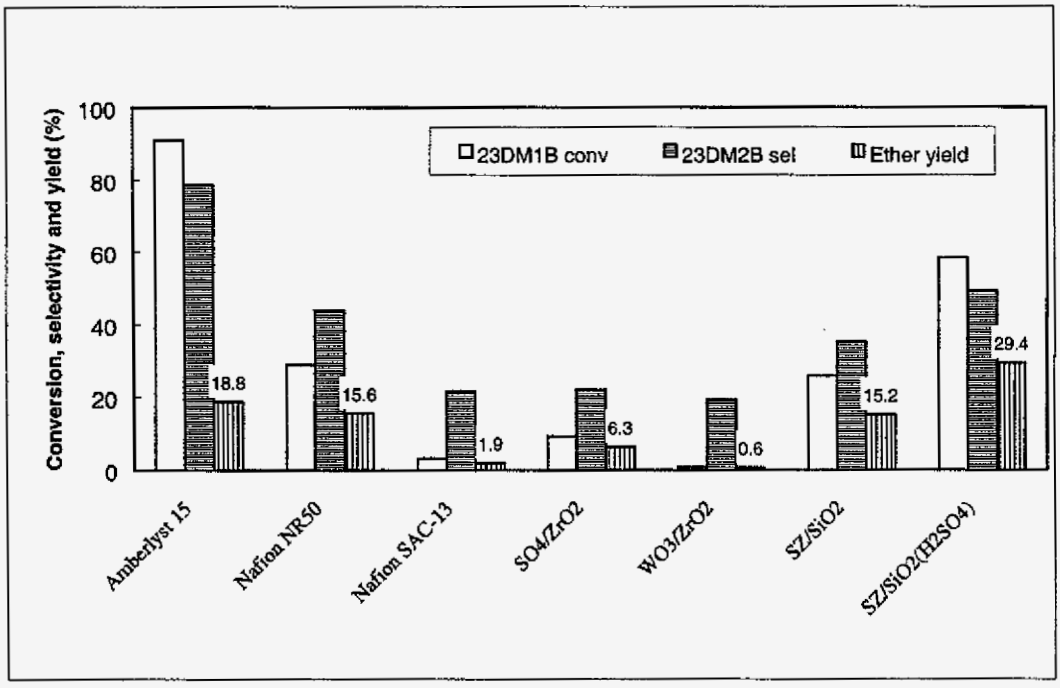

Figure 11. Catalytic activity over commercial ion exchange resin and prepared zirconia-based catalysts.

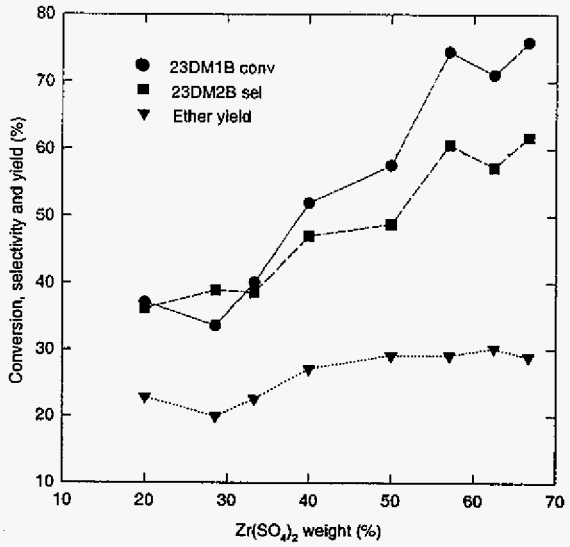

Figure 12. Effect of $Zr(SO_4)_2$ content in $SZ/SiO_2(H_2SO_4)$ system on catalytic activity.

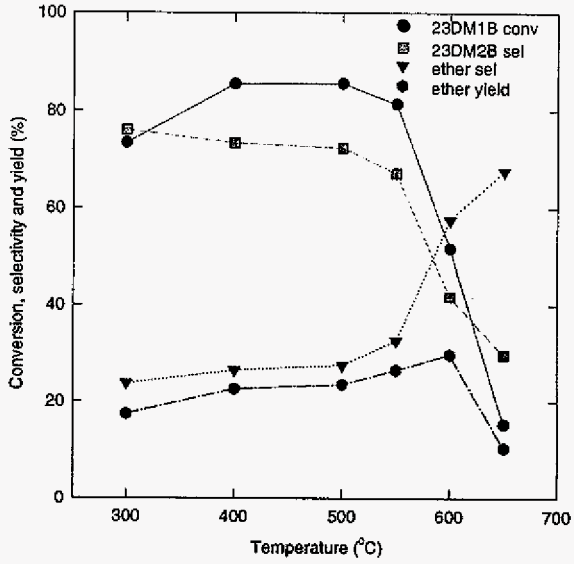

Figure 13. Effect of calcination temperature on activity of $SZ/SiO_2(H_2SO_4)$ catalysts.

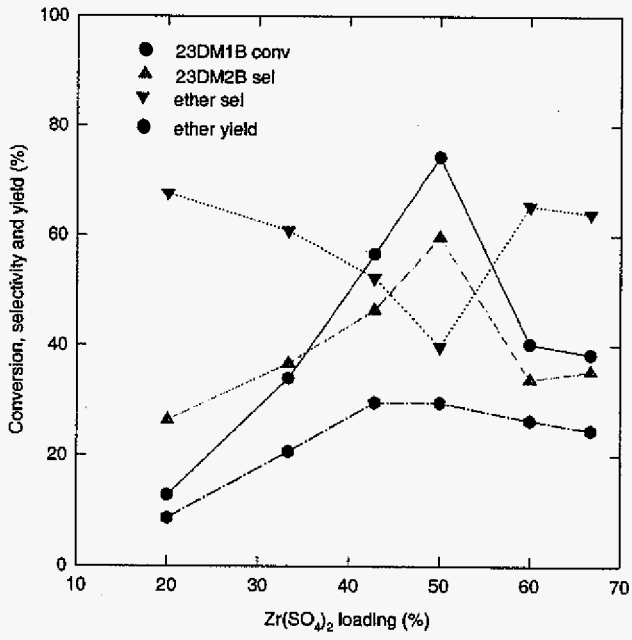

Figure 14. Effect of $Zr(SO_4)_2$ loading in SZ/Si-MCM41 catalysts on catalytic activity.

Synthesis of Organic Carbonates as Possible Transportation Fuel Additives

Annual Report (May 1, 1999 - April 30, 2000)

E. M. Eyring, H. L. C. Meuzelaar and R. J. Pugmire, University of Utah

Introduction

Acting on the counsel of the CFFLS Industrial Advisory Board (IAB) (given at a meeting held November 17, 1999), the University of Utah research team terminated a study of the synthesis of dimethyl carbonate (DMC) from methanol and carbon monoxide. The results of the DMC study (covering the period May 1, 1999 to approximately November 30, 1999) were reported at the national American Chemical Society meeting in San Francisco, CA on April 29, 2000. These results are published in a Fuels Division preprint.[1]

Diethyl carbonate (DEC) was judged by the IAB to be a more promising oxygenated diesel fuel additive than DMC because of the lower volatility and lower water solubility of DEC. The initial research question was: Can DEC be prepared from ethanol and carbon monoxide over a supported copper catalyst in a batch reactor in a manner similar to the synthesis of DMC? The balanced chemical equation describing the desired reaction is:

$$2\,CH_3CH_2OH + CO + \frac{1}{2}O_2 \xrightarrow{Cu^{2+}} O=C(OCH_2CH_3)_2 + H_2O$$

The answer to this initial research question is that the reaction does occur but with some unexpected wrinkles: 1) With a $CuCl_2/PdCl_2$ heterogeneous catalyst (supported on activated carbon) and identical starting experimental conditions (except for using ethanol instead of methanol) one obtains about 20% as much DEC as DMC. 2) The DEC synthesis takes about four times as long to reach completion as the DMC synthesis. 3) There is a greater range of product species in the DEC synthesis than was encountered in the DMC synthesis. Thus mass spectrometry turns out to be a more useful tool for tracking the DEC synthesis than was the case in the DMC synthesis. The dominant byproducts of the DEC synthesis are acetaldehyde and ethyl formate. 4) Pretreatment of the Cu/Pd heterogeneous catalyst with one of several metal

hydroxides greatly improves the reaction selectivity for the DEC product over acetaldehyde and ethyl formate.

Experimental

Catalyst preparation: To approximately 10 g DARCO 20-40 mesh activated carbon one adds 100 mL of 3% $CuCl_2$, 0.25% $PdCl_2$ methanolic solution. The mixture is refluxed for 4 hours with vigorous stirring. Subsequent drying is accomplished in a vacuum oven operated at 26 inches of mercury vacuum and 100 °C. When the effect of hydroxide on the catalyst selectivity for products is to be tested, a metal hydroxide methanolic solution is added to the above described catalyst and is refluxed for 4 hours before redrying in a vacuum oven.

Batch reactor sample preparation: In a typical experiment 3.2 g ethanol(Absolute grade) are poured over the 0.5 g of heterogeneous catalyst sitting in the glass liner of a 625 mL stainless steel reactor. The lid is tightened with 6 bolts and carbon monoxide is admitted to a pressure of 1.7 atm at 25 °C. 3.4 atm of air also is admitted. The reactor is suspended in a preheated fluidized sandbath and the reaction temperature (typically 170 °C) is attained within 20 minutes.

Product identification and quantitation: The first DEC synthesis experiments (in December, 1999) were greatly facilitated by a portable AVS-GC/MS detection system from the laboratory of Prof. Meuzelaar. [AVS stands for ambient vapor sampling.] A two meter long, 50 mm i.d., deactivated fused silica pressure reduction transfer line between the batch reactor and the GC/MS permits real-time monitoring of the volatile reaction products. Most of the experimental DEC data reported below were gathered by on-line GC monitoring with off-line GC/MS product identification after the portable GC/MS was moved by the Meuzelaar group to another experiment.

Results

Better yields of the target DEC are obtained with the $CuCl_2/PdCl_2$ on activated carbon catalyst than with any other heterogeneous catalyst which we have tested so far, see Fig. 1. In all eight reactions the reaction begins with 3.6 mL of ethanol, a pressure of 1. 7 atm of carbon monoxide, 3.4 atm of air, and 0.5 grams of heterogeneous catalyst.

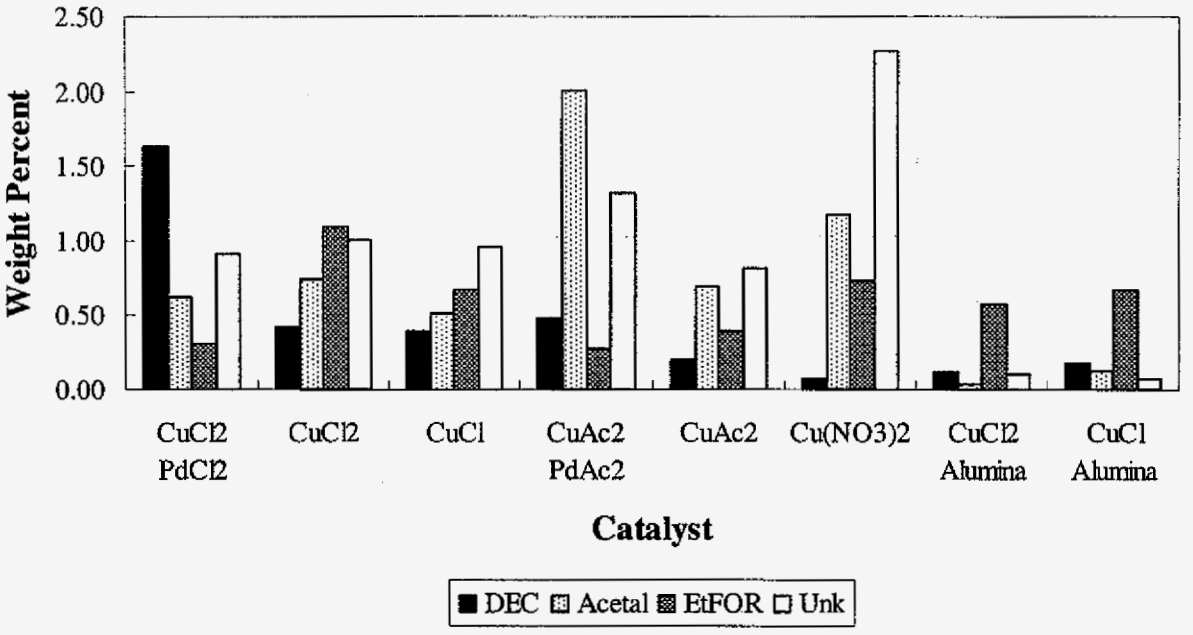

Figure 1. Comparison of product yields after 2 hours at 170 °C for several catalysts. In the first six experiments the support is activated carbon.

Several reaction products have the formulas shown below:

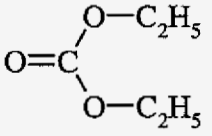

Diethyl Carbonate

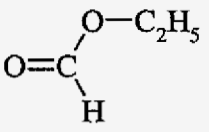

Ethyl Formate

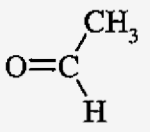

Acetaldehyde

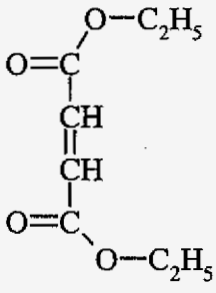

2-Butenedioic acid, diethyl ester

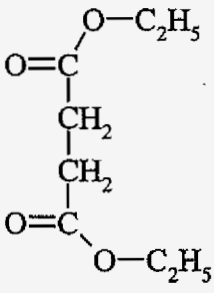

Butanedioic acid, diethyl ester

The influence of hydroxide pretreatment of the heterogeneous catalyst is illustrated in Fig. 2. The yield of the sought after DEC is considerably enhanced by any hydroxide which we have tried with the best results provided by $Ba(OH)_2$. It is evident from the results of the last experiment in Fig. 2 that it is possible to have too much of a good thing: Five times as much NaOH largely shuts down the production of DEC.

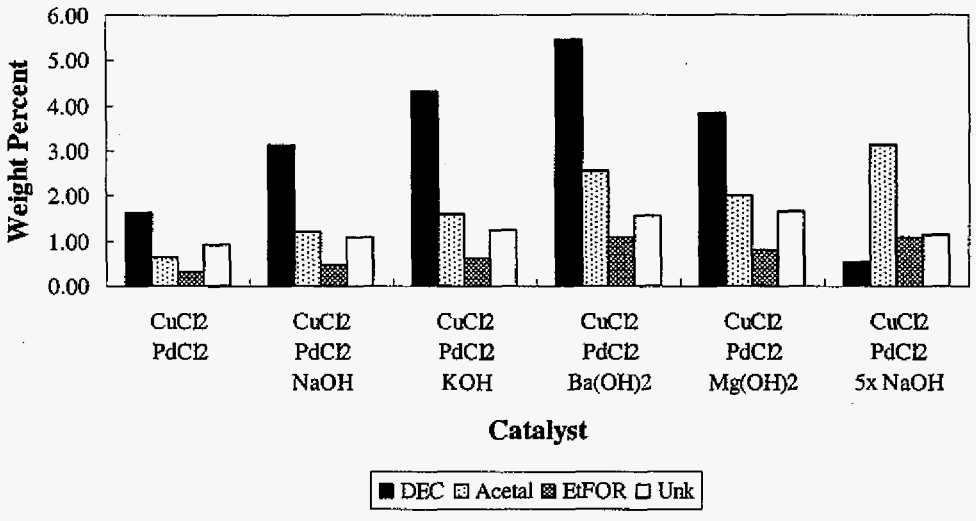

Figure 2. Comparison of product yields at 170 °C and two hours for catalysts pretreated with various metal hydroxides. Note the marked change in the magnitude of the vertical axis from that shown in Fig. 1

In addition to improving product yields the hydroxide pretreatment of the catalyst speeds up the production of DEC. This point is clarified by the time profiles in Fig. 3.

The University of Utah research team has made major strides in two other areas that promise to have a major impact on future research: 1) A flow-through microreactor has been constructed that will address many questions such as the importance of thorough mixing of reactants in the DEC synthesis. It was designed particularly to yield samples of spent heterogeneous catalysts that will be examined by solid state C-13 NMR. 2) A test diesel engine has been acquired and prepared for testing the impact of oxygenated fuel additives on cetane

number and composition of engine exhaust.

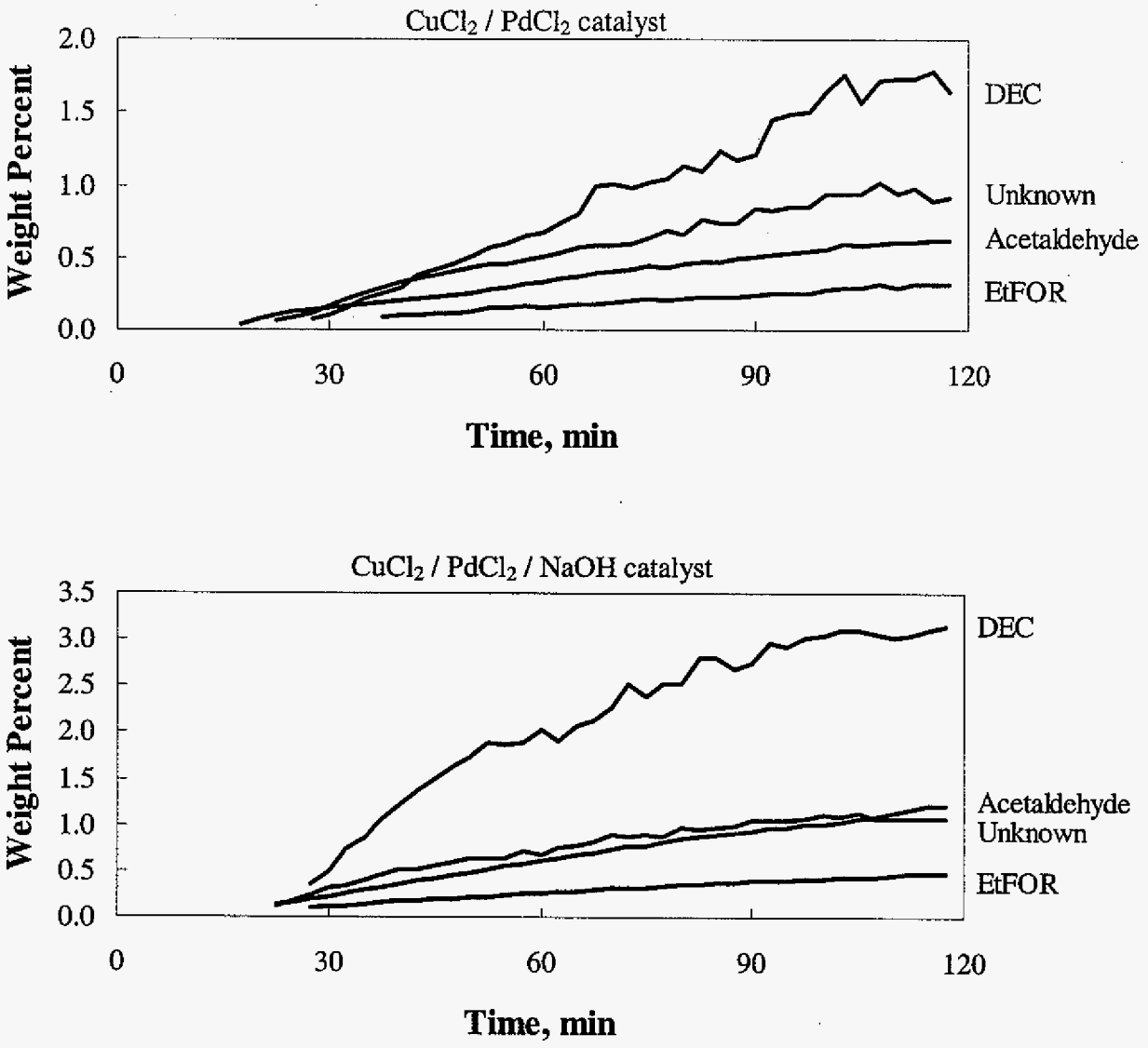

Figure 3. Typical time profiles of heterogeneous reaction showing that hydroxide speeds up the production of DEC.

Projections of Further Work

There are many challenging questions left which merit attention. Some can be resolved more readily than others. Questions are listed below in approximate order of increasing difficulty.

1) What is the oxidation number of the copper species that is catalyzing DEC production?

2) Can better mixing of reactants improve the yield of DEC?

3) Is copper(II) hydroxide the actual catalyst that dramatically enhances selectivity for DEC production?

4) Can an aerogel (a porous glass) provide a better support than activated carbon for the copper clusters that catalyze DEC production?

5) What objective comparisons can be made of cetane number and particulate emissions of oxygenated fuel additives in a diesel engine that will rate DEC against a plethora of other candidate fuel additives?

6) Does the mix of oxygenated products from the copper catalyzed DEC synthesis (from ethanol and CO) work as well in a diesel engine as pure DEC does?

7) Is it true as some have contended that the functional groups in the various potential oxygenated fuel additive molecules are irrelevant to their impact on diesel engine performance and only weight of oxygen in the fuel matters?

8) Over how long a time in a continuous flow reactor will a supported Cu/Pd catalyst continue to put out a reasonable yield of DEC?

9) What are the chemical species left behind on a spent catalyst?

Personnel

People who have participated in this team effort (listed in alphabetical order) are: Genshan Deng (grad. student), Dr. Brian C. Dunn (post-doc), Dr. Jacek Dworzanski (visiting prof.), Dr. Edward M. Eyring (co-P.I.), Catherine Guenneau (visiting teacher from France), Dan Hopkinson (undergrad.), Dr. Jian Zhi Hu (post-doc), Henk L. C. Meuzelaar (co-P.I.), Jorg Pahnke (visiting grad. student from Germany), Dr. Ronald J. Pugmire (co-P.I.), and Dr. Sidney Thornton (post-doc).

References

1. B.C. Dunn, J. Pahnke, D. Hopkinson, E. M. Eyring, G. Deng, J. Dworzanski, H. L. C. Meuzelaar, R. J. Pugmire, "Direct Observation of the Catalytic Production of Dimethyl Carbonate Using On-Line GC/MS," Prepr. Pap. - Am. Chem. Soc., Div. Fuel Chem. 45 (2), 283-287 (2000).

Higher Alcohol Synthesis
A Progress Report

Edwin L. Kugler , Dady B. Dadyburjor, Lawrence Norcio and Abhay Pathania
West Virginia University
Department of Chemical Engineering
Morgantown, WV 26505

Introduction

Additives are important for the performance of fuels. Octane enhancers like tetraethyl lead, MTBE (methyl tertiary-butyl ether), and some aromatic compounds like benzene and toluene are very well known. However these enhancers are being phased out. Alcohols are also octane enhancers, are naturally occurring, and do not appear to cause any environmental problems.

Over the past decade, the synthesis of mixed alcohols has drawn considerable interest due to the increasing demand for octane boosters. Ethanol and methanol have been used as gasoline additives. Higher alcohols now are preferred to methanol because of their lower volatility and higher solubility in hydrocarbons. Alcohols with proper boiling range may be used as diesel fuel additives. These higher boiling alcohols are expected to have positive effects both on increasing cetane index and on reducing particulate emissions.

Mixed alcohols can be produced from synthesis gas using molybdenum, copper and tungsten catalysts. By improving the catalyst and the process, it is possible to increase the selectivity towards higher alcohols .

Objective

The objective of this research is the production of higher alcohols using synthesis gas. This project addresses working with and improving molybdenum and tungsten catalysts, which are known to be active for higher alcohol synthesis. The effects of co-feeding methanol with synthesis gas will also be explored.

Work completed

The work on the project started in January 2000 after the arrival of a new Ph.D. student. The major part of the work to date involved making the alcohol production equipment (Figure 1) fully functional. The mass flow meters for measuring gas flow rates were reconditioned and recalibrated. The gas chromatograph was repaired by installing a new TC detector unit. Equipment shakedown is in progress.

Future work

In the near future we are planning to test equipment by repeating a few sets of experiments using molybdenum-based catalyst prepared in our laboratory previously. Product analysis and material balance determination will be emphasized. Longer-term research will be focused on improving molybdenum and tungsten catalysts, which are known to be active for higher alcohol synthesis.

ACTIVATED C SUPPORT
INCIPIENT WETNESS Mo $(NH_4)_6 Mo_7O_{24} \cdot 4H_2O$ DECOMP 500°C
Ni $Ni(NO_3)_2 \cdot 6H_2O$ 500°C
K KNO_3 300°C

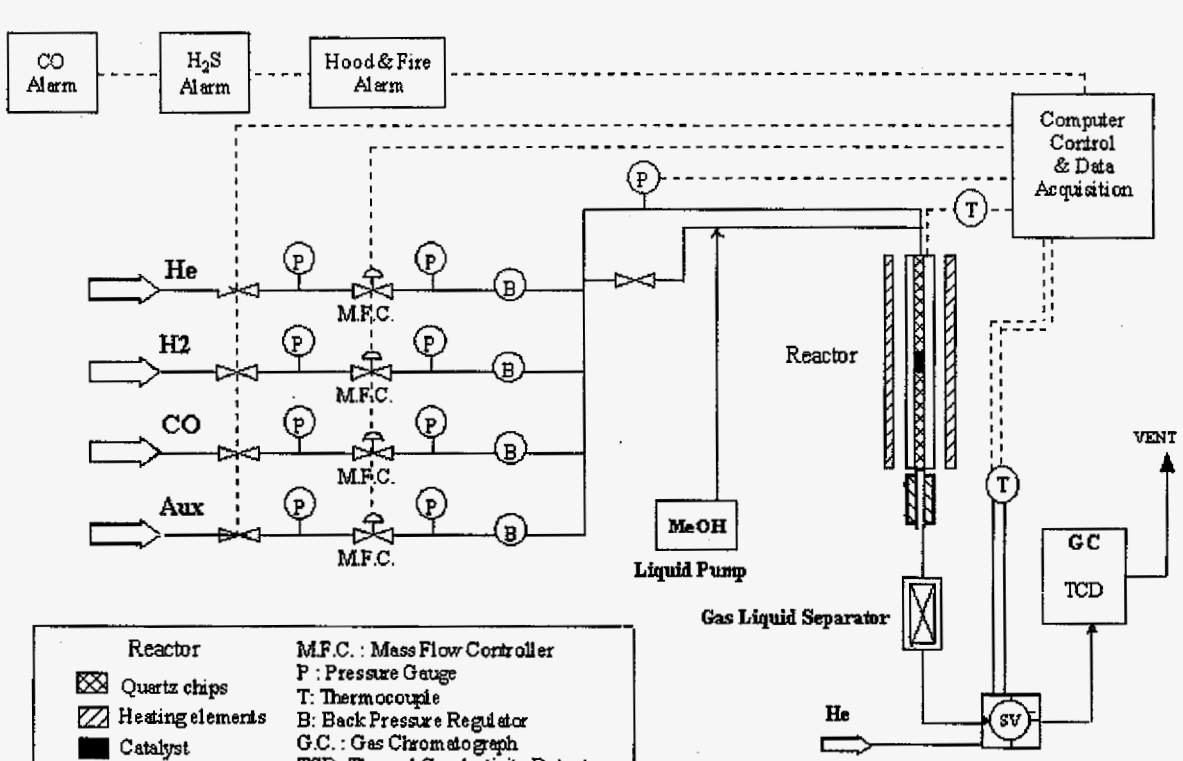

Figure 1: Experimental Setup for Higher Alcohol Synthesis

Conversion of Synthesis Gas to Higher Ethers and Other Oxygenates

Christine W. Curtis
Christopher B. Roberts
Jeff Snelling*
Chemical Engineering Department
*Civil Engineering Department
Auburn University

Synthesis of Higher Ethers from Syngas using a Single-Step Liquid Phase Process

The objective of this research is to develop improved transportation fuels by producing higher ethers and oxygenates for use as additives and blending agents in reformulated gasolines and ultra clean diesel fuels. The addition of oxygenates to gasoline and diesel fuels raises combustion temperatures, improves engine efficiencies, and causes the fuel to burn more cleanly, resulting in lower levels of carbon monoxide and unburned hydrocarbons in the exhaust stream. Ethers are the favored oxygen-containing additives for reformulated gasoline since they have high octane numbers and burn cleanly. Using higher ethers as fuel additives would help achieve the goal of adding oxygenates with lower vapor pressures and lower water solubilities to the fuels while simultaneously increasing the energy density of the added oxygenate.

Single-Step Liquid Phase Process

The focus of this research is to develop a single-step, liquid phase process to produce higher ethers from synthesis gas. The conventional method of producing ethers is first to produce methanol from synthesis gas and then to convert the methanol to an ether. For example, this process is typically used to produce dimethyl ether (DME) from methanol by either a gas or a liquid phase reaction (Snamprogetti; Peng et al., 1998; Sofianos and Scurrell, 1991; Espino and Pletzke, 1973). The conversion of syngas to methanol can be increased by removing, either chemically or physically, the alcohol as it is formed, because this removal lowers the thermodynamic constraints and promotes syngas conversion (Wender, 1996). A single-step, liquid phase DME synthesis reaction has been developed that converts DME directly from

synthesis gas using a bifunctional catalyst that promotes methanol synthesis and methanol dehydration for forming DME (Lewnard et al., 1990). Performing this single-step reaction in a liquid phase environment offers the advantage of heat dissipation, thereby allowing a lower reaction temperature to be maintained. The liquid phase reaction results in less catalyst deactivation and longer catalyst lifetime (Brown et al., 1991)

The objective of this research is to develop a catalytic reaction system to produce higher ethers from synthesis gas and olefins using a single-step liquid phase reaction. In this system, as methanol is produced from syngas, the methanol would react with olefins to produce higher ethers. Diethers could also be synthesized from diolefins. One study (Kazi et al., 1995) has been found that has etherified methanol in a single step reaction for the synthesis of higher ethers. A dual catalyst bed was used with Pd/SiO_2 as the methanol synthesis catalyst and a zeolite as an etherification catalyst. The yield of ether from this reaction, which was operated at 175 °C and 7 atm, was very low. This result was most likely caused by the choice of catalyst. Not only is Pd/SiO_2 a methanol synthesis catalyst but it also serves as an effective hydrogenation catalyst for the added olefin, in this case isobutylene. The work that is currently underway will use a CuO/ZnO on alumina methanol synthesis catalyst and dry Amberlyst 15 as the etherification catalyst at reaction temperatures ranging from 60 to100 ° C.

Current Work: Proof of Concept

A comprehensive literature study has been performed to determine the current state of the literature for the single-step synthesis reactions of high ethers from the reaction of syngas and olefins. The patent literature concerning DME formation and the production of higher ethers and the article by Kazi et al. (1995) indicate the feasibility of developing the process. For the initial studies, the study was divided into two parts: the first part was an analysis of the ether production from the reaction of C_6 and C_8 olefins with alcohols which is described in this report; and the second part is single step process where both methanol and ether synthesis reactions are performed simultaneously. The work described herein evaluated the degree of reactivity of C_6 and C_8 olefins with methanol and the selectivity for production of higher ethers. The initial parametric conditions were selected on the basis of the conditions expected to be encountered from the methanol synthesis reaction.

Experimental

A series of four reactions were performed to determine the efficacy of ether production from the reactions of olefins with methanol. Those reactions were thermal with olefin only; thermal with olefin and methanol; catalytic with olefin only; and catalytic with olefin and methanol. The first three sets of reactions were conducted to establish baseline reactivity of the system without methanol. The reactions were performed using a 25-cm^3 stainless steel tubular reactor, which was immersed and agitated at 100 cpm in a temperature controlled sand bath. The reactions were performed at temperatures of 60 to 150 °C and reaction times from 15 min to 24 hr using a pressure of 200 psig H_2. One experiment was performed at an elevated pressure of 800 psig H_2.

Materials. The olefins used in this study were straight-chain α-olefins, 1-hexene, 1-heptene, and 1-octene, and the branched olefins, 2,3-dimethyl-1-butene, 2,3-dimethyl-2-butene, 2,4,4-trimethyl-1-pentene, and 2,4,4-trimethyl-2-pentene. The reactions with the α-olefins were conducted at higher temperatures of 100 to 150 °C while the reactions with the branched olefins were conducted at temperatures ranging from 60 to 100 °C with most of the experiments being conducted at 70 °C. Reactions were initially performed at a 2:1 ratio of olefin to methanol and then the ratio was changed to a 1:8 ratio of olefin to methanol so that an excess of methanol would be present in the reactor. All of the olefins were obtained from Sigma Aldrich Chemical Co. Methanol was obtained from Fisher Scientific Co.

The catalyst used in the reactions was dry Amberlyst 15 and was charged to the reactor at 10 weight percent of the total charge. Catalyst studies were conducted in which the dry Amberlyst 15 catalyst was compared to wet Amberlyst and to crushed and extrudate HZSM-5. Only the dry Amberlyst showed any reactivity and, hence, was used for the rest of the experiments. Both dry and wet Amberlyst 15 were obtained from Sigma-Aldrich Chemical Co. and the HZSM-5 was obtained from United Catalysts, Inc. Additional reactions using 2,3-dimethyl-1-butene and 2,4,4-trimethyl-1-pentene were performed in which the amount of dry Amberlyst 15 was doubled to 20 weight percent and tripled to 30 weight percent of the total charge; the Amberlyst was also crushed and charged at 10 weight percent.

Analysis. Reaction products were analyzed by gas chromatography using a Varian model 3400 equipped with J&W Scientific DB-5 25m x 0.32mm I.D. with 0.52 μ thickness. The injector was maintained at 200 °C and flame ionization detector was maintained at 210 °C. The initial column temperature was 50 °C and was kept at that temperature. The internal standard used was isooctane. Response factors were obtained for all available reactants and products. Response factors for those products, which were not commercially available, were estimated by obtaining the response factors from structurally similar available compounds.

Results

Straight Chain Olefins. For the produced ethers to be acceptable additives in diesel fuel, the ethers must have sufficient carbon chain length to boil in the range of diesel fuel in order to maintain an acceptable boiling point range. From an environmental perspective, the ethers should have low water solubility and low vapor pressure. The ethers selected to be produced were in the C_7 to C_{10} range.

The initial experimental work focused on determining the reactivity and selectivity of straight-chain olefins when reacted with methanol using dry Amberlyst 15 catalyst. The reaction sets performed were thermal reaction conditions with olefin only, catalytic reaction with olefin only, and thermal and catalytic reactions with olefins and methanol. The reactions using 1-hexene, 1- heptene, and 1-octene, performed at 100 and 150 °C, showed no reactivity under thermal with or without methanol as shown in Table 1a and 1b. Rearrangement of the olefins was observed in the presence of a catalyst regardless of whether methanol was present. While in the presence of methanol, a small amount of higher boiling material was an observed product.

Branched Olefins. The next phase of the experimental work involved reactions of branched C_6 and C_8 olefins, 2,3-dimethyl-1-butene and 2, 4, 4-timethyl-1-pentene, with methanol using 10 weight percent dry Amberlyst. Baseline reactions of the two branched olefins were performed at 80 °C to determine the amount of rearrangement that occurred under thermal and catalytic conditions with the 1- and 2-pentene isomers of 2, 4, 4-timethylpentene and 1-and 2-butene isomers of 2,3-dimethylbutene. In the catalytic reaction, 1-pentene rearranged forming 22% 2-pentene while 2-pentene rearranged yielding 80% 1-pentene. After reacting for 2 hr, the product distributions from both isomers were similar. Similar results were obtained from the C_6

olefin. After 2 hr catalytic reaction regardless of the initial isomer, the reaction composition was similar yielding ~ 90% 2,3-dimethyl-2-butene. When the 2-pentene isomer was reacted in the presence of methanol, 3 mole percent of the ether, 2-methoxy-trimethylpentane was formed while the 1-pentene isomer yielded 7.3 mole percent. Similarly, the reaction with 2-butene yielded 11 mole percent 2-methoxy-2, 3-dimethylbutane while the 1-butene isomer yielded 27 mole percent. In both cases the reaction of the 1-olefin isomer with methanol was favored. Hence, once the 2-butene or 2-pentene isomer was formed, the reaction proceeded very slowly yielding much less ether than the 1-butene or 1-pentene in an equivalent amount of time.

The effect of reaction temperature and time on the production of ether from 2, 4, 4-timethyl-1-pentene and 2,3-dimethyl-1-butene was evaluated. The production of ether, 2-methoxy-2, 4, 4-trimethylpentane, from 2, 4, 4-timethyl-1-pentene in reactions performed at 70, 80, and 100 °C is shown in Table 3. The reactions performed at 70 °C from 1 to 24 hrs showed an increase in ether production from 2.5 to 9.0 mole percent. The reactions performed at 80 °C and 100 °C produced similar amounts of ether as the 70 °C reaction at shorter reaction times. The amount of rearrangement of the 1-pentene isomer to the 2-pentene isomer increased with both temperature and reaction time, which in effect reduced the amount of ether formed since the 2-pentene isomer is less reactive than the 1-pentene. Ether production from 2,3-dimethyl-1-butene after 2 hr reactions at 60, 70, 80, and 100 °C showed little effect of temperature between 70 and 100 °C, with all reactions yielding ~27 to 30 mole percent ether (Table 4). However a substantial increase in ether production from 16.5 to 27 mole percent was observed between 60 and 70 °C. The effect of longer reaction times of 4, 6, 8, and 24 hr was minimal on ether production, which ranged from 27 to 36.5 mole percent. In all of these reactions the amount of rearrangement to the 2,3-dmiethyl-2-butene was substantial yielding nearly 60% of 2-butene isomer after 6 hr as presented in Table 5.

Since this experiment is the second part of single step reaction process, the reaction conditions were initially chosen to simulate as closely as possible the conditions expected to be present in the synthesis of methanol from synthesis gas. The reactions discussed heretofore used a 2:1 olefin to methanol ratio, which was selected because the methanol would most likely be reacted as soon as it is formed. The amount of ether produced was less than 30%. Several parametric factors may have affected the conversion of the olefin to ether. The parameters tested

were the effect of olefin to methanol ratio, of reaction pressure, and of increased catalyst loading. Table 6 shows the effect of changing the olefin to methanol ratio from 2:1 to 1:8 for 2 hr reactions of 2,3-dimethyl-1-butene and 1 and 2 hr reactions of 2,4,4-trimethyl-1-pentene. In the 1-butene reaction at a 1:8 ratio an additional product was formed and is currently being analyzed. The amount of ether formed in the 1:8 was nearly double that obtained in the reaction with 2:1 ratio. In the 1-pentene reaction, the increased ratio had the effect of more than tripling the ether formation, indicating that the reaction had been starved for the methanol reactant. Increasing the pressure from 200 to 800 psig in the reactor that contained a 1:8 ratio of olefin to methanol which was reacted for 2 hr did not affect the amount of ether that was produced as shown in Table 7.

The effect of the catalyst loading on the conversion of 2,3-dimethyl-1-butene and 2,4,4-trimethyl-1-pentene is given in Table 8. The crushed and single loading were both at 10 weight percent of total reactor charge while the double loading was 20 weight percent and the triple was 30 weight percent of total loading. The catalyst loading affected both olefins; however, the 1-butene was affected more than the 1-pentene. The crushed, double and triple loading of catalyst all increased ether production compared to the single loading. The ether production ranges from 48 weight percent for the single loading to 64 weight percent for triple loading. Both the double and triple loading of catalyst increased the ether production from 2,4,4-trimethyl-1-pentene. The increase was not as dramatic as for the C_6 olefin. Therefore, increased ether production was obtained by increasing the amount of methanol available for the reaction and by increasing the number of active catalyst sites available to the olefins for the reaction.

Conclusions and Future Work

The feasibility of producing higher ethers from C_6 and C_8 olefins has been demonstrated at temperatures below 80 °C. Increasing the number of catalyst sites and the amount of methanol available for the reaction raised the ether production to reasonable levels. The branched olefins have a greater reactivity than the straight chain olefins and are better candidates for producing higher ethers as diesel fuel additives. The ethers can be produced at reaction conditions that are favored for the single step reaction of higher ethers from synthesis gas. The next step in the experimentation is to determine the effect of reacting mixtures of olefins and alcohols on the

types and quantity of products produced. Reactions will be performed in the liquid phase using an inert solvent like decalin to dissipate the heat and promote mass transfer.

Liquid phase reaction in which methanol synthesized from synthesis gas is immediately reacted with branched olefins to form higher ethers will be performed in a continuous reactor. A continuous reactor will be built that is similar in design to the super critical continuous reactor described in the next section. Appropriate modifications will be made to outfit the reactor for the reactant feeds, reaction conditions and separation requirements of the single step, liquid phase synthesis of higher ethers from synthesis gas.

References

Wender, Irving, "Reactions of Synthesis Gas", *Fuel Processing Technology,* **1996**, 48(3), 216-218.

Snamprogetti, SpA, German Patent DE 2 362 944.

Peng, Xiang-Dong; Parris, Gene E.; Toseland, Bernard A.; Battavio, Paula J.; "Use of aluminum phosphate as the dehydration catalyst in single step dimethyl ether synthesis", United States Patent US 5,753,716 to Air Products and Chemicals, Allentown, PA, May 19, 1998.

Sofianos, A. C.; Scurrell, M.S. "Conversion of Synthesis Gas to Dimethyl Ether over Bifunctional Catalytic Systems" *Ind. Eng. Chem. Res.* **1991**, 30(11), 2372-2383.

Espino, Ramon L.; Pletzke, Thomas S.; "Methanol Production", United States Patent US 3,888,896, assigned to ChemSystems, Inc., New York, NY, May 29, 1973.

Brown, D.M.; Bhatt, B.L.; Hsiung, T.H.; Lewnard, J.J.; Waller, F.J. "Novel Technology for the Synthesis of Dimethyl Ether from Syngas" *Catalysis Today,* **1991**, 8, 279-304.

Lewnard, J.J.; Hsiung, T.H.; White, J.F.; Brown, D.M. "Single-Step Synthesis of Dimethyl Ether in a Slurry Reactor" *Chemical Engineering Science*, **1990**, 45(8), 2735-2741.

Kazi, A.M.; Goodwin, J.G., Jr.; Marcelin, G.; Oukaci, R. "Synthesis of MTBE during CO Hydrogenation: Reaction Sites Required" *Ind. Eng. Chem. Res.* **1995,** *34,* 718-721.

Table 1a. Thermal and Catalytic Reactions of α-Olefins and Methanol

Reaction time = 2 hours
Pressure: 200 psig H_2
Catalyst: 10 wt%

Reactant	Catalyst	Temperature	Products
Methanol	Amberlyst 15 dry	150 °C	no reaction
1-hexene	none	150 °C	no reaction
1-heptene	none	150 °C	no reaction
1-octene	none	150 °C	no reaction
1-hexene	Amberlyst 15 dry	100 °C	rearrangement
1-heptene	Amberlyst 15 dry	150 °C	rearrangement
1-octene	Amberlyst 15 dry	150 °C	rearrangement

Table 1b. Thermal and Catalytic Reactions of α-Olefins with Methanol

Reaction time: 2 hours
Molar ratio of α-olefin to methanol: 2:1
Pressure: 200 psig H_2
Catalyst: 10 wt%

Reactant	Catalyst	Temperature	Products
1-hexene : methanol	none	100 °C	no reaction
1-heptene : methanol	none	150 °C	no reaction
1-octene : methanol	none	150 °C	no reaction
1-hexene : methanol	Amberlyst 15 dry	100 °C	no reaction
1-heptene : methanol	Amberlyst 15 dry	100 °C	no reaction
1-heptene : methanol	Amberlyst 15 dry	150 °C	rearrangement and 7% of a higher boiling product
1-octene : methanol	Amberlyst 15 dry	150 °C	rearrangement and ~3% high boiling products

Table 2. Thermal and Catalytic Reactions of Branched Olefins

Reaction time: 2 hours
Pressure: 200 psig H_2
Catalyst: 10wt% Amberlyst 15 dry
Temperature: 80 EC; ** 70 EC
Molar ratio of olefin to methanol: 2:1

	Mole Percent of Products (%)			
Reactions of C_8 and C_6 Olefins	**Thermal without Methanol**	**Catalytic without Methanol**	**Thermal with Methanol**	**Catalytic with Methanol**
Starting Material: 2,4,4-trimethyl-1-pentene				
2,4,4-trimethyl-1-pentene	**98**	**78**	**98.4**	**85**
2,4,4-trimethyl-2-pentene	**2.0**	**22**	**0.01**	**8.0**
2-methoxy-2,4,4-trimethylpentane				**7.3**
Starting Material: 2,4,4-trimethyl-2-pentene				
2,4,4-trimethyl-1-pentene	**aborted**	**80**	**0.3**	**5.1****
2,4,4-trimethyl-2-pentene		**20**	**99.2**	**92**
2-methoxy-2,4,4-trimethylpentane				**3.0**
Starting Material: 2,3-dimethyl-1-butene				
2,3-dimethyl-1-butene	**82**	**9.1**	**99.8**	**8.5**
2,3-dimethyl-2-butene	**17**	**89**	**0.06**	**63**
2-hydroxy-2,3-dimethylbutane				**1.5**
2-methoxy-2,3-dimethylbutane				**27**
Starting Material: 2,3-dimethyl-2-butene				
2,3-dimethyl-1-butene	**<1**	**6.0**	**0.01**	**3.1****
2,3-dimethyl-2-butene	**98**	**92**	**97.8**	**84**
2-hydroxy-2,3-dimethylbutane				**2.6**
2-methoxy-2,3-dimethylbutane				**11**

Table 3. Effect of Reaction Time on Reactions of 2,4,4-Trimethyl-1-pentene with Methanol at 70, 80, and 100 °C

Molar ratio of 2,4,4-trimethyl-1-pentene to methanol: 2:1
Pressure: 200 psig H_2
Catalyst: 10 wt% Amberlyst 15 dry

Reaction at 70 °C	Mole Percent of Products at Different Reaction Times				
Reaction Time (hours)	1	2	4	8	24
2,4,4-trimethyl-1-pentene	96	92	87	82	70
2,4,4-trimethyl-2-pentene	2.2	3.4	5.4	9.2	20
2-methoxy-2,4,4-trimethylpentane	2.5	5.1	7.5	9.0	9.6

Reaction at 80 °C	Mole Percent of Products at Different Reaction Times				
Reaction Time (hours)	0.25	0.5	1	2	4
2,4,4-trimethyl-1-pentene	93	91	84	85	77
2,4,4-trimethyl-2-pentene	3.3	4.3	8.5	8.0	16
2-methoxy-2,4,4-trimethylpentane	3.8	5.0	7.8	7.3	7.6

Reaction at 100 °C	Mole Percent of Products at Different Reaction Times			
Reaction Time (hours)	0.25	0.5	1	2
2,4,4-trimethyl-1-pentene	80	76	76	75
2,4,4-trimethyl-2-pentene	14	18	18	15
2-methoxy-2,4,4-trimethylpentane	5.4	5.6	6.2	5.1

Table 4. Effect of Temperature on the Reaction of 2,3-Dimethyl-1-butene with Methanol

Molar ratio of 2,3-dimethyl-1-butene to methanol: 2:1
Pressure: 200 psig H_2
Catalyst: 10 wt% Amberlyst 15 dry
Reaction time: 2 hours

	Mole Percent of Products for Reactions at Different Temperatures			
Temperatures (°C)	60 °C	70 °C	80 °C	100 °C
2,3-dimethyl-1-butene	60.5	14.2	8.5	6.8
2,3-dimethyl-2-butene	18.5	53	63	61
2-hydroxy-2,3-dimethylbutane	4.3	1.2	<1	2.4
2-methoxy-2,3-dimethylbutane	16.5	32	27	30

Table 5. Effect of Reaction Time on Reactions of 2,3-Dimethyl-1-butene with Methanol at 70 °C
Molar ratio of 2,3-dimethyl-1-butene to methanol: 2:1
Pressure: 200 psig H_2
Catalyst: 10 wt% Amberlyst 15 dry
Temperature: 70 °C

	Mole Percent (%) of Products for Reactions at Different Reaction Times				
Reaction Time (hours)	2	4	6	8	24
2,3-dimethyl-1-butene	14.2	6.4	6.3	4.9	6.8
2,3-dimethyl-2-butene	53	57.5	59.5	57.5	59
2-hydroxy-2,3-dimethylbutane	1.2	1.3	0.8	0.87	4.5
2-methoxy-2,3-dimethylbutane	32	34	33.5	36.5	29.5

Table 6. Effect of Olefin to Methanol Ratio at 70 °C on Ether Production from 2,3-Dimethyl-1-butene and 2,4,4-Trimethyl-1-pentene
Pressure: 200 psig H_2
Catalyst: 10 wt % Amberlyst 15 dry

Reaction at 70 °C	Mole Percent of Products at Different Times and Ratios			
Reaction Time	1 hour		2 hour	
olefin to methanol molar ratio	2:1	1:8	2:1	1:8
2,3-dimethyl-1-butene reaction				
2,3-dimethyl-1-butene			14.2	5.2
2,3-dimethyl-2-butene			53	31.5
unknown				11
2-hydroxy-2,3-dimethylbutane			1.2	3.5
2-methoxy-2,3-dimethylbutane			32	48.5
2,4,4-trimethyl-1-pentene reaction				
2,4,4-trimethyl-1-pentene	96	82	92	73
2,4,4-trimethyl-2-pentene	2.2	5.3	3.4	9.2
2-methoxy-2,4,4-trimethylpentane	2.5	13	5.1	18

Table 7. Effect of Pressure on Ether Production from 2,3-Dimethyl-1-butene

Catalyst: 10 wt % Amberlyst 15 dry
Temperature: 70 °C
Reaction Time: 2 hour
Ratio: 1:8 ether to methanol ratio

Reaction at 70 °C	Mole Percent of Products at Different Pressures	
Pressure	200 psig	800 psig
2,3-dimethyl-1-butene	4.9	7.2
2,3-dimethyl-2-butene	59	59
2-hydroxy-2,3-dimethylbutane	0.4	1.2
2-methoxy-2,3-dimethylbutane	35	33

Table 8. Effect of Catalyst Loading on Reactions of C_6 and C_8 Olefins with Methanol at 70 °C

Molar ratio of olefin to methanol: 1:8
Pressure: 200 psig H_2
Temperature: 70 °C
Reaction Time: 2 hours
Catalyst: Amberlyst 15 dry; 10wt% for crushed and single; 20 wt% for double; and 30wt% for triple

Products	Mole Percent of Products for Reactions with Different Catalyst Loading (%)			
	Crushed	Single	Double	Triple
Reaction of C_6 Olefin with Methanol				
2,3-dimethyl-1-butene	2.4	5.2	2.0	1.0
2,3-dimethyl-2-butene	24	31.5	26	26
unknown	22	11	11.5	2.9
2-hydroxy-2,3-dimethylbutane	2.5	3.5	2.3	5.6
2-methoxy-2,3-dimethylbutane	54	48.5	58.5	64
Reaction of C_8 Olefin with Methanol				
2,4,4-trimethyl-1-pentene	66	73	58	58
2,4,4-trimethyl-2-pentene	7.9	9.2	13	15
Unknown	10.2	0.6	7.6	6.2
2-methoxy-2,4,4-trimethylpentane	16	17	22	21

Hydroisomerization of Normal Hexadecane with Platinum-promoted Tungstate-modified Zirconia Catalysts

Irving Wender, John W. Tierney and Gerald D. Holder
Department of Chemical and Petroleum Engineering, 1249 Benedum Hall, University of Pittsburgh, Pittsburgh, PA 15261

The acid-catalyzed isomerization of alkanes is of growing importance in determining the nature of transportation fuels, including environmentally clean high octane gasoline, high cetane diesel fuel, low pour point jet fuel and lubricant base stocks. However, isomerization of long-chain alkanes generally precedes cracking, leading to extensive undesired cracking reactions; this tends to limit catalytic paraffin isomerization to C_4-C_6 alkanes. It is highly desirable to obtain environmentally clean catalysts that can be used to isomerize long-chain paraffins with minimum cracking. Catalysts with a certain optimal balance of metal and acid functions at suitable reaction conditions are needed to suppress cracking in order to achieve high isomerization selectivity for long-chain paraffins.

Work during the past year examined the activity, selectivity and long-term stability of platinum-promoted tungstate-modified zirconia ($Pt/WO_3/ZrO_2$) catalysts for the hydroisomerization of long-chain linear alkanes under relatively mild conditions, using n-hexadecane (C_{16}) as a model compound. A continuous trickle-bed reactor was used to compare the activities and selectivities of three $Pt/WO_3/ZrO_2$ catalysts prepared by different methods and to investigate the effects of tungsten loading and of reaction conditions for hydroisomerization of n-hexadecane. A run of 93.5 h was conducted using the most highly active $Pt/WO_3/ZrO_2$ catalyst which contained 0.5 wt% of well-dispersed Pt and 6.5 wt% of W. Reaction conditions were manipulated and five shutdown (feed stopped, reactor temperature lowered but H_2 flow rate maintained) and restart operations were carried out (Figure 1). This catalyst showed high activity and stability. Considerable success was also achieved in converting n-hexadecane to isohexadecanes for 100 h at temperatures of about 220°C and under H_2 pressure as low as 160 psig (Figure 2). Best results (highest iso-C_{16} yield) were 79.1 wt% n-C_{16} conversion, 89.9 wt % iso-C_{16} selectivity and 71.1 wt% iso-C_{16} yield at 218°C, 160 psig H_2, H_2/n-C_{16} mole ratio = 2 and WHSV=1 h^{-1}. A typical spectrum of hexadecane isomers obtained is show in Figure 3.

The $Pt/WO_3/ZrO_2$ catalyst is rugged and has properties which allow one to propose that it has considerable likelihood of attaining commercial uses.

Research has now shifted to the hydroisomerization and hydrocracking of longer paraffinic chains; C_{24}, C_{28} and C_{32}, as well as to the conversion of Fischer-Tropsch waxes to high cetane diesel and jet fuels.

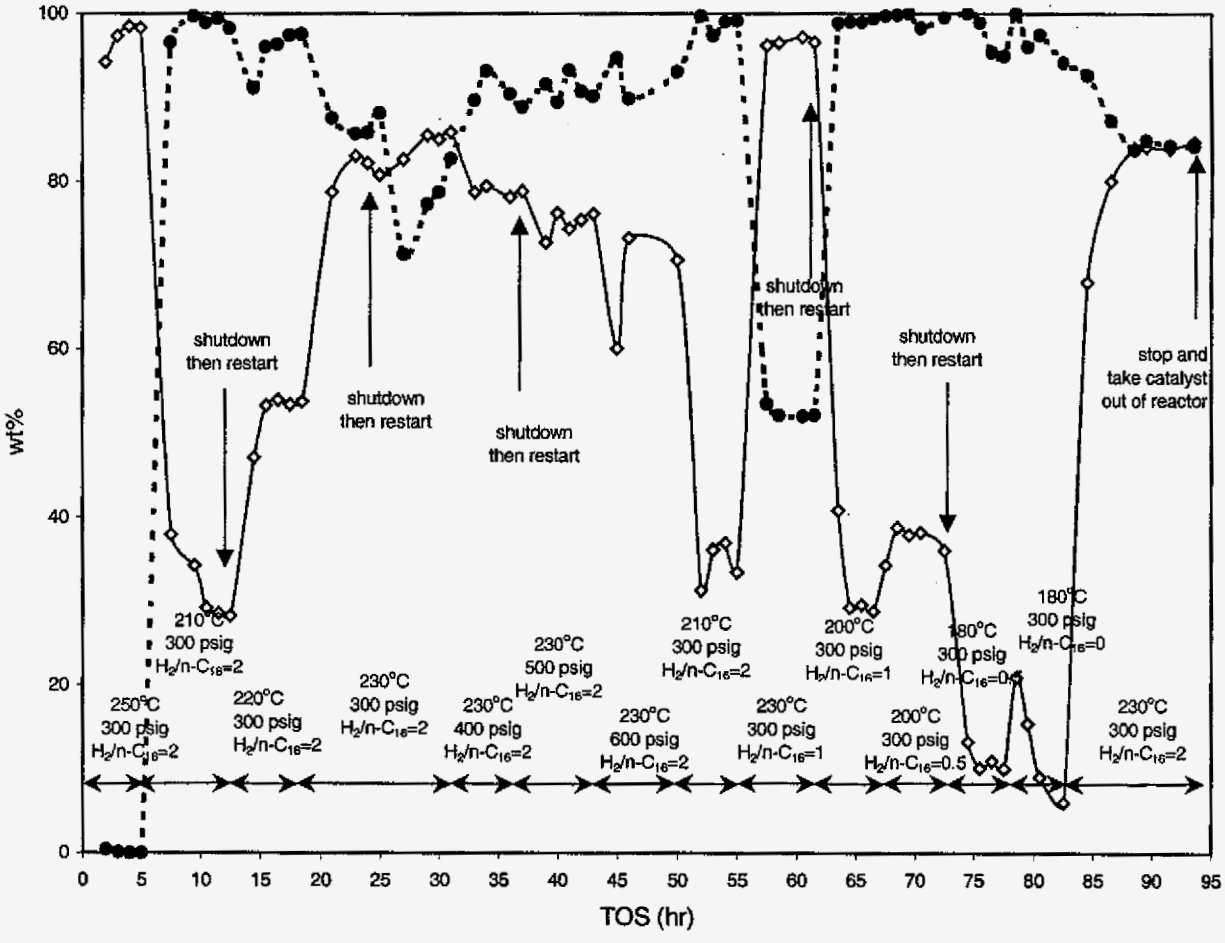

Figure 1. Effect of changes in temperature, pressure and H_2/nC_{16} on hexadecane conversion (solid line) and selectivity (dashed line).

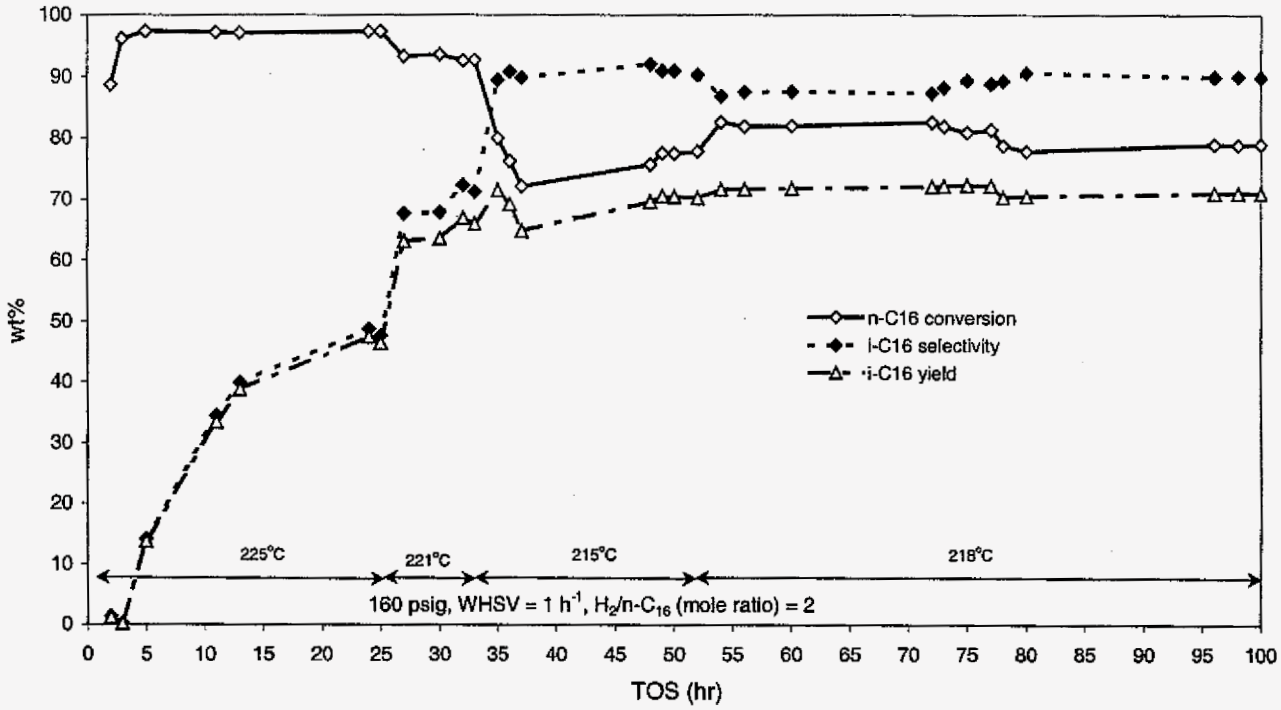

Figure 2. Effect of calcination and reactor shutdown on hydroisomerization of hexadecane.

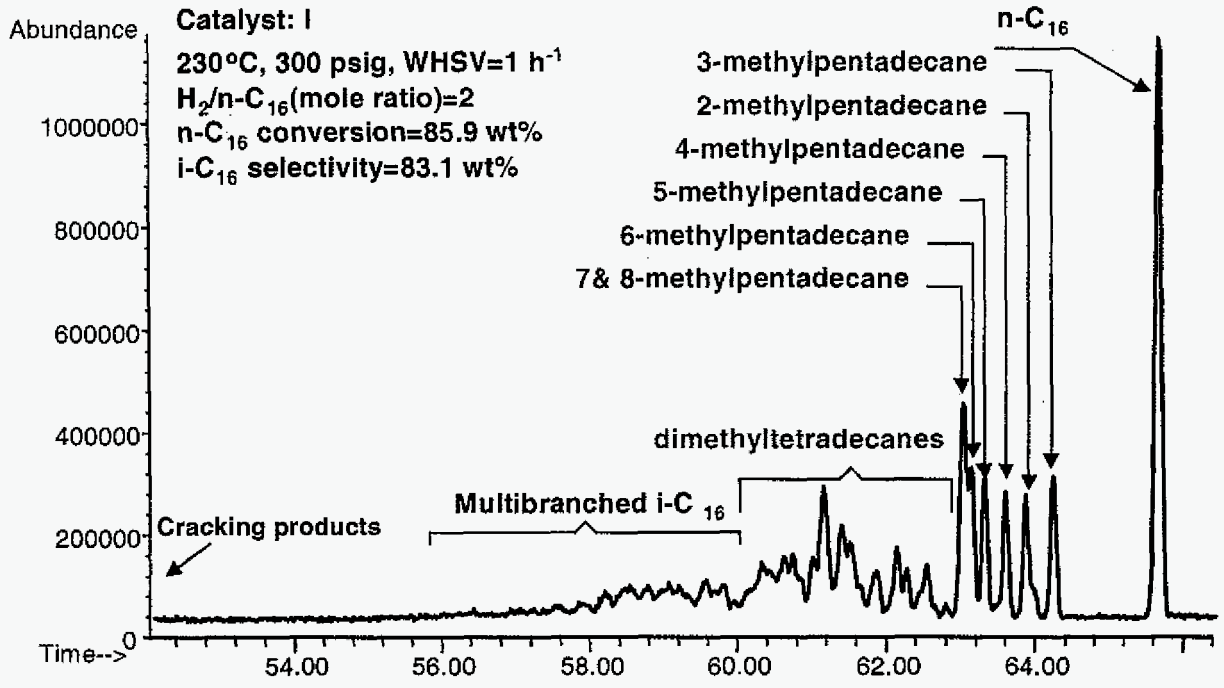

Figure 3. Typical GC-MS spectrum of hexadecane isomers in the products of n-C_{16} hydroisomerization.

Supercritical Fluids as an Alternative Reaction Medium for Fischer-Tropsch Synthesis

Christopher B. Roberts, Christine W. Curtis, and Xiwen Huang
Department of Chemical Engineering, Auburn University, Alabama, 36849

Introduction

The Fischer-Tropsch (F-T) synthesis reaction conducted in the solid-catalyzed gas-phase reaction system is inevitably accompanied by local overheating of the catalyst surface as well as by production of heavy wax, which may lead to the deactivation of catalyst and also the increase of methane selectivity. The slurry phase F-T reaction process, in which the slurry is composed of fine powdery catalyst and mineral oil, is used as an alternative reaction medium and has been developed to overcome defects of the gas-phase process[1]. However, the diffusion of syngas into the micropores of the catalysis is slow in the slurry phase such that the overall rate is markedly lower than that in the gas-phase reaction[2]. Further more, the concentration of solid catalyst particles in the slurry medium must be limited to low levels in order to maintain slurry fluidity. Other disadvantages of slurry reactors are the accumulation of high molecular weight products and the in situ separation of fine catalyst particles from the heavy products. These considerations have driven research on F-T synthesis to the application of supercritical conditions, which combines the desirable properties of gaslike diffusivity and liquidlike solubility.

It is well known that a supercritical fluids have unique characteristics in their molecular diffusion and solubility parameters[3]. As a result, supercritical fluids possess properties that make them attractive media for chemical reactions. Conducting chemical reactions at supercritical conditions affords opportunities to manipulate the reaction environment by manipulating pressure to enhance the solubility of reactants and products, to eliminate interphase transport limitations on the reaction rates, and to integrate reaction and separation unit operations. For the application of supercritical FT synthesis, there are at least four distinct advantages[4-7]: (1) the in-situ extraction of heavy hydrocarbons from the catalyst surface and their transport out of the pores before they are transformed to consolidated coke, thereby extending catalyst lifetime; (2) the enhancement of the pore-transport of syngas to the catalyst surface thereby promoting desired reaction pathways; (3) the enhanced desorption of primary products preventing secondary reactions that adversely affect product selectivity; (4) and the elimination of interphases, which may exist in multicomponent systems under ordinary conditions which can result in significantly enhanced mass transfer under supercritical conditions.

Outcomes

An optimum operating condition for the F-T synthesis reaction is expected within the SCF solvent region. Comparison of the conversions and product selectivities in the SCF media will be made with those in traditional gas- and liquid-phase operation. The unique and adjustable properties of the SCF reaction medium will provide several advantages in the F-T synthesis of fuels and oxygenates including: (1) increased heat transfer from the catalyst surface, compared to gas phase F-T, leading to improved product selectivities, (2) enhanced mass transport into and out of the catalyst pores that will improve overall product yields and selectivities, (3) and enhanced desorption and in situ extraction of desired products which will improve catalyst lifetimes.

Current Status of the SCF Project

Recently, we have developed a continuous fixed-bed reactor system equipped with an on-line GC analysis system. This reactor will be used to perform continuous catalytic reaction studies of SCF-FT synthesis in both CO_2 and hydrocarbon solvents over a variety of solvent conditions, reaction feed compositions, flowrates and catalyst materials. The function checks and tests of the entire reaction system have been accomplished. In addition, a detailed and accurate on-line analysis strategy for the gas and liquid phase products has been developed, and the corresponding calculation methods of the syngas conversion, product selectivity and carbon number distribution have been created.

Schematic Diagram of the SCF Fischer-Tropsch Reaction and Analysis System

BPR: back pressure regulator; BV: ball valve; CT: cold trap; CV: check valve
MFC: mass flow controller; MMV: micrometering valve
HT: hot trap; PT pressure transducer; SM: static mixer
SV: solenoid valve; SH/RD: safety head/rupture disc

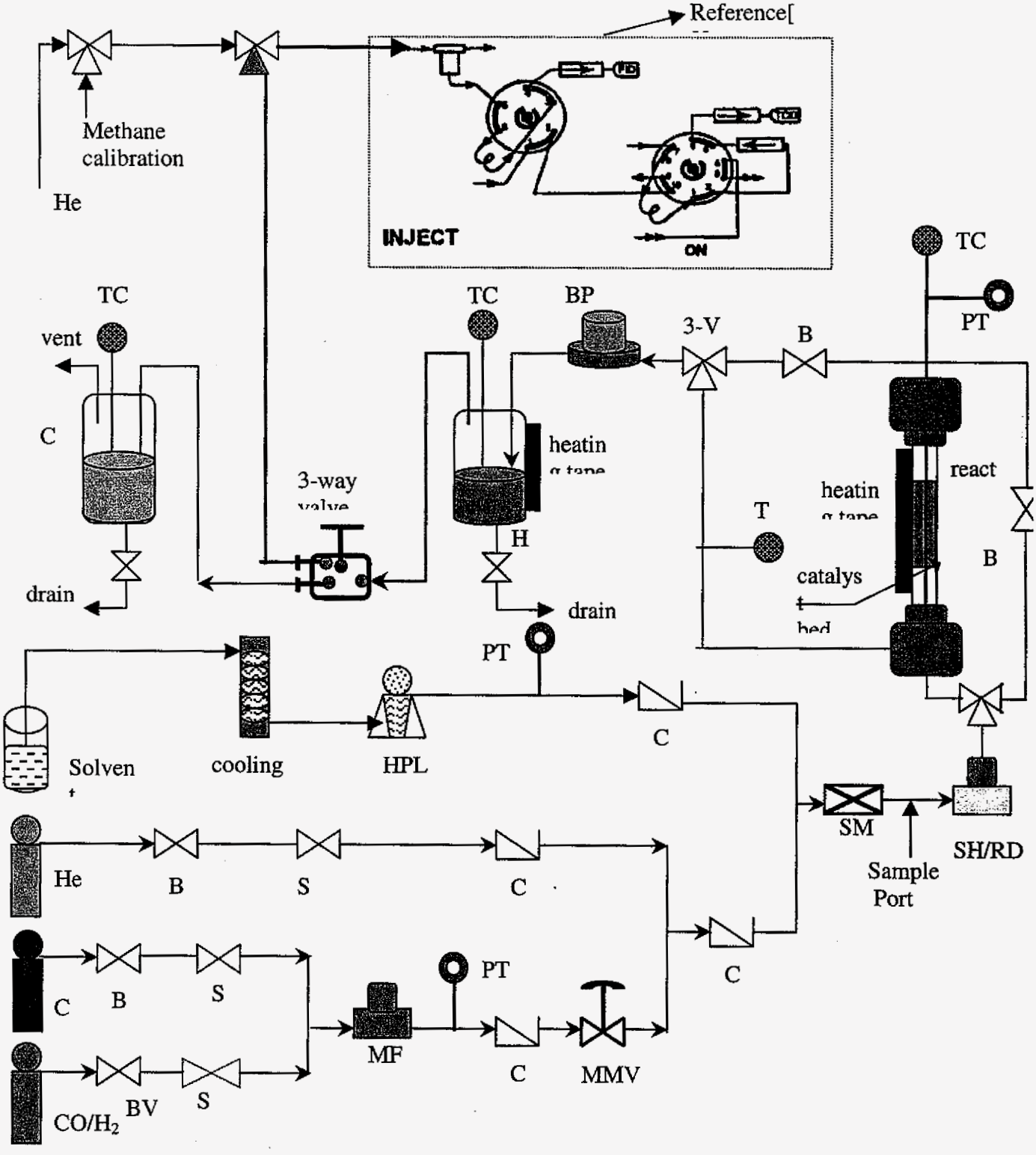

Experimental Conditions

Reactor	• Fixed bed(1.27cm(0.5in)*25.4cm(10in) with an effective volume:32 cm^3)
Catalyst	▪ **Traditional** Fe&Co supported on SiO_2 and Al_2O_3 with promoter potassium: $Fe/Cu/K_2O/SiO_2$ **Recent** Ru on Al_2O_3, Co-Ni on ZrO_2 • **Others**
Supercritical Solvent Medium	• **Pure SCF Solvents**: CO_2 (Pc=72.9atm, Tc=304.2K) , acetone (Pc=47atm, Tc=508.1K) ethane (Pc=48.8atm, Tc=305.4K) , hexane (Pc=29.7bar, Tc=233.7°C), propane (Pc=42.5atm, Tc=369.8K), n-pentane (Pc=33.7atm, Tc=469.6K) propylene (Pc=46.2atm, Tc=365.0K), • **Mixtures of SCF Solvents:** Mixtures of $CO_2 + C_nH_{2n+2}$ Mixtures of C_nH_{2n+2} **Flowrate:**1.0 ml/min
Syngas	**Space velocity:** 50 sccm/g cat **Ratio:** H_2/CO:0.1~ 1.0
Pretreatment	**Reducing gas type:** CO, H_2, CO/H_2 **Flowrate:** 50sccm **Time:** 20 hr **Temperature, Pressure:** 280°C, atmospheric pressure
Reaction Conditions	**Temperature:** 1.1-1.5Tc **Pressure:** 1.2-2.4Pc Time**: the reactions are run for 10hrs once steady state has been reached**
Targeted Results	**Syngas(H_2+CO) conversion, Carbon number distribution(selectivity)** **Catalyst activity(volume, surface area)**

Analytical Procedure

Two gas chromatographs (GCs) are being used in the on-line analysis system. The first involves a Varian 3300 GC equipped with a capillary column (DB-5) and FID for the analysis of C1-C20 hydrocarbons and oxygenates. The second consists of a Varian CP-3800 GC with a packed column and TCD for the analysis of permanent gases and C_1-C_5 hydrocarbons and oxygenates.

Analytical Conditions

Sample	Size	50uL gas, Capillary Column GSV 100uL gas, Packed Column GSV
Column	Capillary Packed Analytical	DB5 HayeSep D
Injection Source	Source Hold Time	Packed and Capillary GSVs 20 seconds
Zone Temperatures	Capillary Injector	250°C
	Valve Oven	250°C
	TCD	140°C
	FID	300°C
	Sample transfer Line	220°C
Column Oven Parameters	Oven Equilibration Time	3 minutes
	Oven Maximum Temperature	290°C
	Oven	on
Column Oven Temperature program	-25°C(0 minute) to 280°C at 4C/min. , hold	
Detector Information	TCD: Reference GAS Flow Rate(30°C) 40cc/min	
	FID: make-up GAS Flow Rate(30°C) N_2, 30cc/min	
	H_2 Flow Rate(30°C), 30cc/min	
	Air Flow Rate(30°C), 300cc/min	
Pressure and Flow	Capillary Column: carrier gas flow rate(30°C): He 13cm/s Pressure Program: 25psig(27min.) to 70psig at 5psig/min, hold Packed Column: Carrier Gas: Helium	

Quantitative Analysis

Concentration Calculations: All of the expected components that are being analyzed by the packed column are gases at standard conditions and appropriate gas standards have been obtained and used to calibrate the analytical equipment. Hence, external

standard curves could be generated for each compound in the packed column chromatogram. In the capillary chromatography, only the hydrocarbons up to pentane have been obtained within gas mixtures. None of the oxygenates are gases at standard conditions. An alternate we are exploring involves relating the quantities of nongaseous hydrocarbons and oxygenates to a light hydrocarbon. A technique has been devised for using the external standard curve of methane to calculate quantities for all compounds present in the capillary column chromatogram, which involve converting the peak area of any peak in the capillary chromatogram to an "equivalent" methane peak area. For example, for the hydrocarbon concentration:

$$A_1^e = \left(\frac{M_{CH4}}{M_2} \right) A_2 = A_{CH4}^e$$

Thus the peak area is multiplied by the ratio of molecular weights of methane to the component of interest and the resulting equivalent area is fed to calibration equations for methane.

Current Experimental Plan

- SCF-based FT reactions are to be performed with SCF CO_2 and SCF alkanes using temperatures that range from 100 to 250 °C, pressure from 70 to 200 bar, syngas and SCF solvent feed composition from 1:1 to 1:5 and H_2/CO from 0.5 to 2. Solvent/syngas flowrates will be varied at each of the desired operating conditions. A variety of FT catalysts are to be used in these reactions including iron and Co-based catalysts, as well as ruthenium catalysts. The reaction products are analyzed to determine the effect of the SCF reaction parameters and catalysts on product conversions and selectivities.
- The influence of the SCF solvents on the adjustable solubilities of the products is to be determined. Specifically, in the case of mixed supercritical solvent systems, the determination of phase boundaries using a high temperature and high pressure view cell are being performed to ensure single-phase operation throughout the FT system.

[1] H. Koelbel, M.Ralek, Catal. Rev. Sci. Eng., 21(1980)225
[2] D. Stem, A. T. Bell, H. Heinemann, Chem. Eng. Sci., 38(1983),597
[3] P.G. Debenedetti, R.C.Reid, AIChE J., 32(1986)2034
[4]Baiker, A., Chem. Rev., 1999, 99,453
[5] Subramaniam, B., Energeia, 1999, (10),3, 1
[6] Bian, B.; Fan, L.; Fujimoto, K., Ind. Eng. Chem. Res., 1997, 36, 2580-2587

[7] Xiaosu Lang, Aydin Akgerman and Dragomir Bukur, Ind. Eng. Chem. Res., 1995, 34, 72-77
[8] William K. Snavely, M.S. Thesis, University of Kansas, 1992.

Hydrogen Production by Hydrocarbon Cracking

Naresh Shah, Devadas Panjala, Sidhartha Pattanaik, Frank E. Huggins and Gerald P. Huffman University of Kentucky, Lexington, KY

Introduction

The goal of this project is to develop catalysts and reaction conditions for catalytic cracking of hydrocarbons to produce hydrogen. Methane is the major component of natural gas. Traditionally, dry (with CO_2) reforming, wet (with H_2O) reforming and partial oxidation of methane is employed to produce synthesis gas and hydrogen is produced using the water-gas shift. In this project, we are exploring non-oxidative methods to produce hydrogen from hydrocarbon. Due to the lack of oxygen, there is no formation of carbon monoxide, which is a poison for catalysts used in fuel cells.

In the current project, nanoscale, binary, iron-based catalysts, supported on alumina, are being investigated to determine their activities for catalytic decomposition of hydrocarbons and reforming reactions.

Catalyst synthesis

In previous work, our group has demonstrated that nanoscale, binary ferrihydrite catalysts are readily formed by co-precipitation techniques.[1,2] The metal component of these binary ferrihydrite (FHYD) catalysts typically consists of 90-95% iron and 5-10% of a secondary element. Characterization of $FHYD_{90\text{-}95}$ /$M_{5\text{-}10}$ (M = Si, Al, Mo, Cr) using a range of techniques (TEM, XRD, XAFS spectroscopy, Mössbauer spectroscopy, SQUID magnetometry) has established that:

1. Particle sizes in the as-precipitated state are typically in the range from 5 to 50 nm.
2. The secondary element is often concentrated at the surfaces of the particles.
3. Binary ferrihydrites resist agglomeration much better than pure ferrihydrite at elevated temperatures.

To date, we have synthesized binary FHYD/M catalysts with M = Mo, W, V, Pd, Ir, Ni, and Si. Pure ferrihydrite treated with a citric acid solution to promote chemisorption

of organic ions at the particle surfaces [3] was also prepared. The surface organic ions also cause the ferrihydrite nano-particles to resist agglomeration at elevated temperatures.

Supported catalysts were prepared by first adding an aqueous solution of metal catalyst to a slurry of γ-alumina (150 m^2/gram) and then precipitating metal oxyhydroxide on alumina by raising the pH of the slurry with ammonia. The slurry was washed with distilled water and dewatered. The paste was extruded and vacuum dried to form pellets.

For this report, we are limiting the discussion of reaction study results to the following three catalyst systems:

1. 5% Fe on alumina
2. 0.5% Mo - 4.5% Fe on alumina
3. 5% Mo on alumina

Reaction and gas analysis system

Methane is a good carburizing agent and will carburize 304 and 316L stainless steel reactors rapidly. Hence, all of the current experiments were performed in quartz reactors. To quantify the gaseous reaction products, we use a six port sampling valve with a 50 microliter sample loop that does not saturate the TCD detector.

Methane can be cracked non-catalytically at higher temperatures. This thermal cracking reaction is dependent on the contact time and temperature. Since we have to use quartz wool to support the catalyst in the down-flow reactor, the amount of quartz wool used was kept constant to minimize any effect on the variation in contact time.

Catalyst pre-treatment

The as-prepared, supported, iron catalyst exists in a ferrihydrite structure. Prior to reaction, the catalysts was subjected to the following three pretreatments.

(1) The catalyst was oxidized under flowing air at 1000 °C.

(2) The catalyst was reduced in flowing hydrogen (50ml/min) for two hours at 1000 °C to produce a metallic state.

(3) The catalyst was first reduced to the metallic state in H_2 at 1000 °C, then carburized by treatment in flowing 20% CH_4 – 80% H_2 at 700 °C to produce metal carbide.

Results

Figure 1 shows changes in methane and hydrogen concentrations by volume in the product stream as different catalysts in their reduced states are heated to increasing temperatures. It is clear that the catalysts have a profound effect in lowering the temperature for methane cracking as compared to thermal cracking over an alumina support with no added metal catalyst. Both the 5% Fe/Al_2O_3 and the 0.5%-4.5%Fe/Al_2O_3 lower the methane decomposition temperatures by over 300 °C.

Though not so obvious, it is also noted that the product gas stream did not contain any appreciable amounts of C_2 and higher hydrocarbons. Since both hydrogen and methane are measured independently, it is seen that the product stream contains more than 98% of only these two gases. Except in the case of non-catalytic cracking, there was a complete absence of any liquid products in all experiments.

Figure 2 shows the effect of different pretreatments on 5%Fe/alumina catalysts for the same cracking reaction. For clarity, no methane concentrations are plotted (they are complimentary to the hydrogen concentrations). Oxidized Fe is not an active catalyst. However, under reaction conditions, it may be converted to metallic/carbide state, resulting in the observed activity. There is not much difference in activity between metallic and carbide phase. However, this may be due to rapid conversion of the metallic phase to carbide phase under reaction conditions. Thus, the catalyst state may be quite similar in both reaction experiments, even though they were pre-treated to produce different states. However, the carburized catalyst produced much more carbon and the experiment had to be stopped due to reactor clogging by carbon at temperatures above 850 °C.

References:

1. Jianmin Zhao, Zhen Feng, F.E. Huggins, and G.P. Huffman, Energy & Fuels, **1994**, *8*, 38-43.
2. G.P. Huffman, J. Zhao and Z. Feng, "Binary Ferrihydrite Catalysts,", U.S. Patent Number 5,580,839, Dec.3, 1996.
3. J. Zhao, Z. Feng, F.E. Huggins, and G.P. Huffman, *Energy & Fuels*, **1994**, *8*, 1152-1153.

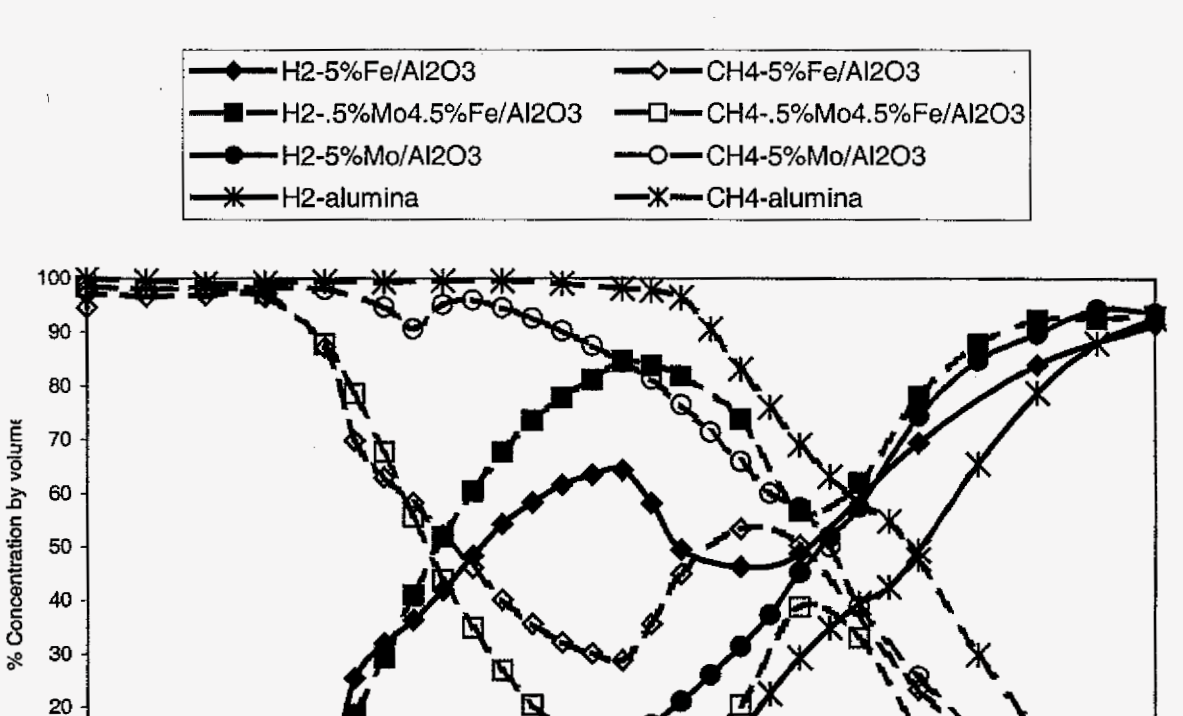

Figure 1. Catalytic CH4 cracking - Effect of catalyst - 5%Fe/Al2O3, 0.5%Mo/4.5%Fe/Al2O3 and 5%Mo/Al2O3 - Reduced in hydrogen at 1000C for 2 hrs.

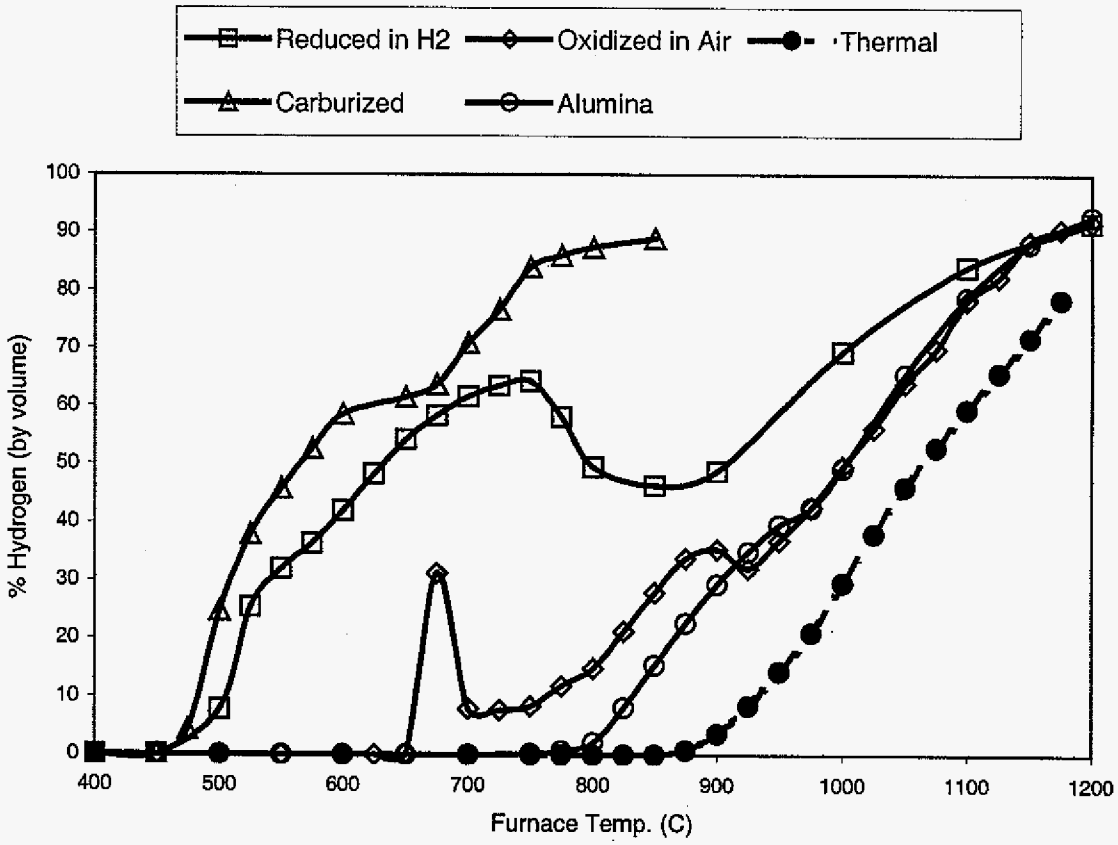

Figure 2. Hydrogen production from CH_4 cracking - Thermal and 5%Fe/Al_2O_3.

Methane Reforming with Carbon Dioxide
A Progress Report

Edwin L. Kugler, Dady B. Dadyburjor, Lawrence Norcio and Mahesh Iyer
West Virginia University
Department of Chemical Engineering
Morgantown, WV 26506

Introduction

The reforming of methane with carbon dioxide for the production of synthesis gas is appealing because it produces synthesis gas with higher purity and lower H_2-to-CO ratio than either partial oxidation or steam reforming.[1] Lower H_2-to-CO ratio is a preferable feedstock for the Fischer-Tropsch synthesis of long-chain hydrocarbons. On the environmental perspective, methane reforming is enticing due to the reduction of carbon dioxide and methane emissions as both are viewed as harmful greenhouse gases.[2] Commercially, nickel is used for methane reforming reactions due to its inherent availability and lower cost compared to noble metals. However, nickel also catalyses carbon formation via methane decomposition and CO disproportionation (Boudouard reaction).[3] Thus, notable efforts have been concentrated on exploring new catalysts, which are resistant to carbon formation. Sulphur passivated nickel catalysts and noble metals have been shown to exhibit resistance to carbon formation.[4] But the low activity of sulphur passivated nickel and the high costs and limited availability of the noble metals have limited their application.

There has been considerable interest in the catalytic properties of metal carbides. The production of metal carbides is abundant and their price is cheap compared to noble metals. It has been suggested that they can replace the rare and expensive noble metals in catalysis.

---

[1] van Kuelen, *et al.*, Journal of Catalysis, **166**, 306 (1997).
[2] Bradford and Vannice, Applied Catalysis, **142**, 73 (1996).
[3] Claridge, *et al.*, Journal of Catalysis, **180**, 85 (1998).
[4] Rostrup-Nielsen, Journal of Catalysis, **85**, 31 (1984).

Identifying better catalysts would reduce process costs for methanol, ammonia, and Fischer-Tropsch plants. The objective of this research is to develop new metal carbide catalysts for syngas production from methane reforming with carbon dioxide.

The Catalyst Testing Unit

The catalyst testing unit is shown in Figure 1. The unit is computer-controlled and is located in a walk-in hood. The computer monitors alarms for CO and H_2S, and for flows of reactive gases, hood velocity, ambient hood temperature, reactor temperature, reactor pressure, and electric power. The unit automatically shuts down in the event of hood failure, or CO leak detection, or if a gas flow or the reactor temperature exceeds the preset operating ranges.

The unit has four lines of gas feed, each independently controlled. The reactor is a stainless steel tube (SS 304L) placed in a single-zone furnace. The catalyst samples are placed in the center of the reactor between quartz chips. The product stream is sampled immediately downstream of the reactor at the pressure of the reactor and at a minimum temperature of 150°C. The products are analyzed on-line, using a Hewlett-Packard 5890 gas chromatograph. The Hayesep D packed column is connected to a thermal conductivity detector, which provides quantitative analysis for CH_4, He, CO_2, CO, H_2, and H_2O. Helium is used as an internal standard for quantitative analysis.

Results

Preliminary experiments were conducted to check the working condition of the catalyst testing unit. Two catalysts were used for this purpose. The first catalyst was Ni/Al_2O_3 obtained

from United Catalyst, Inc. and the second catalyst was Pt/ZrO_2, which was prepared in-house. Prior to catalytic testing, blank reaction tests were performed without catalysts to determine the activity of the reactor and the thermocouple itself. Results show that the reactor and thermocouple were not catalytically active up to 750°C. However, at reaction temperatures 800 and 850°C, the % CH_4 conversions were 1.23 and 1.29%, respectively.

Commercial Catalyst

The commercial Ni/Al_2O_3 catalyst has a BET surface area of 1.5-5 m^2/g and pore volume of 0.1-0.2 cc/g. It contains 14%-wt. Ni, 80-86%-wt. Al_2O_3, and less than 0.1%-wt. C. The catalyst pellets were crushed and sieved into grains of 0.3-0.6 mm (10-20 mesh) and 90-125μm (120-170 mesh) in size. Typically, 300 mg of the catalyst was tested. As recommended by United Catalysts, Inc., the commercial catalyst was pretreated by heating to 149°C and holding that temperature for 2 hours. Then, the temperature was raised to 204°C and CO_2 gas was passed through the reactor for 1 hour, before adjusting to the desired reaction temperature. The feed ratio used was CH_4: CO_2: Ar = 1: 3.7: 4.9 with a total feed rate of 170 cc/min. Both small and large particle-size catalysts were tested at various reaction temperatures ranging from high temperature (700°C) to low temperature (400°C) with increasing and decreasing temperature modes.

Figure 2 shows an example of a chromatogram obtained from testing the commercial catalyst. Pure component injections were used to identify the major peaks. Figures 3 and 4 show examples of the % CH_4 and % CO_2 conversions obtained from running the commercial catalyst. As expected, the % conversions increase as the reaction temperature increases.

Moreover, the smaller particle size catalyst has higher % conversion compared to that of the larger particle size catalyst. It was also found that this catalyst is very stable.

It was hypothesized that there were three major reactions taking place: methane reforming, reverse water gas shift (RWGS), and carbon deposition. Reaction rates were calculated based on these reaction models. Figure 5 shows the reaction rates of the three reactions at various reaction temperatures. The order of increasing reaction rates is: rate of carbon deposition < rate of methane reforming < rate of RWGS.

Pt/ZrO_2 Catalyst

The Pt/ZrO_2 catalyst was prepared in our laboratory. Zirconium oxide powder, as received, was first calcined at 852°C for over 18 hours in flowing air. The calcined support was isostatically pressed into pellets at 6000 bar. The pellets were crushed and sieved to give grains having diameters between 0.3-0.6mm. The grains were impregnated with H_2PtCl_6 solution to yield 0.31%-wt. Pt. The water was removed by heating the catalyst at 92°C for 2 hours in a rotating evaporator followed by drying overnight at 92°C in static air. The impregnated grains were calcined at 650°C for 15 hours. The BET surface area of the catalyst was determined to be 4-5 m^2/g. The Pt/ZrO_2 catalyst was pretreated in flowing H_2 at temperatures between 400 to 800°C, *in situ*, before testing. The same reaction conditions, feed ratio, and feed rate used in testing the commercial catalysts were used in testing the Pt/ZrO_2 catalyst.

Results show very low % conversions for the Pt/ZrO_2 catalyst. Pretreating at higher temperatures with H_2 showed no significant effect on its conversion. Later, it was found that the catalyst was deactivating within 2 hours into the reaction. Thus, this prepared catalyst was found to be very unstable. No further study was made for this catalyst.

Future Work

The catalyst testing unit was found to be in good working condition. Future work includes preparation and catalyst testing of molybdenum and tungsten carbide catalysts. A new experimental setup will be fabricated for the preparation of molybdenum carbide. Catalytic testing for Co_6W_6C catalyst is now in progress.

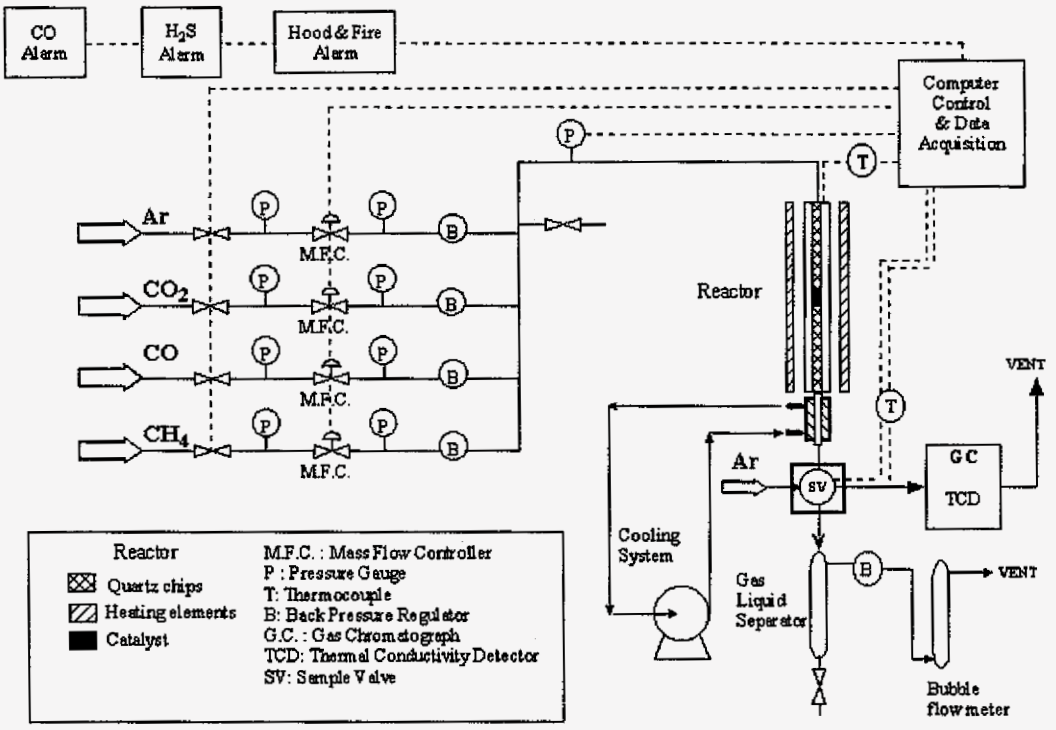

Figure 1- Flow sheet for catalyst testing unit

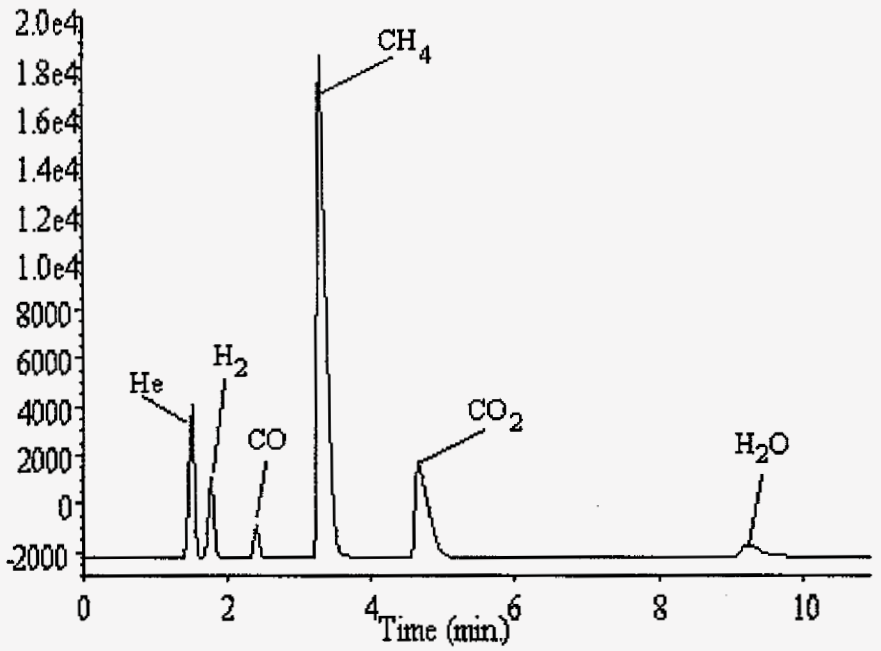

Figure 2- A typical chromatograph obtained from Ni/Al_2O_3 catalyst (120-170 mesh size). Reaction conditions: T= 700 °C; feed ratio = CH_4: CO_2:Ar = 1:3.7:4.9

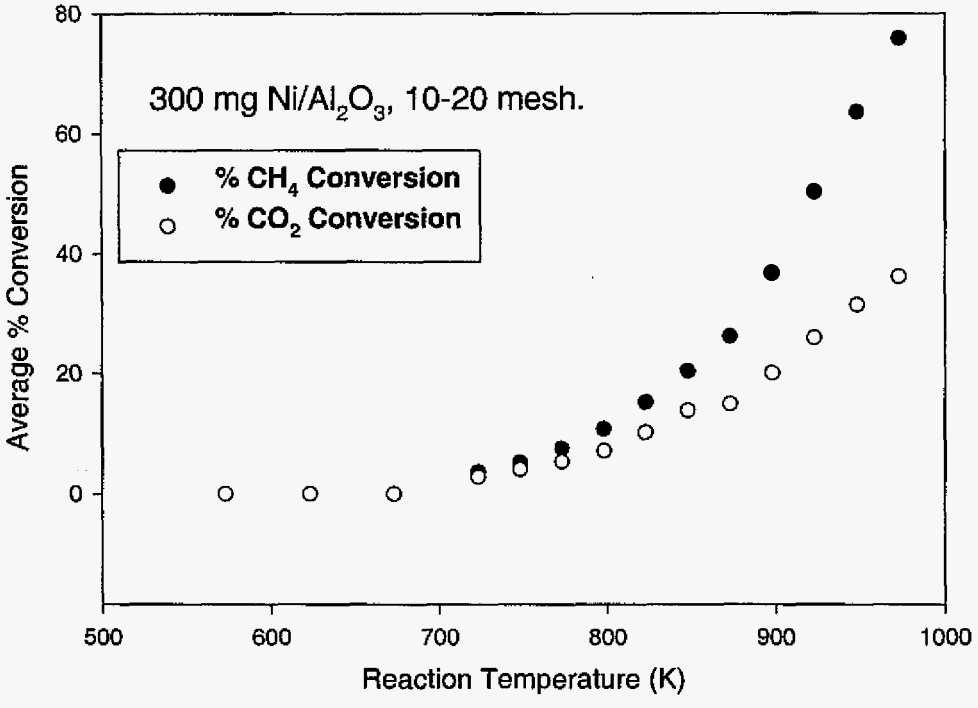

Figure 3- Conversion plots for large particle size commercial catalyst with decreasing temperatures

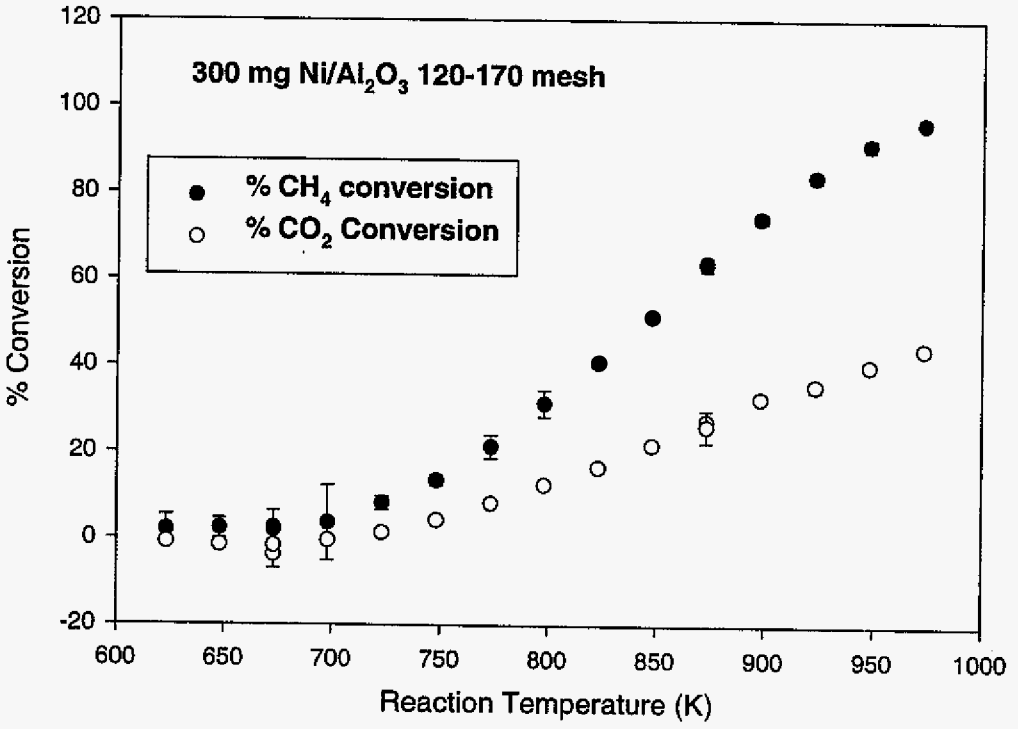

Figure 4- Conversion plots for small particle size commercial catalyst with decreasing temperatures.

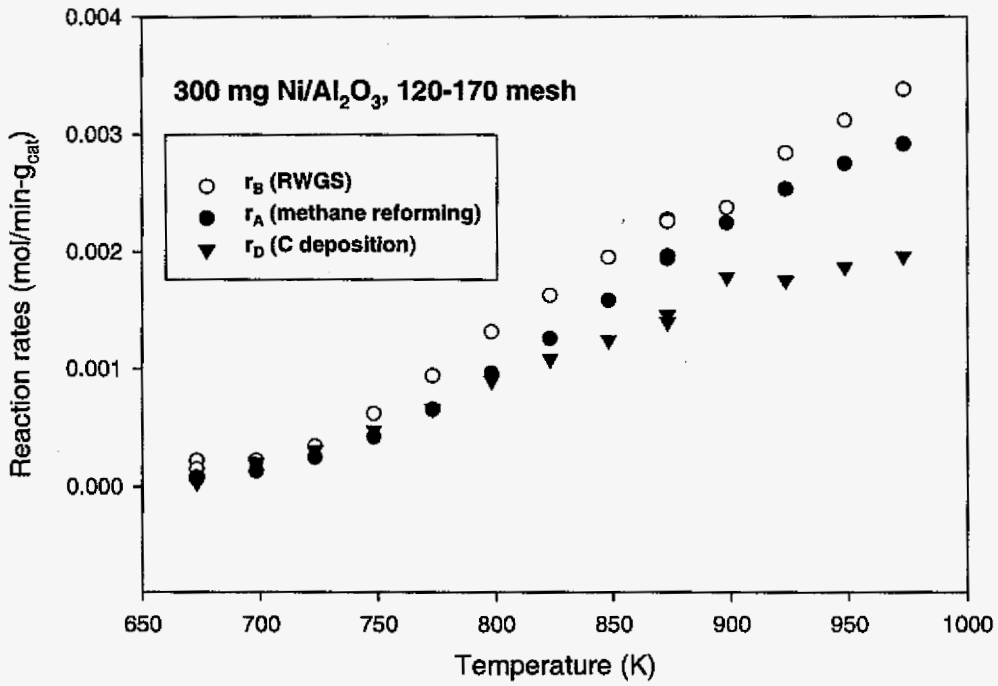

Figure 5- Reaction rates of methane reforming, RWGS, and C-deposition with decreasing temperature using small particle size commercial catalyst.

Carbon Dioxide as an Oxidizing (Dehydrogenating) Agent

Irving Wender and John W. Tierney
Department of Chemical and Petroleum Engineering, 1249 Benedum Hall,
University of Pittsburgh, Pittsburgh, PA 15261

There have been several publications on the reaction of two greenhouse gases, carbon dioxide and methane, to form hydrogen and carbon monoxide (synthesis gas), valuable reactants for conversion to fuels and chemicals. Our attention was brought to the fact that CO_2 is a weak oxidizing or dehydrogenation compound. [Oxidation is equivalent to dehydrogenation.] We have therefore carried out research on using CO_2 as a reagent for the dehydrogenation of hydrocarbons, a manner of using this greenhouse gas as a reactant while providing useful, environmentally clean products with a possible saving in energy.

Dehydrogenation of hydrocarbons requires high temperatures due to thermodynamic limitations. A high steam-to hydrocarbon ratio is used to supply heat for the reactions, dilute the reactants to increase equilibrium conversion and avoid coke deposition on the catalyst. CO_2 could play a role similar to steam in these reactions. Utilization of CO_2 in the dehydrogenation of hydrocarbons could be used to produce chemicals efficiently and, at the same time, convert this greenhouse gas to valuable carbon monoxide (CO) gas.

Styrene, a high volume, high value chemical, is a raw material for polymers; it is produced by dehydrogenation of ethylbenzene in the presence of steam and a catalyst. The problems encountered in ethylbenzene dehydrogenation are similar to those generally met in the dehydrogenation of hydrocarbons. High steam-to-hydrocarbon ratios (7 to 12) and high temperatures (above 600°C) are used in commercial plants. A new process using CO_2 instead of steam has been reported. A comparable yield of styrene was obtained at 580°C (50° lower than the commercial process). The energy consumption using CO_2 instead of steam is 1.9×10^8 cal/t-styrene, only 12.7% of the energy consumption of the commercial process (15.0×10^8 cal/t-styrene).

Commercial catalysts for dehydrogenation of ethylbenzene are not suitable for this new process; new catalysts are under investigation.

A series of catalysts on various supports were prepared by incipient wetness techniques, drying and calcinations. Catalyst performance was measured in a continuous reactor. 0.5g of catalyst, mixed with 1g of quartz sand, was loaded into a tubular reactor. Ethylbenzene was introduced with a syringe pump and vaporized before entering the reactor. CO_2/ethylbenzene ratios were maintained at 10 in most experiments. A LHSV of one for ethylbenzene was used. The products were analyzed online using two gas chromatographs.

Thermodynamic calculations were conducted for this reaction system. Coupling the reverse water gas shift reaction with the dehydrogenation of ethylbenzene is not favored for lowering the standard free energy for styrene production. However, higher concentrations of CO_2 will shift the equilibrium to obtain high conversions of styrene. Equilibrium conversion for the dehydrogenation of ethylbenzene was about 15% higher in the presence of CO_2 than that in steam. From thermodynamic results, a similar conversion could obtained at 50°C lower in the presence of CO_2.

Some reaction results at 550°C are listed in Table 1. The table shows that Al_2O_3 is a better support for iron catalyst than is SiO_2. In some cases, potassium promotion was favorable. Active carbon (AC) supported iron catalysts had very high initial activities but the catalysts deactivated rapidly.

A $Pt/WO_3/ZrO_2$ catalyst showed comparable activity for the dehydrogenation of ethylbenzene in the presence of CO_2. All three components in this catalyst are essential because activities of Pt and WO_3/ZrO_2 were very low. The activity increased with increase in WO_3 concentration in the $Pt/WO_3/ZrO_2$ catalyst.

Figure 1 shows the effect of CO_2 on the dehydrogenation of ethylbenzene. Obviously, CO_2 improves the activity and stability of Fe/Al_2O_3 catalysts. Similar effects were observed with $Pt/WO_3/ZrO_2$ and Fe/AC catalysts. It can also be seen from Table 1 that a substantial amount of valuable CO is produced when CO_2 is used in the dehydrogenation reaction.

Dehydrogenation of ethylbenzene could involve the following reactions:

CO_2 + ethylbenzene → CO + styrene + H_2O (1)

Ethylbenzene → styrene + H_2 (2)

$H_2 + CO_2 \rightarrow CO + H_2O$ (3)

CO could be produced either by reaction (1) or by a combination of reactions (2) and (3). A study of the reverse water gas shift reactions shows that reaction (3) is approaching thermodynamic equilibrium at 550°C. It is difficult to distinguish these two routes. From the promotion effect of CO_2 on this reaction, one can conclude that CO_2 is involved in the activation of ethylbenzene. CO_2, as a weak oxidant, would react with the weak bonds in adsorbed ethylbenzene to increase the oxidation rate.

Carbon dioxide could also be used in the dehydrogenation of isobutane to isobutene. Our search for improved catalysts for incorporating CO_2 into dehydrogenation processes to produce high values chemicals is nearing completion.

Figure 1. Effect of CO_2 on Dehydrogenation of Ethylbenzene with Fe/Al_2O_3 Catalyst

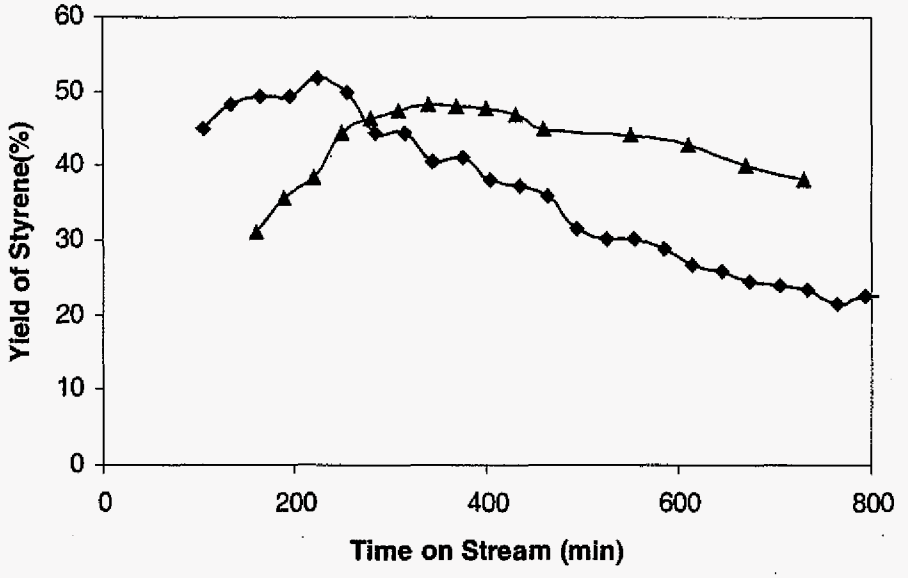

Table 1. Dehydrogenation of Ethylbenzene on Various Catalysts.

Catalyst	TOS (min)	Conversion (%)	Yield of Styrene (%)	Selectivity to Styrene (%)	Yield of CO (%)
Fe/Al_2O_3	50	42.8	39.9	93.3	NA
	200	27.9	27.8	97.9	NA
	500	22.6	22.6	100	NA
KFe/Al_2O_3	50	33.3	31.2	93.6	4.6
	200	47.3	47.3	100	43.6
	500	42.3	42.3	100	37.1
KFe/SiO_2	35	1.08	1.08	100	0
	200	1.34	1.34	100	0
	500	1.59	1.59	100	0.02
Fe/AC	60	27.8	67.8	93.9	NA
	200	58.3	41.4	99.3	NA
	500	21.2	18.8	100	NA
KFe/AC	60	27.4	63.4	76.8	85.5
	200	71.5	28.5	100	32.4
$PtWO3/ZrO_2$ (No CO_2)	60	62.7	37.3	100	-
	200	72.9	27.1	100	-
	500	80.0	20.0	100	-

Reaction conditions:

Temperature:550°C, WHSV of ethylbenzene:1, CO_2/ethylbenzene:10

Analytical Characterization of Catalyst Structure and Product Distribution

Principal Investigator: M. S. Seehra, Eberly Professor of Physics, West Virginia University

Coinvestigators: Alex Punnoose, P. Roy, A. Manivannan and Heidi Magnone

Annual Report: May 1, 1999 to April 30, 2000

I. INTRODUCTION

The objectives of our program are to characterize various catalysts used in the C-1 Chemistry reactions in order to determine their structural and electronic properties relevant to catalysis. The experimental techniques employed include x-ray diffraction (XRD), electron spin resonance (ESR) spectroscopy, magnetometry, thermogravimetric analysis (TGA) and transmission electron microscopy (TEM). Some catalysts were synthesized in our laboratory (nanoparticles of CuO and Si-doped ferrihydrites, FHYD) while others were obtained from the research groups of Huffman et al (Kentucky), Wender et al (Pittsburgh) and Eyring et al (Utah). In this brief report, a summary of the major findings from this research carried out during the past one year is given. A more detailed account is available in the publications listed at the end of the report.

II. SUMMARY OF RESULTS

A. Structure, properties and roles of the different constituents in $Pt/WO_x/ZrO_2$ catalysts:

Platinum-promoted tungstated zirconia catalysts ($Pt_{0.5}/WO_x/ZrO_2$) have been used by Wender et al in the hydroisomerization of long-chain linear alkanes since they provide good stability and selectivity. However, a number of questions had remained unresolved which our recent studies have clarified. First, ZrO_2 exists in both the tetragonal and monoclinic forms. However, the exact role of the two phases was not clear. Our studies have shown that it is the tetragonal phase of ZrO_2 which supports the WO_x species and that WO_x is highly dispersed in the catalyst up to 600°C since no diffraction peaks due to crystalline WO_3 are observed (Fig. 1). Above 700°C, crystalline peaks due to WO_3 begin to appear, along with the conversion of tetragonal ZrO_2 to monoclinic ZrO_2 (Fig. 1). At 1000°C, WO_3 is crystallized and the tetragonal ZrO_2 is absent. These observations along with other supporting data reported in Publication #1

establishes the correlation of dispersed WO_x with tetragonal ZrO_2. These observations also show that the catalyst becomes unstable above 700°C.

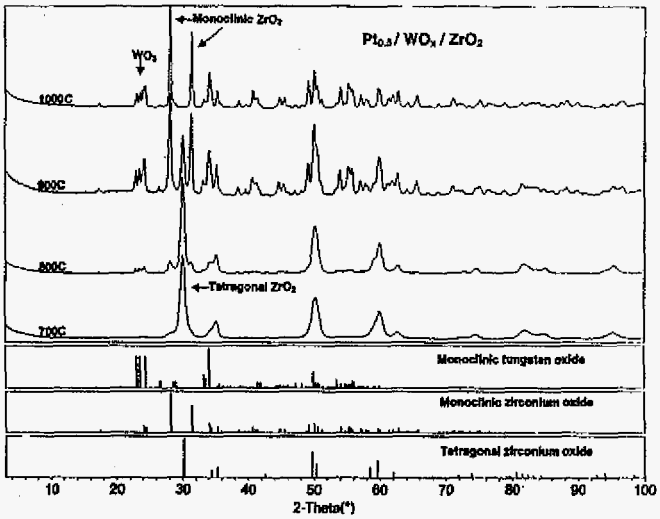

Fig. 1: Changes in X-ray diffractogram of $Pt/WO_3/ZrO_2$ upon annealing at different temperatures.

The second important question is the nature of electronic state of Pt. Since the catalysts contained only 0.5 wt.% of Pt, no information on the state of Pt could be determined from x-ray diffraction. However we used temperature-dependent magnetic measurements to show that in fresh $Pt/WO_x/ZrO_2$ catalysts, Pt exists in the form of Pt-oxospecies and that under the hydroisomerization conditions, these Pt-oxides are reduced to metallic Pt. Also, co-impregnation of tungsten and platinum to ZrO_2 support appears more favorable for the formation of Pt oxo-species. Details are given in Publication #1.

B. Structural and electronic properties of doped-ferrihydrite catalysts

Nanoparticles of ferrihydrites $(FeOOH)\cdot nH_2O$ with particle size of about 4 nm and ferrihydrites (FHYD) doped with Si, Al, Ni, Mo, Ir are under study by the Kentucky group (Huffman et al) in a number of C-1 Chemistry reactions. During the past year, we have made enormous progress in understanding the structural and electronic properties of the undoped and doped ferrihydrites, by employing the techniques of x-ray and neutron diffraction, magnetometry and ESR spectroscopy (Publications #2, 3, 4 and 5). Neutron diffraction studies showed that the two-line undoped FHYD order antiferromagnetically at $T_N \simeq 350$ K. The magnetic measurements show that each particle carries a magnetic moment $\mu_p \simeq 300\ \mu_B$, corresponding to

50 Fe^{3+} uncompensated ions, each with a magnetic moment of about 6 μ_B. Doping of FHYD with Si (viz. Si_x/FHYD), for x up to 0.5 have shown that μ_p decreases rapidly as x increases for initially dopings (Fig. 2). A detailed analysis on the magnetic properties of Si_x/FHYD for x = 0, 0.02, 0.05, 0.10, 0.15, 0.20, 0.26, 0.40 and 0.50 has been carried out (Publication #5) and the following picture has emerged from these studies.

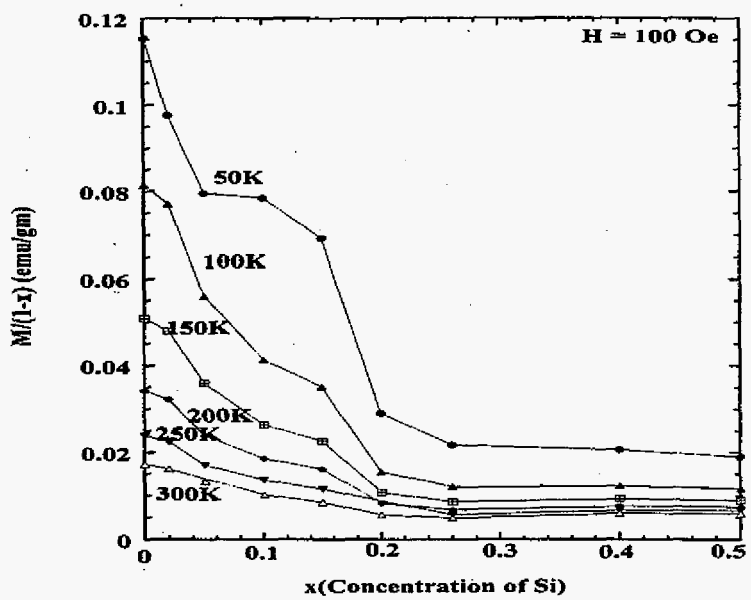

Fig. 2: Plot showing changes in the magnetization of Si_x/FHYD with x at different temperatures

For a particle of diameter ≃ 40 Å, there are about 2500 Fe^{3+} spins out of which about 500 are in a surface shell of thickness ≃ 1.5 Å. However, only about 50 ($\sqrt{2500} = 50$) Fe^{3+} spins on the surface are magnetically uncompensated which give the measured moment of 300 μ_B/particle. Since Si favors the tetrahedral bonding of the surface spins, initial doping by Si preferentially replaces the surface Fe^{3+} ions, leading to a dramatic decrease in the magnetization M (Fig. 2). When all the 500 surface Fe^{3+} are replaced by Si at x = 500/2500 = 0.2, additional doping by Si begins to replace the Fe^{3+} ions in the core of the nanoparticles, with the resulting increase in the amorphous nature of the particles. This is quite evident in the x-ray diffraction patterns where shift and broadening of the lines is observed for the higher x-values (Fig. 3).

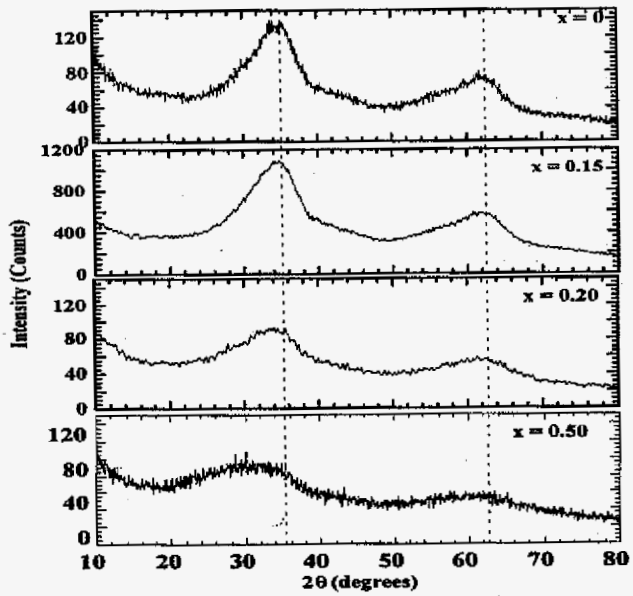

Fig. 3: X-ray diffractograms of Six/FHYD samples

Magnetic measurements on samples doped with 5% Ni, Mo, Ir and Al show that except for the case of Ni, magnetization M decreases upon doping with Mo, Ir and Al, similar to the case of Si doping. This is understandable since except for Ni all the other dopants are non-magnetic. For the Ni-doped FHYD, the magnetization increases. In ESR spectroscopy, the ESR line is broadened by different amounts by the different dopants (Fig. 4) except for Ni

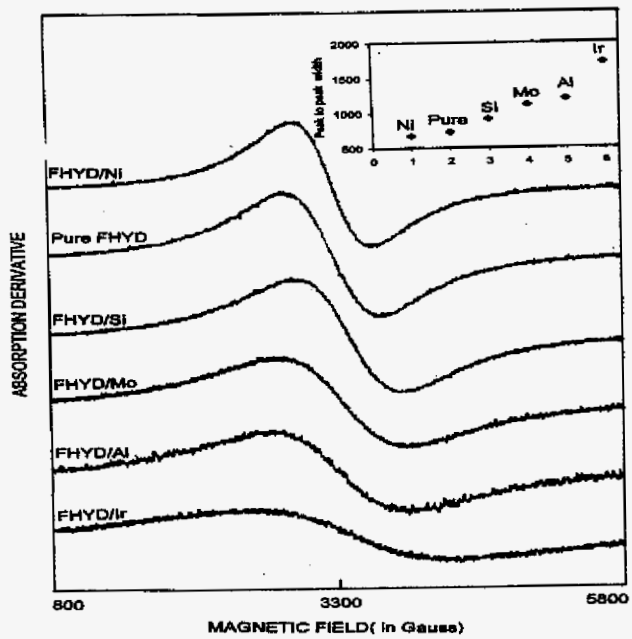

Fig. 4: Plot showing the effect of different dopants on the ESR spectrum of FHYD at 300K

which narrows the line. For Si_x/FHYD, there is a strong correlation between the intensity of ESR line and the measured magnetization (Fig. 5). These results clearly show that the ESR line is due to the magnetically uncompensated surface Fe^{3+} ions. A detailed quantitative analysis is in progress upon completion of which a paper on this work will be submitted for publication (Publication #8).

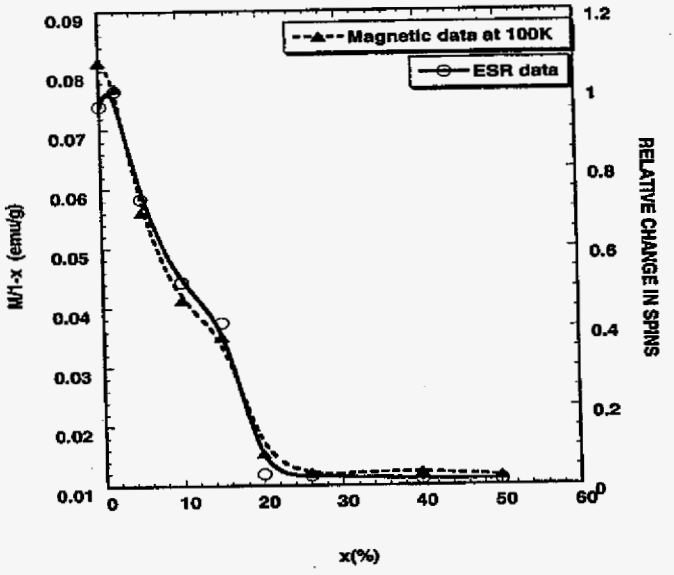

Fig. 5: Plot showing the correlation between ESR line intensity and magnetization of Si_x/FHYD

The above results have important implications for the catalytic properties of the doped FHYD nanoparticles. It is noted that catalysis usually involves unpaired electrons of a catalyst and the ESR signal and the magnetization are a measure of the density of the unpaired electrons. Therefore the changes observed in the ESR signal and magnetization upon doping provides a probe for the catalytic properties. Some of the samples investigated here were obtained from Huffman et al whereas most of the Si and Al doped FHYD were prepared in our laboratory. In the near future, we expect to receive some samples from Huffman et al which have been exposed to catalytic reactions. These samples will be similarly investigated to provide further insights into various catalytic processes. The results obtained so far show that the magnetically uncompensated surface spins for Fe^{3+} are likely to play the most important role in catalysis and that with appropriate dopants, the electronic and structural properties of FHYD can be manipulated.

Publications #7 and 8 on the properties of nanophase carbons provide important insights for catalysis since these carbons are often used as catalyst supports.

III. WORK IN PROGRESS

Other catalyst systems currently under investigation include $CuCl_2/PdCl_2$/carbon obtained from Eyring et al (Utah), and a number of Fe and Mo catalysts supported on Al_2O_3 obtained from Huffman et al (Kentucky). In addition, we have recently synthesized CuO nanoparticles in the size range of 6 to 30 nm as potential catalysts. X-ray diffraction studies on all these catalysts have been completed which have provided information on the crystalline components and their crystallite size. Magnetic and ESR studies are now in progress which are expected to be completed during the coming year. For the $CuCl_2/PdCl_2$/carbon catalyst, x-ray diffraction shows very high dispersion of $CuCl_2/PdCl_2$ on the carbon support. Magnetic and ESR measurements provide evidence of unpaired spins on Cu, with evidence for nanoparticle magnetism. More details on these results will be provided in future reports.

IV. PERSONNEL

Graduate assistant Paromita Roy completed her M.S. thesis in May, 2000 on the "Magnetic properties of Si-doped ferrihydrite nanoparticles". A new student, Heidi Magnone, has joined the group recently. She has successfully synthesized the CuO nanoparticles with assistance from Dr. Alex Punnoose. Dr. Punnoose joined the group in October 1999 and he has the major responsibility for the experimental studies in this program. Dr. A. Manivannan, Research Assistant Professor, has made contributions in magnetic studies in the early stages of the Program and in the measurements of the particle sizes by TEM (Transmission Electron Microscopy). The TEM measurements were carried out at NIOSH (National Institute of Safety and Health) in Morgantown, with the kind assistance of Diana Schwegler-Barry. Others collaborators on the publications listed below include J. W. Lynn of NIST, a former research associate V. S. Babu, and Professor N. C. Giles at WVU, Prof. Wender at Pittsburgh and Professor Huffman at Kentucky.

V. PUBLICATIONS & PRESENTATIONS

1. Structure, properties and roles of the different constituents in $Pt/WO_x/ZrO_2$ catalysts, A. Punnoose, M. S. Seehra and I. Wender, Journal of Catalysis (submitted).
2. Neutron scattering and magnetic studies of ferrihydrite nanoparticles, M. S. Seehra, V. S. Babu, A. Manivannan and J. W. Lynn, Physical Review B 61, 3513-3518 (2000).
3. Hysteresis loop shifts in magnetic field cooled FeOOH nanoparticles, M. S. Seehra, P. Roy and A. Manivannan, Proc. Materials Research Soc. June 2000 (in press).
4. Influence of chemisorption on the magnetism of interacting ferrihydrite nanoparticles, M. S. Seehra, V. S. Babu, P. Roy and A. Manivannan, Cluster and Nanostructure Interfaces World Scientific, June 2000 (in press).
5. Effects of Si doping on the magnetism of ferrihydrite nanoparticles, P. Roy, A. Manivannan and M. S. Seehra, Physical Review B (submitted).
6. Interaction of oxygen with nanophase carbons investigated by electron spin resonance spectroscopy, A. Manivannan, A. Punnoose, and M. S. Seehra, Proc. Materials Research Soc., June 2000 (in press).
7. Microstructure, dangling bonds and impurities in activated carbons, A. Manivannan, M. Chirila, N. C. Giles and M. S. Seehra, Carbon 37, 1741-1747 (1999).
8. Correlation of ESR parameters and magnetization in doped ferrihydrite nanoparticles, A. Punnoose, M. S. Seehra and G. P. Huffman (manuscript near completion).
9. Synthesis and magnetic properties of CuO nanoparticles, A. Punnoose, H. Magnone and M. S. Seehra, paper presented at the 10th Annual Conference on Computational & Structural Materials, hosted by West Virginia University; manuscript for publication under preparation.

Mössbauer and XAFS Investigation of C1 Catalysts

F. E. Huggins, S. Pattanaik, N. Shah, and G. P. Huffman

CFFLS, 533 S. Limestone St., 111 Whalen Bldg., University of Kentucky, Lexington, KY 40506

Mössbauer spectroscopy: As described elsewhere in this report, various C1 catalyst formulations are being prepared, treated, and reacted. In addition, considerable catalyst characterization is being undertaken to determine the chemistry and properties of these catalysts. Although such work is incomplete at this time, significant Mössbauer and x-ray absorption fine structure (XAFS) spectroscopic examination of various catalysts have been undertaken. In this section, we report a preliminary account of the iron Mössbauer spectroscopy of various C1 catalysts prepared and treated in the C1 laboratory at the University of Kentucky (UK).

As described elsewhere, the catalysts are prepared as either binary ferrihydrites or as impregnated alumina (Al_2O_3). Table 1 summarizes Mössbauer results for the two types of catalyst. As can be seen from this table, the as prepared catalysts are found exclusively as ferrihydrite or similar species. Selective spectra are shown in Figures 1-3.

The most interesting result is the formation of iron carbide in the 5%Fe/Al_2O_3 catalysts after reaction under a methane atmosphere, regardless of how the catalyst was prepared (Figure 1). There is no evidence for iron carbide formation under any other conditions. There appear to be some remnant phases left over that clearly reflect the initial treatments of the catalyst. For example, the 5%Fe/Al_2O_3 catalyst heated to 1000°C in air before methane reaction (not shown) exhibits a ferric doublet in its spectrum, whereas the same catalyst reduced at 1000°C exhibits Fe^{2+} phases and metallic iron, in addition to the carbide spectrum (Figure 1). These ferrous and ferric phases are thought to have formed by reaction of the iron oxide with the alumina support and prevent complete reduction of the iron to the metallic state. The temperature of reduction makes a significant difference as the Mössbauer spectrum of the 0.5%Mo/4.5%/Al_2O_3 catalyst reduced at 1000°C (Figure 3) is clearly much different from that obtained from the catalyst reduced at 700 (Figure 2) or 500°C (not shown). Further work is needed to identify the very narrow doublet in Figure 3 that has an unusually low value for the isomer shift of –0.23 mm/sec. We have tentatively identified it as a Fe-Mo alloys phase.

Table 1: Summary of Mössbauer Results on Prepared and Treated Catalysts

Sample ID	Treatment	Fe metal	Fe_3C	Austenite	Fe^{2+}	Fe^{3+}
10%Mo!0%Si/FHYD MK2608	As rec'd	--	--	--	--	100 (fhyd)
5%Mo/5%Si/FHYD MK2607	As rec'd	--	--	--	--	100 (fhyd)
#12 5%Fe/Al_2O_3 MK2598	R @ 1000 C CH_4 rxn	13	43	10	34	--
#13 5%Fe/Al_2O_3 Mk2606	C @ 1000 C CH_4 rxn	33	19	11	37	--
#14 5%Fe/Al_2O_3 MK2597	O @ 1000 C CH_4 rxn	Trace	65	15	--	20
#23 Mo/Fe/Al_2O_3 MK2599	R @ 1000 C C @ 725 C	18	--	25	--	57
#27 Mo/Fe/Al_2O_3 MK2603	O @ 1000 C	--	--	--	--	100 (spinel?)
#28 Mo/Fe/Al_2O_3 MK2600	R @ 1000	22	--	--	--	29*
#29 Mo/Fe/Al_2O_3 MK2601	R @ 500 C	5	--	--	61	34
#30 Mo/Fe/Al_2O_3 MK2602	R @ 700 C	4	--	30	--	66
#31 Mo/Fe/Al_2O_3 MK2604	R @ 500C C @ 500C	11	--	--	39	50
#32 Mo/Fe/Al_2O_3 MK2605	R @ 700C C @ 700C	13	--	--	40	47
0.5%Mo/4.5%Fe/Al_2O_3 MK2596	As prep'd	--	--	--	--	100 (fhyd)

*Includes 49% unknown doublet (-0.23,0.37) Mo-Fe alloy?

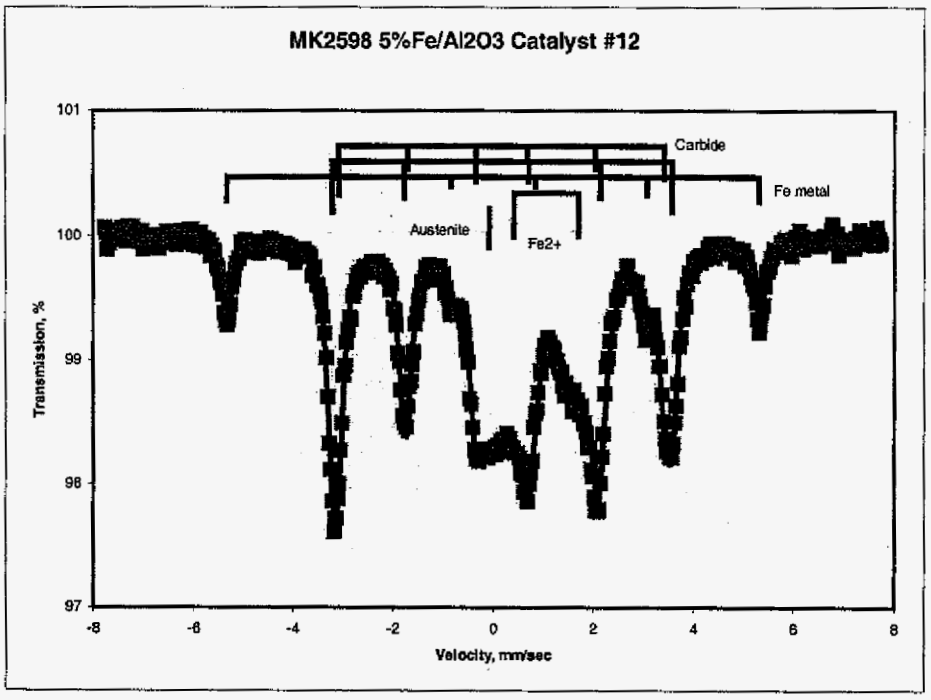

Figure 1: Mössbauer spectrum of 5%Fe/Al_2O_3 catalyst. Sample 12 after reduction in hydrogen at 1000°C followed by reaction in a methane atmosphere.

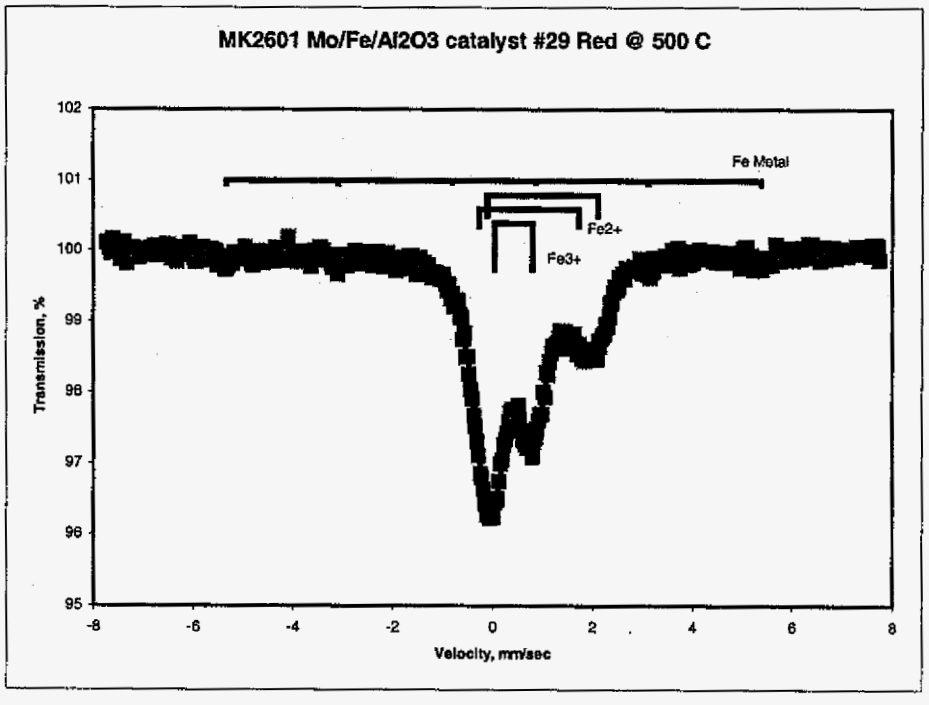

Figure 2: Mössbauer spectrum of 0.5%Mo/4.5%Fe/Al_2O_3 catalyst. Sample #29 after reduction at 500°C in hydrogen.

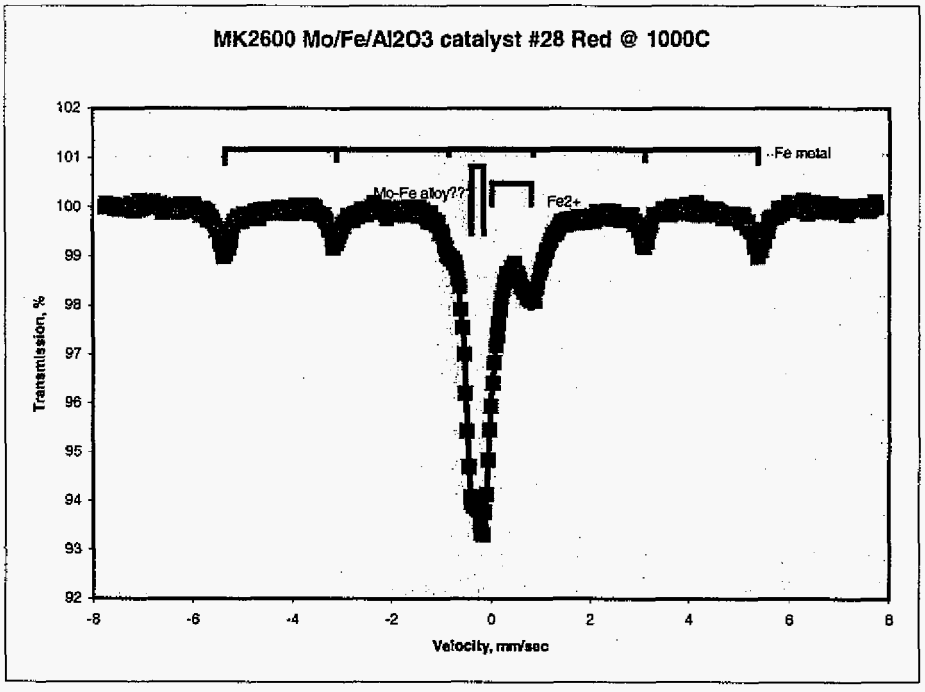

Figure 3: Mössbauer spectrum of 0.5%Mo/4.5%Fe/Al_2O_3 catalyst. Sample 29 after reduction in hydrogen at 1000°C.

XAFS spectroscopy: X-ray absorption fine structure (XAFS) spectra have been obtained from a number of the catalysts synthesized and reacted in the C1 laboratory at UK. Although detailed analysis and interpretation of these spectra is incomplete, some preliminary conclusions can be reported. Qualitative interpretations of the XAFS spectra obtained from 5%Fe/Al_2O_3, 4.5%Fe/0.5%Mo/Al_2O_3, and 0.5%Mo/Al_2O_3 catalysts at both the Fe and the Mo K-edges are given in Table 2. The Mössbauer results for several samples are also indicated in the table. Briefly, it is found that the catalysts subjected to reduction treatments at 700 and 1000 °C or to reduction treatments followed by carburization at 700 °C exhibit ~20-50% Fe metal in their Fe K-edge XAFS spectra, and some evidence of metallic forms of Mo in their Mo K-edge XAFS spectra. However, there is little indication of carbide formation for either metal. For the four samples reacted in methane subsequent to reduction or reduction plus carburization, the Fe XAFS data indicate that Fe metal is the dominant component. The as-prepared 4.5%Fe/0.5%Mo/Al_2O_3 catalyst exhibits spectra consistent with the Mo being present in the form

of a molybdate anion, MoO_4^{-2}. Subsequent reduction appears to produce lower oxides and a metallic form of Mo. For the 4.5%Fe/0.5%Mo/Al_2O_3 catalysts, the Mo generally appears to be less reduced than the Fe after reducing treatments. More detailed analysis of these spectra is in progress.

Unfortunately, the analysis of catalyst samples after reaction may be deceptive, since exposure of small metallic catalyst particles to air when they are removed from the reactor may convert them to oxide. Therefore, much of the current effort in XAFS analysis is focused on the development of an in situ XAFS cell that will allow structural data to be obtained from catalysts during C1 reactions. An in situ cell has been designed and built that should allow investigation of C1 catalysts at temperatures up to 700 °C. It will be tested at the National Synchrotron Light Source at Brookhaven National Laboratory in mid-July of this year.

Table 2. Mössbauer & XAFS Data Summary for C1 Catalysts

Sample no. and description	MK no.	XAFS elem.	Mössbauer results	XAFS results (qualitative analysis)
47 - AP 4.5Fe/0.5Mo/Al2O3	2596	Mo	100% Fe^{+3} (ferrihydrite)	XANES edge at ~ same location as MoO_3 with similar shoulder. FT - large peak at 1.3 A (O), small at 2.9 A. Very similar to Mo0.05/FHYD data (MoO_4^{2-}).
27 - O-1000 4.5Fe/0.5Mo/Al2O3		Mo		Nearly identical to as prepared sample (47).
48 - AP 0.5Mo/Al2O3 & 40 - O-700 0.5Mo/Al2O3		Mo		Both show an O FT peak at 1.5-1.55 A and an XANES and an XANES shoulder at ~7 eV, similar to MoO_3.
41 - R-700 0.5Mo/Al2O3		Mo		Both XANES and FT look like mixture of MoO_3 and Mo metal.
42 - R & C – 700 0.5Mo/Al2O3		Mo		FT peaks at 1.37, (~1.7), & 2.4 A, slightly different from 41. XANES very similar to 41. FT suggests some Mo carbide.
28 - R-1000 4.5Fe/0.5Mo/Al2O3	2600	Mo	28% Fe metal, 29% Fe^{3+}, 49% Fe-Mo alloy.	Mixture of oxide and metallic forms of Mo. Mo appears to be mainly molybdate (MoO_4^{2-}).
30 - 0 R-700 4.5Fe/0.5Mo/Al2O3	2602	Mo	4% Fe metal, 66% Fe^{3+}, 30% austenite.	XANES and FT indicate Mo is still predominantly molybdate (MoO_4^{2-}).
32 - R-700, C-700 4.5Fe/0.5Mo/Al2O3	2605	Mo	13% Fe metal, 40% Fe^{2+}, 47% Fe^{3+}.	FT – strong peak at 1.57 A (MoO_3 or MoO_2 nn O shell) and weaker peak at ~2.5 (Mo_2C nn metal shell). XANES more metallic but still show an oxide shoulder like MoO_3.
28 - R-1000 4.5Fe/0.5Mo/Al2O3	2600	Fe	28% Fe metal, 29% Fe^{3+}, 49% Fe-Mo alloy.	Both FT and XANES indicate partial conversion (~50%) to metallic form.
30 - R-700 4.5Fe/0.5Mo/Al2O3	2602	Fe	4% Fe metal, 66% Fe^{3+}, 30% austenite.	FT indicates ~20-30% conversion to Fe metal, balance hematite. XANES is consistent with this estimate.
32 - R-700, C-700 4.5Fe/0.5Mo/Al2O3	2605	Fe	13% Fe metal, 40% Fe^{2+}, 47% Fe^{3+}.	FT and XANES about the same as 30.

33 - R-700, CH4 rxn 4.5Fe/0.5Mo/Al2O3		Fe		FT – strong peak at 2.12 A (Fe metal) and broad weak peak at ~4.0. XANES close to Fe metal, missing edge shoulder. Appears to be mostly Fe metal.
34 - R-700, C-700, CH4 rxn, 4.5Fe/0.5Mo/Al2O3		Fe		Virtually identical to 33.
17 - R-1000, CH4 rxn 5%Fe/Al2O3		Fe		Both FT and XANES indicate Fe metal with minor secondary component.
18 - R-1000, C-725, CH4 rxn 5%Fe/Al2O3		Fe		Both FT and XANES indicate Fe metal with minor secondary component.
39 - R-700, C-700, 5%Fe/Al2O3		Fe		FT – strong O peak 1.5 A, weaker Fe metal peak, 2.17 A, oxide Fe peak – 2.85 A. XANES - mixture of oxide and metal.
37 - R-700, 5%Fe/Al2O3		Fe		Nearly identical to 39.

AP – as prepared.
O – oxidized in air.
R – reduced in H_2.
C – carburized in 20% CH_4, 80% H_2.
CH_4 rxn – reacted in CH_4.
FT – Fourier transform.
XANES – x-ray absorption near edge structure.
700, 1000 – 700 °C, 1000 °C.

Diethyl carbonate (DEC) synthesize using the Pulse-quench reactor

J. Z. Hu and R. J. Pugmire, Chemical & Fuels Engineering Department, University of Utah

The Pulse-quench reactor

Solid state NMR can be efficiently utilized as a complementary analytical tool to GS/MS for characterizing catalyst reaction (see Figure 1).

In order to facilitate the ongoing NMR investigation as well as to provide a constant flow reactor with the flexibility of controlling experimental parameters for the reaction, we have built a Pulse-quench Reactor depicted in Figure 2. Currently, the reactor has the following main features.

(1). The maximum temperature inside the catalyst bed is about 420 °C with a temperature control stability of ±1°C.

(2). Constant flow of the reagents, e.g., CH_3CH_2OH, CO and O_2 as well as the carrier gas N_2. The flow rates are controllable over a range from 0 to 200 sccm for the reactants, and 1000 sccm for the carrier N_2.

(3). Pressure control over a range of 0-140 psi.

(4). Pulse injection of the regents with sequence of timing under computer control.

(5). Quenching of the reaction inside the catalyst bed using liquid nitrogen under computer control.

Experimental results

Figure 3 shows a typical temperature profile inside the reactor versus the quenching time with no catalyst placed inside the reactor. It is obvious that in less than 1s, the temperature can be brought from about 450 °C down to room temperature. With catalyst in place, the time needed for a complete quenching is lengthened accordingly depending on the length and the packing density of the catalyst bed.

Currently, we are using the constant flow feature of the pulse-quench reactor for the DEC catalytic reaction. A typical GS spectrum of the eluted products is given in Figure 4. Though the yield of the DEC under the specified condition is low, only 6.7 wt %, the products are simple,

containing CH_3CH_2OH, DEC and only one major unknown byproduct. Preliminary results are summarized in Table 1.

Some interesting results are observed from Table 1. (1) Comparing the experiments #2, 3 and 4, the yield of DEC decreases with the increase of the flow-rate of CO in contrast to the dimethyl carbonate reaction, probably due to the side reaction of $CO + O_2 = H_2O$. So far, the best yield of DEC was observed at the balanced molar ratio condition, i.e., 6 sccm of CO and 3 sccm of O_2 (#2). (2) The wt% of the side products is increased, while the yield of DEC is decreased at decreased temperature (see #1 and #3).

Future work

1. Search the optimum conditions that give the highest yield of DEC by changing the relative ratio of CH_3CH_2OH, CO, O_2 and the carrier gas flow rates, the values of temperature and the pressure.
2. Screen different types of catalyst.
3. Investigate the effects of residence time of the reactants at the catalyst bed.
4. Once optimum experimental conditions are established using the constant flow conditions, pulse-quench experiments will be carried out to provide samples for solid state NMR to study the species adsorbed on the catalyst bed with particular emphasize on the transition period of the catalytic reaction process (see Figure 1).

Table 1. Summarize of the ending products eluted from the catalyst bed under various experimental conditions.

Experiments (#)	CH_3CH_2OH (ml/h)	CO (sccm)	O_2 (sccm)	Temperature (°C)	DEC (wt %)	Byproducts (wt %)
1	**1.18**	**48**	**3**	**155**	**5.0**	**4.0**
2	**1.18**	**6**	**3**	**110**	**6.7**	**2.6**
3	**1.18**	**48**	**3**	**110**	**4.3**	**6.5**
4	**1.18**	**96**	**3**	**110**	**0.8**	**4.8**

Note: The flow rate of the carrier gas N_2 and the pressure at the catalyst bed for all experiments are 48 sccm and 100 psi, respectively. The catalyst was 2.96g $CuCl_2/PdCl_2/NaOH$. The reaction time was 6 hours in order to collect sufficient liquid (2-8ml). The GS measurement was performed immediately after the reaction.

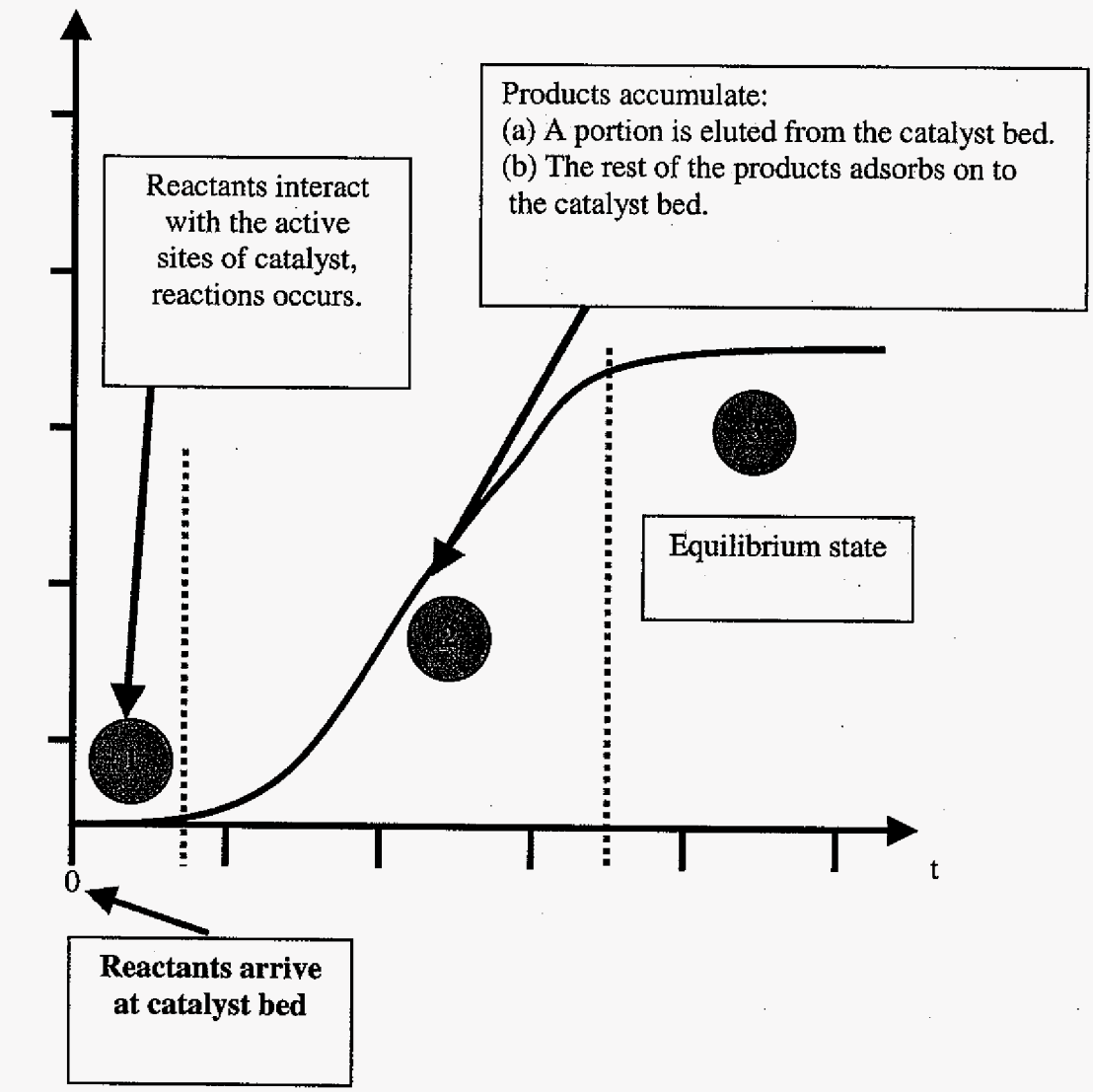

Figure 1. Postulated kinetic process in DEC reaction at constant temperature(i.e., 135 °C). NMR is good for stages (1) and (2) by investigating the product adsorbs at catalyst bed. GC/MS is useful for stages (2) and (3).

Figure 2. The diagram of pulse-quench reactor

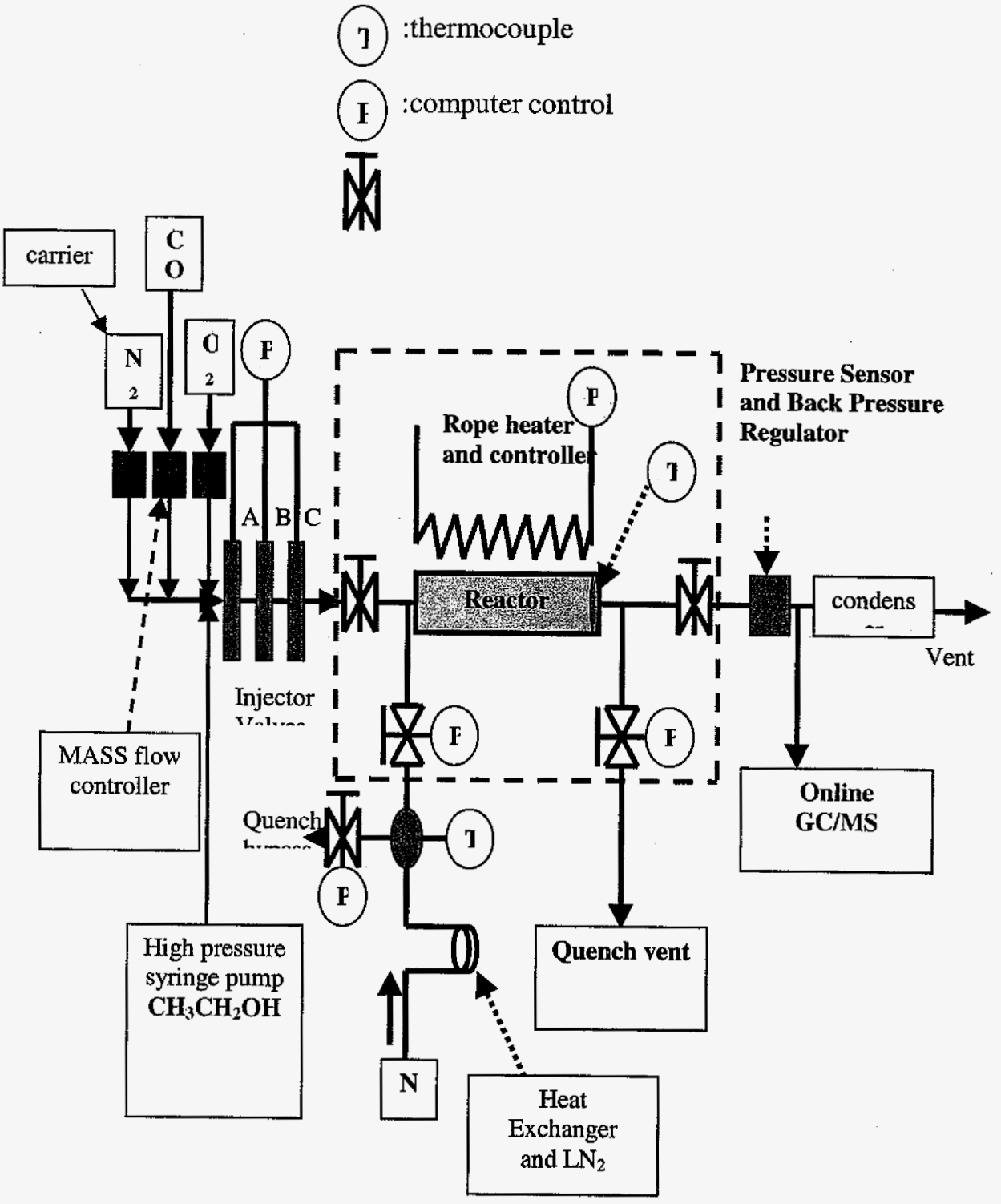

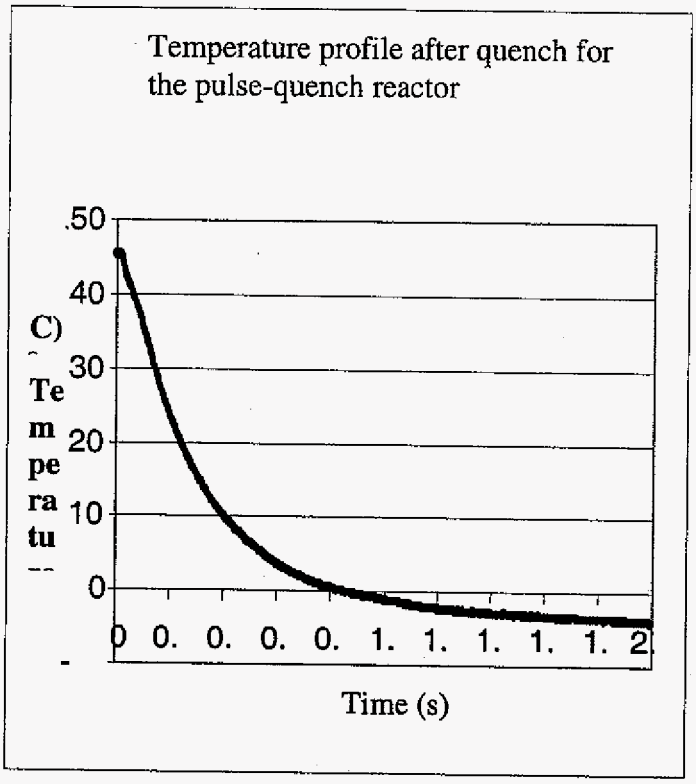

Figure 3. The temperature profile in the middle of the reactor versus the quench time. Note that the temperature can be dropped from 450 °C to room temperature (25 °C) in approximately 0.6s.

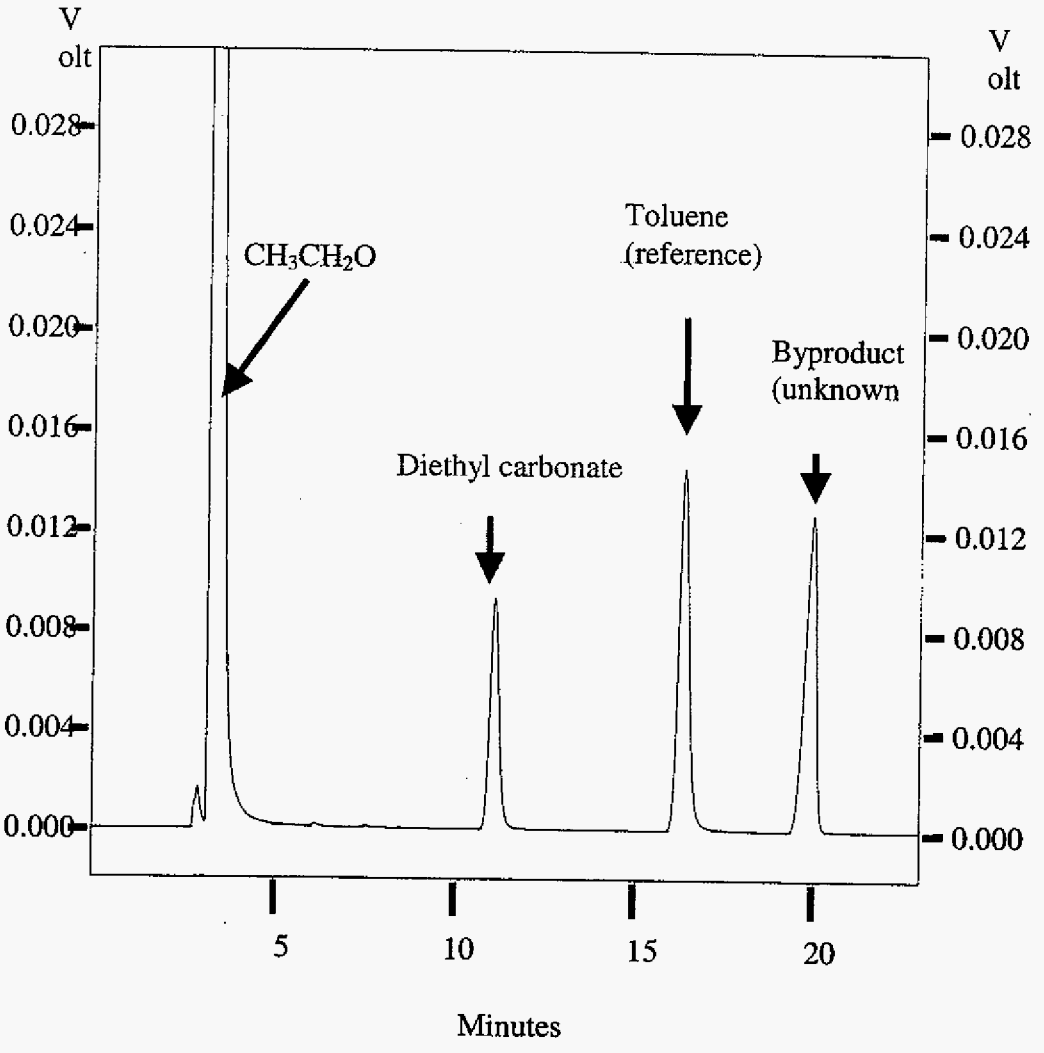

Figure 4. The GS spectrum of the ending products from the Pulse-quench reactor working at the constant flow condition in experiment #2.

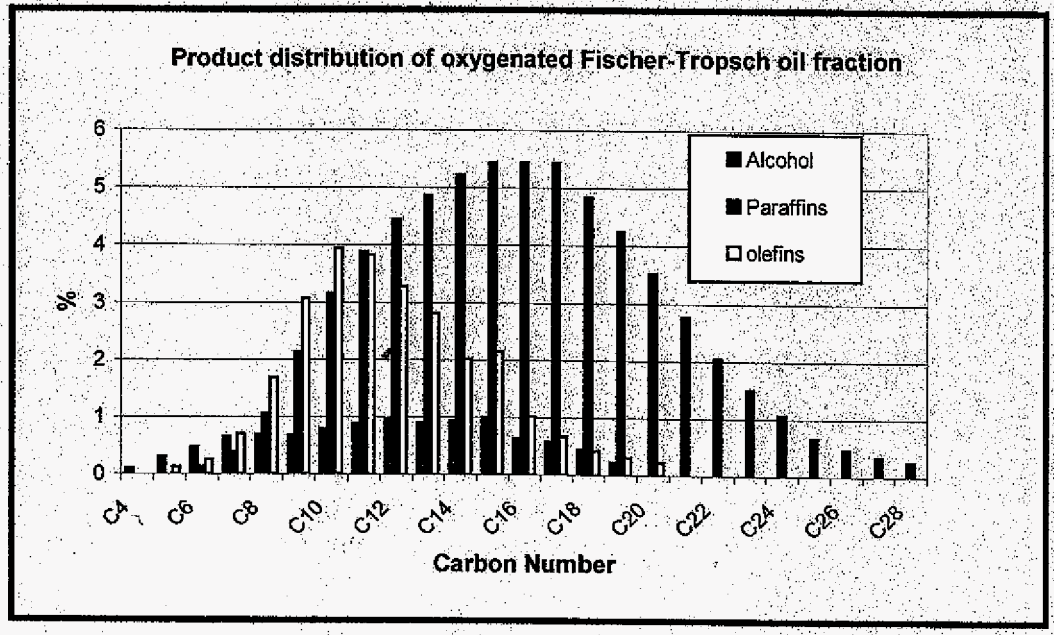

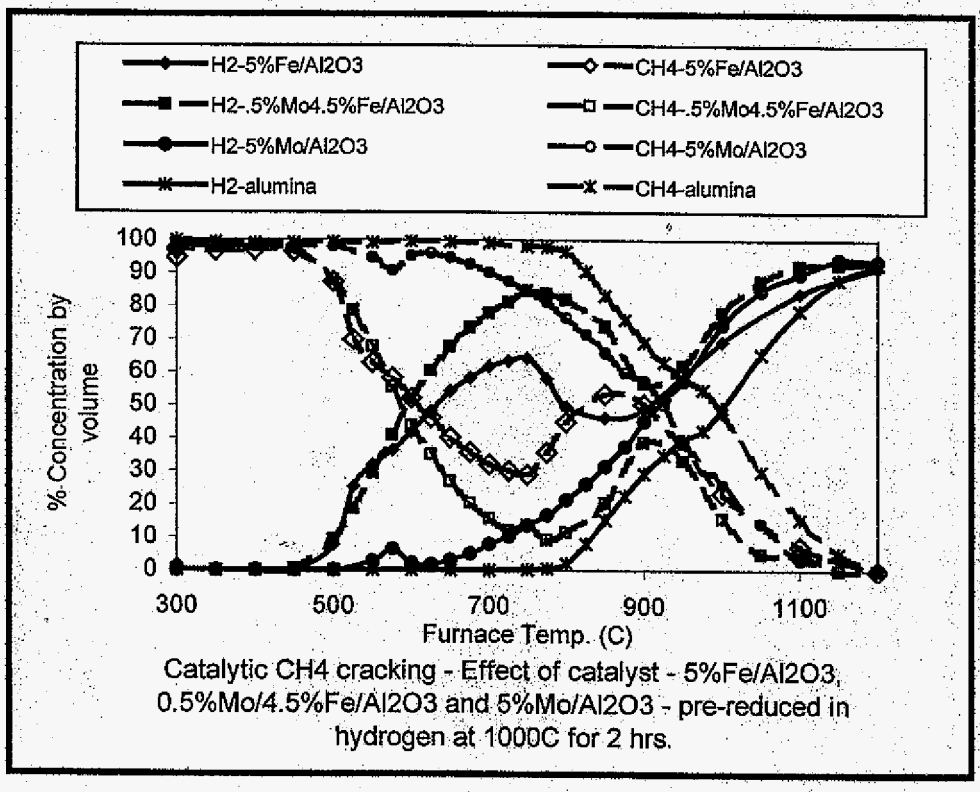

Catalytic CH4 cracking - Effect of catalyst - 5%Fe/Al2O3, 0.5%Mo/4.5%Fe/Al2O3 and 5%Mo/Al2O3 - pre-reduced in hydrogen at 1000C for 2 hrs.